TECHNICAL REPORT HL-88-4

US Army Corps of Engineers

STABLE RIPRAP SIZE FOR OPEN CHANNEL FLOWS

by

Stephen T. Maynord

Hydraulics Laboratory

DEPARTMENT OF THE ARMY
Waterways Experiment Station, Corps of Engineers
PO Box 631, Vicksburg, Mississippi 39180-0631

March 1988
Final Report

HYDRAULICS LABORATORY

Prepared for DEPARTMENT OF THE ARMY
US Army Corps of Engineers
Washington, DC 20314-1000
Under CWI Work Unit No. 31028

Destroy this report when no longer needed. Do not return it to the originator.

The findings in this report are not to be construed as an official Department of the Army position unless so designated by other authorized documents.

The contents of this report are not to be used for advertising, publication, or promotional purposes. Citation of trade names does not constitute an official endorsement or approval of the use of such commercial products.

Unclassified
SECURITY CLASSIFICATION OF THIS PAGE

REPORT DOCUMENTATION PAGE

Form Approved
OMB No. 0704-0188

1a. REPORT SECURITY CLASSIFICATION Unclassified	1b. RESTRICTIVE MARKINGS
2a. SECURITY CLASSIFICATION AUTHORITY	3. DISTRIBUTION/AVAILABILITY OF REPORT Approved for public release; distribution unlimited.
2b. DECLASSIFICATION/DOWNGRADING SCHEDULE	
4. PERFORMING ORGANIZATION REPORT NUMBER(S) Technical Report HL-88-4	5. MONITORING ORGANIZATION REPORT NUMBER(S)
6a. NAME OF PERFORMING ORGANIZATION USAEWES Hydraulics Laboratory 6b. OFFICE SYMBOL (If applicable) WESHS-S	7a. NAME OF MONITORING ORGANIZATION
6c. ADDRESS (City, State, and ZIP Code) PO Box 631 Vicksburg, MS 39180-0631	7b. ADDRESS (City, State, and ZIP Code)
8a. NAME OF FUNDING/SPONSORING ORGANIZATION US Army Corps of Engineers 8b. OFFICE SYMBOL (If applicable)	9. PROCUREMENT INSTRUMENT IDENTIFICATION NUMBER
8c. ADDRESS (City, State, and ZIP Code) Washington, DC 20314-1000	10. SOURCE OF FUNDING NUMBERS See reverse PROGRAM ELEMENT NO. / PROJECT NO. / TASK NO. / WORK UNIT ACCESSION NO

11. TITLE (Include Security Classification)
Stable Riprap Size for Open Channel Flows

12. PERSONAL AUTHOR(S)
Maynord, Stephen T.

13a. TYPE OF REPORT	13b. TIME COVERED	14. DATE OF REPORT (Year, Month, Day)	15. PAGE COUNT
Final report	FROM _____ TO _____	March 1988	122

16. SUPPLEMENTARY NOTATION
Available from National Technical Information Service, 5285 Port Royal Road, Springfield, VA 22161. (Continued)

17. COSATI CODES			18. SUBJECT TERMS (Continue on reverse if necessary and identify by block number)
FIELD	GROUP	SUB-GROUP	Channel stabilization; Revetments; Erosion control; Riprap design

19. ABSTRACT (Continue on reverse if necessary and identify by block number)

Riprap revetment is one of the most widely used methods for protecting the boundaries of erodible channels. Determining riprap size is one of the most important steps in the design process. Some of the existing methods for riprap sizing use the critical shear stress relations and the logarithmic velocity laws to determine stable riprap size. Flume data used in this investigation show that the use of a constant Shields coefficient in the critical shear stress relations is not valid for high relative roughness problems like riprap design. Similarly, the logarithmic velocity laws are not valid for high relative roughness problems. Another limitation of existing riprap sizing methods is the lack of variation relative to the effects of gradation, thickness, or shape.

Using flume data, a riprap sizing method is developed based on average local velocity and depth. Variation in riprap gradation uniformity is described by using d_{30} as the

(Continued)

20. DISTRIBUTION/AVAILABILITY OF ABSTRACT	21. ABSTRACT SECURITY CLASSIFICATION
☒ UNCLASSIFIED/UNLIMITED ☐ SAME AS RPT ☐ DTIC USERS	Unclassified
22a. NAME OF RESPONSIBLE INDIVIDUAL	22b. TELEPHONE (Include Area Code) / 22c. OFFICE SYMBOL

DD Form 1473, JUN 86 *Previous editions are obsolete.*

SECURITY CLASSIFICATION OF THIS PAGE
Unclassified

10. WORK UNIT ACCESSION NO. (Continued).

Funding provided by Civil Works Research and Development Program under Civil Works Investigation Work Unit No. 31028, "Effects of Water Flow on Riprap in Flood Channels," sponsored by Headquarters, US Army Corps of Engineers.

16. SUPPLEMENTARY NOTATION (Continued).

Originally submitted in partial fulfillment of the requirements for the degree of Doctor of Philosophy in Civil Engineering to Colorado State University, Fort Collins, Colorado.

19. ABSTRACT (Continued).

characteristic size. Thicker riprap blankets allow a reduction in size, and shape effects within the range tested are insignificant.

Existing side slope relations used in the critical shear stress equation overestimate the decrease in stability that occurs when a particle is placed on a sloping bank. Comparison of velocity profiles over channel side slopes in straight and curved reaches shows that for the same average velocity over the toe of the side slope, the velocity and shear stress on the side slope are significantly higher on the outer bank of the curved channel. Depth and average velocity over the toe of the side slope are measured in straight and curved flume tests of riprap stability and are used to develop sizing relations for side slope riprap. Results are compared to field data, and safety factors are recommended. A sizing nomograph and an example design are presented.

PREFACE

The study described herein was performed at the US Army Engineer Waterways Experiment Station (WES) during the period 1980-1986 for the Headquarters, US Army Corps of Engineers (USACE), as part of the Civil Works Research and Development Program. Funds were allotted under Civil Works Investigation Work Unit No. 31028, "Effects of Water Flow on Riprap in Flood Channels," under USACE Program Monitor Mr. Tom Munsey. This study was accomplished under the direction of Messrs. H. B. Simmons, former Chief of the Hydraulics Laboratory, F. A. Herrmann, Jr., Chief of the Hydraulics Laboratory, J. L. Grace, Jr., former Chief of the Hydraulic Structures Division, and G. A. Pickering, Chief of the Hydraulic Structures Division. The WES tests were conducted by Messrs. S. T. Maynord, project engineer, E. L. Jefferson, and R. Bryant under the direct supervision of Mr. N. R. Oswalt, Chief of the Spillways and Channels Branch. This report was written by Dr. S. T. Maynord and edited by Mrs. Marsha Gay, Information Technology Laboratory.

This report was also submitted to the Academic Faculty of Colorado State University, Fort Collins, Colorado, in partial fulfillment of the requirements for the degree of Doctor of Philosophy in Civil Engineering.

COL Dwayne G. Lee, CE, is the Commander and Director of WES. Dr. Robert W. Whalin is the Technical Director.

TABLE OF CONTENTS

CONVERSION FACTORS, NON-SI TO SI (METRIC)
UNITS OF MEASUREMENT

Non-SI units of measurement used in this report can be converted to SI (metric) units as follows:

Multiply	By	To Obtain
cubic feet	0.02831685	cubic metres
degrees (angle)	0.01745329	radians
feet	0.3048	metres
inches	2.54	centimetres
pounds (mass)	0.4535924	kilograms
pounds (mass) per cubic foot	16.01846	kilograms per cubic metre
square feet	0.09290304	square metres

STABLE RIPRAP SIZE FOR OPEN CHANNEL FLOWS

CHAPTER 1

INTRODUCTION

The transport of water through natural and man-made open channels carries the possibility of scour if the channel boundaries are erodible. While many different methods have been used to protect channel boundaries, riprap revetment continues to be one of the most widely used methods. Riprap is long-lasting, flexible, easily placed and repaired, and natural in appearance. However, in some locations riprap is not readily available or the available stone is too small for riprap. In other locations, a limited number of available gradations, rather than design guidance, determines the size used. Transportation costs for riprap from quarry to jobsite are often greater than the cost of the rock alone. In spite of these limitations, the large amount of riprap used requires guidance to ensure optimum design.

Determining riprap size is one of the most important factors in defining the optimum riprap gradation. Existing riprap sizing methods have limitations which include the following:

1. Many existing riprap sizing methods have evolved from sediment transport concepts which use shear stress to define particle stability. Critical shear stress for a given riprap size is determined by the well-known Shields coefficients. Most sediment transport and riprap sizing techniques use a constant Shields coefficient for rough turbulent flow. Existing riprap design techniques also use logarithmic velocity laws to relate

velocity to shear stress. However, several investigators have found the Shields coefficient to vary at high relative roughness while others have found the logarithmic velocity laws to be affected by high relative roughness. Since most riprap stability problems involve high relative roughness, many of the existing riprap sizing methods may not be applicable.

2. Existing riprap sizing methods that use shear stress have an additional liability. As stated by Neill and Hey (1982),

> Researchers tend to favor shear stress criteria for stability and bed movement. From a practical engineering viewpoint, local shear stresses are difficult to measure and to conceptualize, compared to velocities. Researchers might pay more attention to expressing results in velocity terms for practical applications.

3. Existing riprap sizing methods also lack variation relative to the effects of riprap gradation, thickness, and shape.
4. The analytical techniques used to determine the decrease in stability that results from placing riprap on a channel side slope need to be tested against experimental data.

Considering these limitations of existing riprap sizing methods, the objectives of this study are as follows:

1. Evaluate the applicability of existing riprap sizing methods that use a constant Shields coefficient or the logarithmic velocity laws.
2. Develop a riprap method based on velocity. Determine which velocity (bottom, average, surface, or maximum) to use in the riprap sizing method.
3. Incorporate riprap gradation, thickness, and shape variation into riprap sizing method.

4. Evaluate side slope effects on riprap stability and incorporate into riprap sizing method for straight and curved channels.

A series of flume tests were used to accomplish these objectives by studying the stability and resistance to flow of riprap having gradation, thickness, and shape similar to that used for scour protection in open channels. Results are limited to channels with slopes less than 2 percent, and the ratio of flow depth to average riprap size must be greater than 4. Riprap sizing for placement in highly turbulent flow downstream of hydraulic structures or for placement on embankments subject to overtopping flows is not covered in this study.

The following chapters present first a review of existing literature relative to these four objectives. Next, the experimental investigation is explained, and then the analysis and results to achieve each of these four objectives are presented. Finally the conclusions from the study and recommendations for further studies are presented.

CHAPTER 2

LITERATURE REVIEW

In the study of open channel riprap stability, many investigations have been conducted that are applicable to this engineering problem. This review of existing information focuses on four different topics which correspond to the four objectives in the Introduction. First, studies concerning the effects of relative roughness on Shields coefficient and logarithmic velocity equations will be reviewed to see if existing sizing techniques are valid. Second, the literature will be searched for existing riprap sizing methods based on velocity. Third, previous studies will be reviewed to determine the present knowledge regarding the effects of thickness, shape, and gradation on particle stability. Fourth, existing concepts of side slope particle stability will be reviewed and summarized.

2.1 APPLICABILITY OF EXISTING RIPRAP SIZING METHODS USING A CONSTANT SHIELDS COEFFICIENT OR THE LOGARITHMIC VELOCITY LAWS

One of the most common methods for evaluating riprap stability is the critical shear stress method (also called tractive force). The shear stress stability concept was used by Dubuat (1786) but did not become popular until Schoklitsch (1914). Lane (1953) used the tractive force method for stable canal design in noncohesive material. Anderson, Paintal, and Davenport (1968) developed the tractive force approach into a riprap design method which includes the effects of side slopes and

channel bends. The work of Anderson, Paintal, and Davenport is used as the basis for riprap design by the US Department of Transportation (1975). The Office, Chief of Engineers (OCE), (1970 and 1971) riprap design guidance is based on the tractive force approach. Li et al. (1976) and Stevens and Simons (1971) developed tractive force methods which incorporate probability and safety factors into the design method.

The shear stress exerted on the boundary in uniform flow is

$$\tau = \gamma_w DS \tag{2.1}$$

where

τ = tractive force imposed by flowing water[1]

γ_w = specific weight of water

D = flow depth

S = energy slope

or using hydraulic radius

$$\tau = \gamma_w RS \tag{2.2}$$

where R is the hydraulic radius.

The imposed force calculated from either Equation 2.1 or 2.2 is equated to the ability of the particle to resist movement or the critical shear stress. Using the analysis of Carter, Carlson, and Lane (1953), which is an equilibrium force analysis, yields

$$\tau_c = C_1 \left(\gamma_s - \gamma_w\right) d \tan \Phi \tag{2.3}$$

where

τ_c = critical tractive force for given particle size on bottom

---

[1] For convenience, symbols and unusual abbreviations are listed and defined in the Notation (Appendix A).

C_1 = coefficient

γ_s = specific weight of stone

d = particle size

Φ = angle of repose

Formulations of the shear relations from dimensional analysis depend on which parameters are considered significant. Vanoni (1977) uses the parameters T_c, $\gamma_s - \gamma_w$, d, the fluid density ρ, and viscosity ν, to define incipient motion. This results in the same form derived by Shields (1936) or

$$\frac{T_c}{(\gamma_s - \gamma_w)d} = f\left(\frac{U_* d}{\nu}\right) \qquad 2.4$$

where

U_* = shear velocity = $\sqrt{gDS}$

g = universal gravitational constant

For rough turbulent flow (particle Reynolds number $\frac{U_* d}{\nu} > 400$), the right side is often assumed constant and called the Shields number or Shields coefficient, herein denoted as C_c. Most of the stability investigations concerning Shields coefficient have been related to sediment transport. According to Graf (1971), the definition of the critical Shields coefficient has been subject to the interpretation of the researcher. The riprap design procedures by OCE (1970) and Anderson, Paintal, and Davenport (1968) use a constant Shields coefficient for safe design.

The use of a constant Shields coefficient has been questioned by Meyer-Peter and Muller (1948), Yalin (1965), Barr and Herbertson (1966), Blench (1966), Neill (1967 and 1968), Bogardi (1968), Ashida and Bayazit

(1973), Bathurst, Graf, and Cao (1982), Daido (1983), and Bettess (1984), who propose that Shields coefficients should vary with relative roughness. Bathurst, Graf, and Cao (1982) and Bettess (1984) have found this variation with relative roughness to be limited to high relative roughness below which Shields coefficient becomes constant. Meyer-Peter and Muller (1948) found that the limiting shear stress is proportional to particle diameter and relative roughness and proposed an equation

$$C_c = C_2 \left(\frac{d}{R}\right)^{1/9} \qquad 2.5$$

An explanation for a changing Shields coefficient with relative roughness has been offered by Escoffier (1968). At high relative roughness (low depth/d_{50}), turbulence generated at the boundary is hindered by the presence of the free surface. Consequently the fluctuations in velocity are decreased. At low relative roughness (large depth/d_{50}), the boundary-generated turbulence is not hindered by the free surface and fluctuations in velocity are not reduced. Since the magnitude of turbulent fluctuations is critical for riprap stability, this provides an explanation for the variation of Shields coefficient with relative roughness. Chen and Roberson (1974) and Bayazit (1976) found that measured turbulence intensity decreased with increase of relative roughness in the region near the wall. Bayazit (1982) proposed that this "can be explained by the fact that a substantial part of the energy of the mean flow is converted into turbulence in the separation zones between the roughness elements in the case of large scale roughness." Gessler (1971) stated that relative roughness does not influence Shields coefficient because incipient conditions depend only on conditions at the bed and not on the boundary layer thickness (or depth in open channels).

Some of the existing riprap procedures (OCE 1970 and Li et al. 1976) use the logarithmic velocity laws to determine the relation between velocity and shear stress on the boundary. The universal velocity distribution law for rough surfaces is

$$\frac{V_y}{U_*} = \frac{2.3}{\kappa} \log \frac{30(y + y_o)}{K_s} \qquad 2.6$$

where

V_y = local velocity at distance y

κ = von Karman coefficient

y = distance above origin

y_o = distance below top of roughness element to origin of profile

K_s = equivalent sand grain roughness

Equation 2.6 is integrated over the depth to determine the mean velocity relations (Keulegan 1938). For wide channels, with essentially two-dimensional flow, the mean velocity relation is

$$\frac{V}{U_*} = \frac{2.3}{\kappa} \log \frac{11.1D}{K_s} \qquad 2.7$$

where V is the average flow velocity.

Several difficulties arise in application of the logarithmic velocity laws to rough surfaces.

1. Origin for Velocity Profile. Several investigators, including Einstein and El-Samni (1949), O'Loughlin and McDonald (1964), Knight and McDonald (1979), Bayazit (1982), and Coleman, Hodge, and Taylor (1984), have shown that the velocity profile origin for rough surfaces lies below the tops of the roughness elements. There is no general agreement as to the location of the origin. The relation between velocity and tractive force is

sensitive to the origin location, particularly at high relative roughness.

2. K_s Value. Previous studies have used K_s values ranging from d_{50} (OCE 1970) to $3.5d_{84}$ (Hey 1979). Particle sizes d_{50}, d_{84}, etc., refer to the size of which a given percentage is finer by weight. Kamphius (1974) found $K_s = 2d_{90}$ for depth/$d_{90} > 10$. Van Rijn (1982) determined an average value of $K_s = 3d_{90}$.

3. Effects of Relative Roughness. Yalin (1977) has shown that Equation 2.6 is not valid at relative depth D/d_{90} less than approximately 10 because K_s/d_{90} varies below $D/d_{90} = 10$. Other investigators have also suggested limiting application of the logarithmic velocity equations to small scale roughness. Bathurst, Graf, and Cao (1982) give $D/d_{84} > 6$ for small-scale roughness. Van Rijn (1982) places the strictest requirement by limiting application of the logarithmic velocity laws to $D/K_s > 10$. Van Rijn (1982) found $K_s = 3d_{90}$ which implies a limitation $D/d_{90} > 30$ on the logarithmic laws.

4. Von Karman κ. There has been considerable disagreement over the von Karman κ and its constancy in clear versus sediment-laden flow. Coleman (1981) found that by evaluating κ in the lower 15 percent of the flow, κ was the commonly used 0.4 for clear or sediment-laden flow. However for high relative roughness $D/d = 4.0$ and 8.5, Bayazit (1982) found $\kappa < 0.4$ for clear water flow in the region near the bed. Uram (1981) found von Karman's κ both higher and lower than 0.4 depending on the nature of the roughness.

Summarizing, other investigators have suggested that a constant Shields coefficient and the logarithmic velocity laws should not be used for problems involving high relative roughness.

2.2 EXISTING CRITICAL VELOCITY METHODS FOR PARTICLE STABILITY

Some of the earliest stability relations used particle size or weight as a function of velocity. Graf (1971) presented the general relation

$$\frac{V_b^2}{\left(\frac{\rho_s}{\rho} - 1\right) gd} = \frac{2K_3 \ (\tan \Phi \cos \alpha - \sin \alpha)}{C_d \ K_1 + C_\ell \ K_2 \tan \Phi} \qquad 2.8$$

where

V_b = bottom velocity

ρ_s = stone density

K_1, K_2, K_3 = coefficients

α = bottom angle with horizontal in flow direction

C_d = drag coefficient

C_ℓ = lift coefficient

Graf referred to the right side of Equation 2.8 as the sediment coefficient which varies with particle characteristics (shape, size, uniformity, texture, repose angle) and flow characteristics.

Forchheimer (1914) reported that as early as 1753, A. Brahms presented the relation

$$V_b = C_3 \ W^{1/6} \qquad 2.9$$

where W is the unsubmerged stone weight. Equation 2.9 is a simple form of Equation 2.8. Isbash (1935) related stone size for dam closures to a bottom velocity called the "velocity against the stone."

Equation 2.8 is the form used by Isbash and serves as the basis for Hydraulic Design Criteria (HDC) Sheet 712-1 (US Army Corps of Engineers). Average velocity is used in HDC 712-1 instead of bottom velocity, which may cause these curves to be rather conservative for low turbulence flows. The National Crushed Stone Association (1978) presents guidance for sizing riprap based on average velocity. The California Division of Highways (1970) uses a design equation having the same form as Equation 2.8.

Blodgett and McConaughy (1986) proposed the following relation for stable rock size based on extensive prototype data

$$d_{50} = 0.01\ V_a^{2.44} \qquad 2.10$$

where V_a is the cross-section average channel velocity. Adjustments for bank angle, unit stone weight, channel shape, etc., are not used in this design procedure.

Critical velocity relations using average velocity and depth are also used for particle stability. They have been rewritten in a common form to assist in their comparison. Straub (1953) presented the average velocity and depth relation

$$\frac{d}{D} = 0.31 \left[\left(\frac{\gamma_w}{\gamma_s - \gamma_w} \right)^{1/2} \frac{V}{\sqrt{gD}} \right]^3 \qquad 2.11$$

Neill (1967) used dimensional analysis to determine the pertinent relationships for stability of coarse, uniform bed material and conducted scour tests using the incipient criterion of first movement by visual observation. His conservative design curve is represented by the equation

$$\frac{d}{D} = 0.32 \left[\left(\frac{\gamma_w}{\gamma_s - \gamma_w} \right)^{1/2} \frac{V}{\sqrt{gD}} \right]^{2.5} \qquad 2.12$$

Neill and Van Der Giessen (1966) suggested that relative roughness, which results from the dimensional analysis, is connected with the intensity of turbulent fluctuation. Neill (1968) stated that because the flume size and test section area were constant, the first movement criterion was more severe for the smaller particles and Equation 2.12 may not be valid. Because the test section contained smaller particles, and therefore more particles, a greater probability of movement exists. Neill (1968) also stated that the equation is applicable to problems such as riprap stability. Bogardi (1968) presented particle stability data covering a wide range of d/D and determined the relation

$$\frac{d}{D} = 0.26 \left[\left(\frac{\gamma_w}{\gamma_s - \gamma_w} \right)^{1/2} \frac{V}{\sqrt{gD}} \right]^{2.47} \qquad 2.13$$

which is almost identical to Neill (1967). Cooper (1970) analyzed sediment transport data for low rates of transport (concentration = 1 part per million) and found good agreement with Neill's (1967) relation. Grace, Calhoun, and Brown (1973), Maynord (1978), and Reese (1984) used the riprap stability relation

$$\frac{d_{50}}{D} = C_4 \left[\left(\frac{\gamma_w}{\gamma_s - \gamma_w} \right)^{1/2} \frac{V}{\sqrt{gD}} \right]^{3} \qquad 2.14$$

which is identical to Straub (1953).

Combining and rearranging Equations 2.4 and 2.7 results in the OCE (1970) procedure for riprap design using average velocity and depth:

$$d_{50} = \frac{\gamma_w V^2}{C_c \left(\gamma_s - \gamma_w\right) \left(32.6 \log \frac{11.1D}{d_{50}}\right)^2} \qquad 2.15$$

With the appropriate coefficients, Equations 2.14 and 2.15 give similar results over a wide range of d/D. Reese (1984) demonstrated that these two relations differ only by the velocity profile used. Equation 2.14 is based on a power velocity profile while Equation 2.15 is based on a logarithmic velocity profile.

Determining which velocity to use is an important step in developing a riprap sizing method based on velocity. Some form of bottom velocity is the most representative because it is closest to the bed. However bottom velocities are difficult to predict and measure (Bogardi 1978) because the velocity near the bottom varies rapidly with distance from the bed. Surface velocities are easy to measure but difficult to predict and are not representative because they are far removed from the bed. Bogardi (1978) recommended the use of mean velocity in critical velocity relations. Mean velocity is the easiest to calculate using both numerical and physical modeling techniques.

2.3 PREVIOUS STUDIES ON THE EFFECTS OF GRADATION, THICKNESS, AND SHAPE ON RIPRAP STABILITY

The effects of gradation on particle stability or resistance are generally accounted for by determining a characteristic size which represents any gradation. In the case of resistance, the larger size fractions are generally used for the characteristic size (van Rijn 1982, Bayazit 1982). In the case of stability, the characteristic size is found to vary. Einstein (1942) found d_{35} to be the effective size for movement of sand mixtures. Schoklitsch (1962) used d_{40} in stability

relations. The California Division of Highways (1970) used W_{33} in the riprap sizing relation. Peterka (1958) used d_{40} in the riprap sizing relation for placement downstream of stilling basins. Shen and Lu (1983) found d_{30} to be the characteristic size of nonuniform surface material on an armored bed. Shen and Lu suggested that increased turbulence caused by the larger particles decreases the stability of nonuniform materials. Anderson, Paintal, and Davenport (1968) conducted flume tests showing that nonuniform ripraps are less stable than uniform ripraps having the same average size. These results show that the characteristic size is less than the average size. Maynord compared the stability of various riprap gradations and found that d_{50} was the characteristic size for riprap placed to a thickness of $1d_{100}$. However, these tests differed from prototype placement of riprap because the careful placement techniques used in the model prevented segregation of sizes with the nonuniform ripraps. Many riprap sizing relations have used d_{50} as the characteristic size (OCE 1970, Anderson, Paintal, and Davenport 1968, US Department of Transportation 1975, Blodgett and McConaughy 1986).

Standardized riprap gradations have been used by OCE (1971), California Division of Highways (1970), and the US Army Engineer Division, Lower Mississippi Valley (1982). Simons and Senturk (1977) and the US Department of Transportation (1975) present a single curve defining riprap gradation.

Studies were not found on the effects of varying blanket thickness on riprap stability. Present OCE (1971) guidance requires a thickness of $1d_{100}$ (maximum) or $1.5d_{50}$ (maximum), whichever is larger, for placement in the dry.

Shape effects on riprap stability are important in determining which shapes are acceptable. Neill (1968) compared the stability of spheres and "irregular grains" and found no significant difference if the equivalent spherical diameter (volume basis) was adopted as the size of the irregular grains. Olivier (1967) conducted tests on overflow rock dams and found that rounded stone had to be approximately 15 percent larger than crushed stone for equivalent stability. This was attributed to surface smoothness, not shape. Present OCE (1970) guidance for riprap shape is as follows:

1. Stone predominantly angular
2. No more than 25 percent of stones having a stone length ℓ to stone thickness b ratio of > 2.5
3. No stone having $\ell/b > 3.0$

2.4 EFFECTS OF SIDE SLOPE ON PARTICLE STABILITY

Since most riprap is placed on channel banks, the influence of side slope angle on riprap stability is important. Carter, Carlson, and Lane (1953) presented the effects of side slopes on particle stability by defining forces parallel and normal to the angle of repose of the material. The equilibrium condition given by Carter, Carlson, and Lane is

$$\tan \Phi = \frac{\sqrt{W_s^2 \sin^2 \Theta + a^2 \tau_s^2}}{W_s \cos \Theta} \qquad 2.16$$

where

W_s = submerged weight of stone

Θ = angle of side slope with horizontal

a = effective area of particle

T_s = critical tractive force for particle on side slope

Carter, Carlson, and Lane defined the tractive force ratio K as the ratio of force on sloping side to that on level surface necessary to cause impending motion

$$K = \frac{T_s}{T_c} = \cos \Theta \sqrt{1 - \frac{\tan^2 \Theta}{\tan^2 \Phi}} = \sqrt{1 - \frac{\sin^2 \Theta}{\sin^2 \Phi}} \qquad 2.17$$

Equation 2.17 is used in many riprap design procedures including Anderson, Paintal, and Davenport (1968), US Department of Transportation (1975), and OCE (1970, 1971).

An alternate formulation by Graf (1971) includes lift force F_L and the angle of inclination of the drag force or shear stress as a result of secondary motion β, which is especially pronounced in channel bends. The equilibrium condition is alternately written

$$\tan \Phi = \frac{\sqrt{W_s^2 \sin^2 \Theta + 2aT_s W_s \sin \Theta \sin \beta + a^2 T_s^2}}{W_s \cos \Theta - F_L} \qquad 2.18$$

Lack of information on the angle β has prevented evaluation of this form of the side slope stability analysis. Christensen (1972) developed a side slope stability analysis which included lift and showed that the relation given by Equation 2.17 is not conservative. Stevens and Simons (1971) determined the stability of coarse particles on a side slope based on equilibrium of moments instead of forces. Relative safety factors can be determined with this method and the authors concluded that the Carter, Carlson, and Lane (1953) method yields larger sizes than required by the Stevens and Simons method.

No investigations were found that test these side slope equations for open channel flow. There have been tests in the wave environment that test the applicability of the Hudson (1958) equation, which follows:

$$W = \frac{\gamma_s H^3}{K_D \left(\frac{\gamma_s}{\gamma_w} - 1 \right)^3 \cot \theta} \qquad 2.19$$

where

H = wave height

K_D = stability coefficient

Since wave forces act up and down the side slope, the effects of side slope angle are expected to be more severe than that in open channel flow where forces act along the slope. Comparing 1V:1.5H and 1V:3H side slopes in Hudson's equation gives the wave effect:

$$\frac{d\ (1V:1.5H)}{d\ (1V:3H)} = 1.26$$

Using the open channel Equation 2.17 with ϕ = 40 deg[2] (OCE 1970) gives the velocity effect:

$$\frac{d\ (1V:1.5H)}{d\ (1V:3H)} = 1.71$$

This comparison suggests that the tractive force relation (which has not been tested against stability data) overestimates the effects of side slope angle on stability.

2.5 SUMMARY

Several investigators have proposed that Shields coefficient should

---

[2] A table of factors for converting non-SI units of measurement to SI (metric) units is found on page iii.

vary with relative roughness. Many of the existing riprap design techniques use a constant Shields coefficient.

Past studies have shown that the logarithmic velocity laws should be limited to small-scale roughness. Present riprap guidance does not place any limitations on use of these laws. Other factors, including determining the correct values of K_s, κ, and the profile origin, compound the difficulty in using these laws for surfaces having high relative roughness.

Several different velocity-based riprap sizing methods have been developed. Average velocity is recommended for use in these equations.

Previous studies on gradation effects on the stability of riprap have used a characteristic size ranging from d_{30} to d_{50}. No studies were found addressing the effects of riprap thickness on stability.

Side slope stability equations have used equilibrium of both forces and moments. Information was not found in which these equations were tested against stability data. Comparison of the side slope equations for open channel flow with equations tested against wave data suggests that the existing side slope relations for open channel flow overestimate the effects of side slope angle.

CHAPTER 3

EXPERIMENTAL INVESTIGATION

Experimental studies were conducted to determine the stability and resistance to flow of riprap having gradation, thickness, and shape similar to riprap used in the prototype installations. This chapter describes facilities, model riprap, failure criteria, test procedures and data collection, and data restrictions. Additional information on the Colorado State University (CSU) studies can be found in Fiuzat, Chen, and Simons (1982), Fiuzat and Richardson (1983), Ruff et al. (1985), and Ruff et al. (1987).

3.1 TEST FACILITIES

One flume at CSU, Fort Collins, Colorado, and three flumes at the US Army Engineer Waterways Experiment Station (WES), Vicksburg, Mississippi, were used to conduct the riprap tests. The CSU flume is 200 ft long by 8 ft wide by 4 ft deep and can be tilted from 0 to 2 percent bottom slope. Maximum discharge is 100 cfs. The sides and bottom of the flume are made primarily of aluminum. A portion of the side of the flume is made of Plexiglas to allow observation of the test section. Two gates installed at the downstream end of the flume allow control of the water level in the flume under subcritical flow conditions. A motorized carriage can travel along the flume for carrying data collection instruments and photographic equipment. A schematic diagram of the flume and the test section is shown in Figure 3.1. The initial 100 ft

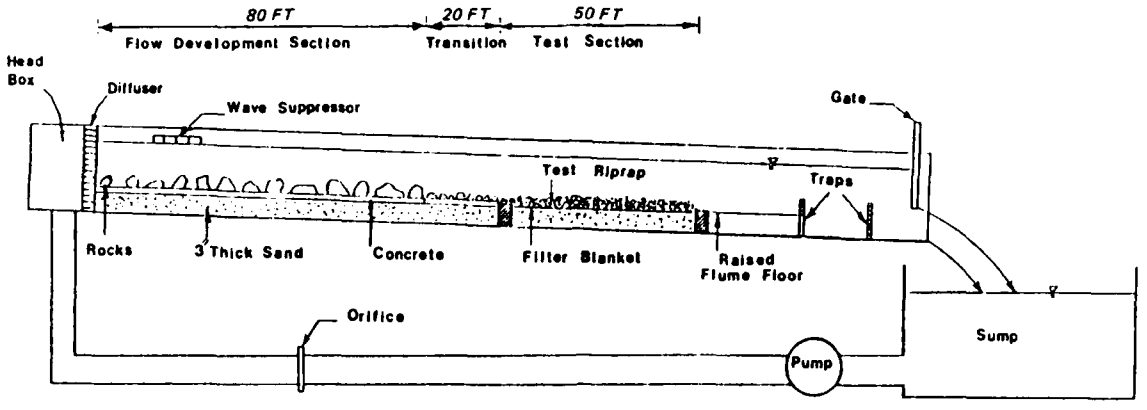

Figure 3.1. CSU tilting flume

of the flume was used for flow development and transition into the test section.

The CSU tests consisted of four phases. Phases I-III addressed stability of bottom riprap having varying gradation, thickness, and shape. The Phase IV tests addressed stability of side slope riprap. In Phase I and II test series, large 6- to 10-in. rocks cemented to the flume floor between stations 0 and 80 produced a fully developed hydraulically rough boundary flow at the beginning of the 20-ft transition. Rock similar in size to that in the test section was placed in the 20-ft transition to eliminate the abrupt change in roughness between the flow development section and the test section. In the Phase III test series, the large 6- to 10-in. rocks were placed in the initial 60-70 ft of the flume. A 40-ft-long transition was used in the Phase III tests. The test section varied from 40 to 50 ft in length for Phases I-III. Details of the Phase IV test facility, in which a 1V:2H side slope was tested, are shown in Figure 3.2.

The WES trapezoidal channel model is described in Maynord (1978). This facility had a 5-ft bottom width with 1V:2H, 1V:3H, and 1V:4H side slopes. Discharge capacity was 35 cfs, and a constant bottom slope of

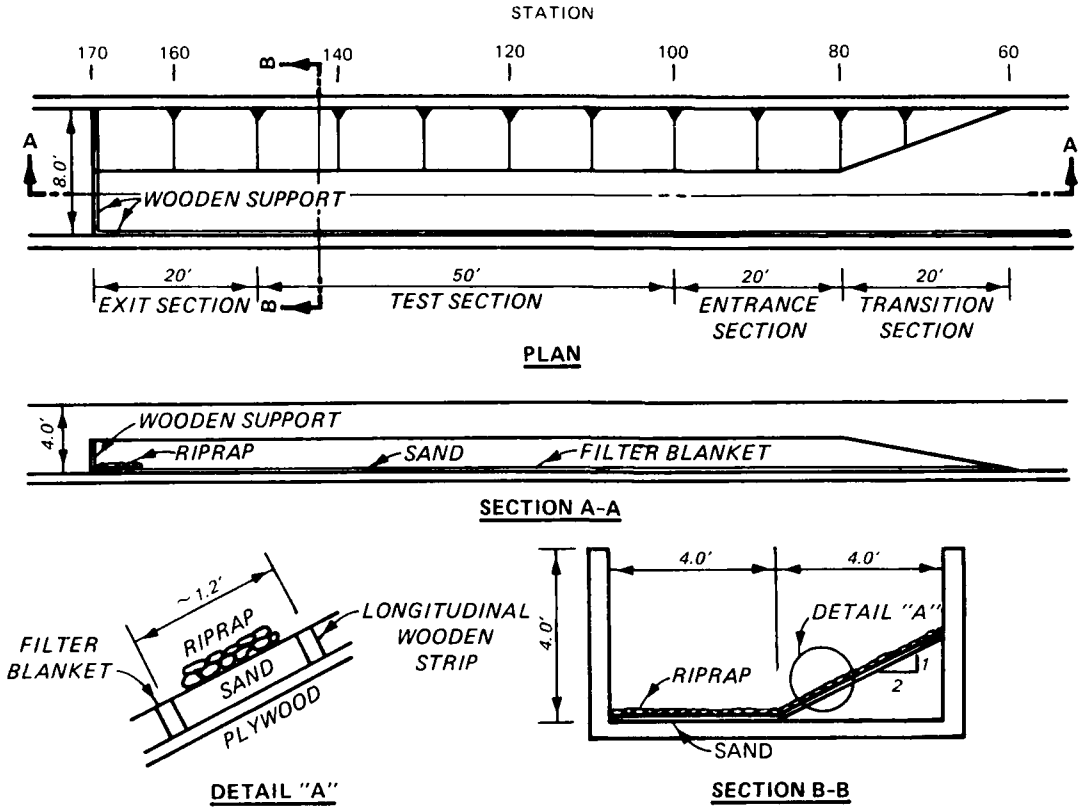

Figure 3.2. CSU Phase IV side slope test flume

0.008 ft/ft was used in all tests. A tailgate was used to control depth of flow.

The WES tilting flume is 3 ft wide by 1 ft deep by 75 ft long. Maximum discharge is 5.6 cfs. Bottom slope can be varied from 0 to 2.2 percent, and a tailgate at the downstream end of the model is used to control depth of flow for subcritical flows. Steel rails set to grade are used to support instrumentation devices.

The WES curved channel model is shown in Figure 3.3. This trapezoidal channel has two 100-deg bends with a centerline radius of 22 ft. The bends are separated by a 15-ft straight reach, and the straight reach on each end of the channel is 25 ft in length. The bottom width is 7.0 ft, and side slopes are 1V:2H. The bottom slope is 0.0025 ft/ft, and the discharge varies up to 15 cfs.

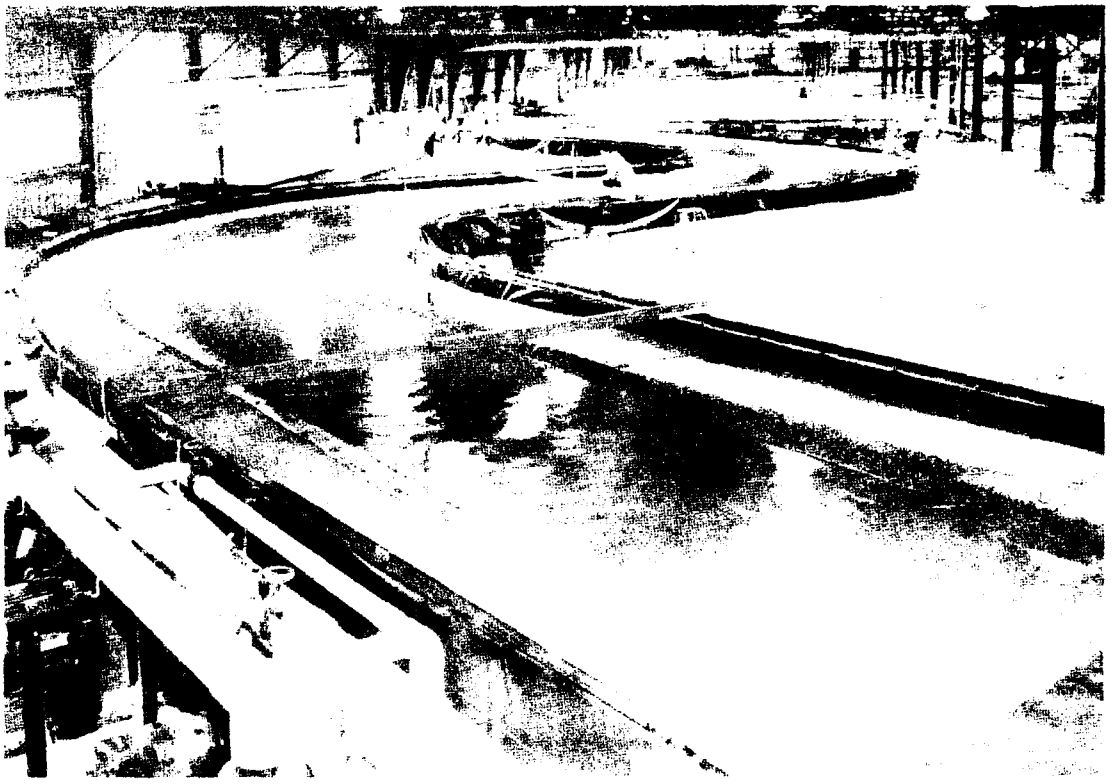

Figure 3.3. WES curved channel model

3.2 MODEL RIPRAP

The characteristics of the model riprap used in these investigations are given in Table 3.1. Gradations for the CSU flume are shown in Figures 3.4-3.7.

All model riprap was crushed rock. Shape characteristics of the model riprap are shown in Table 3.2.

3.3 FAILURE CRITERIA

At the outset of these experimental studies, an acceptable failure criterion had to be determined. The selected failure criterion must be able to be used to determine riprap stability for a range of riprap gradation and blanket thicknesses. Most sediment transport studies using uniform materials have weighed the transported material for various flow rates and extrapolated the transport rate to zero to determine what is

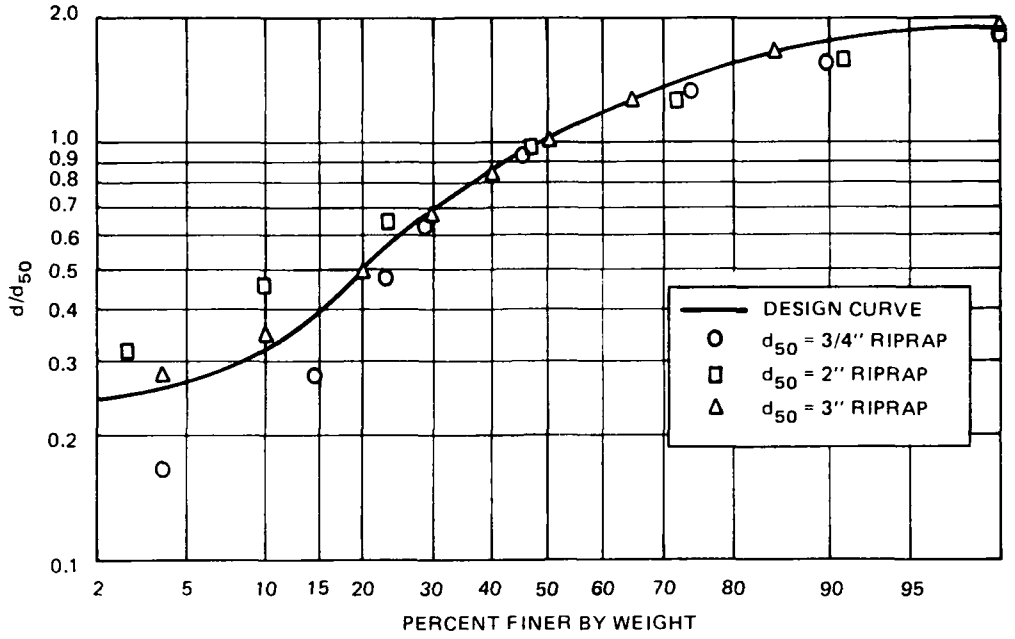

Figure 3.4. Size distribution for CSU Phase I

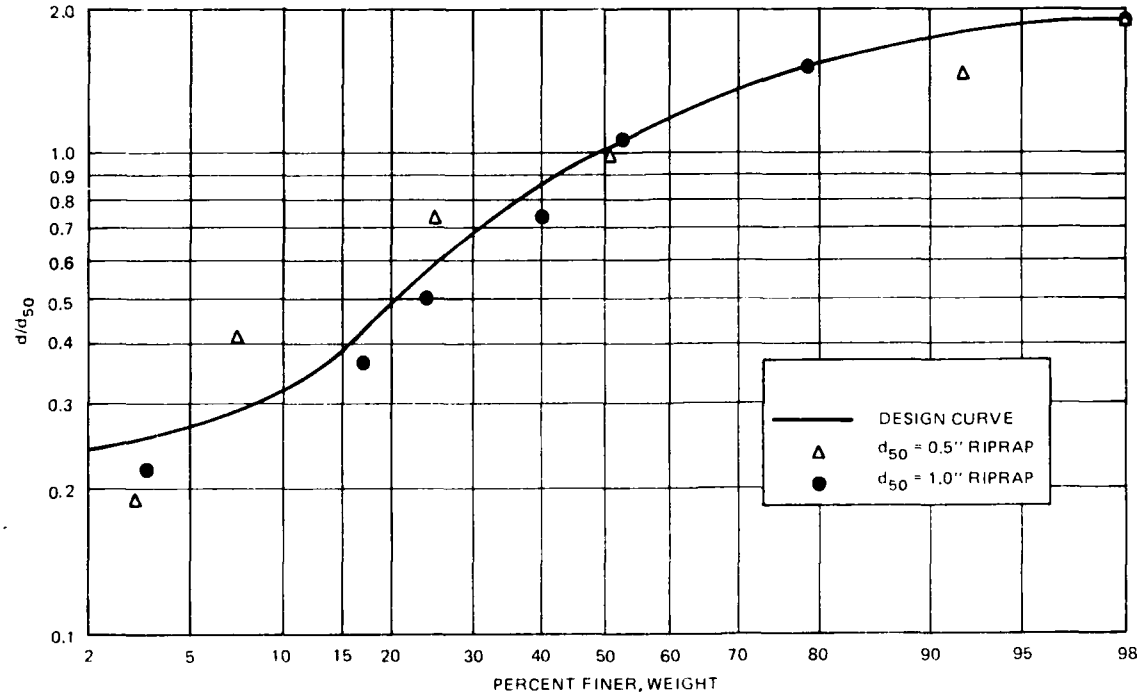

Figure 3.5. Size distribution for CSU Phase II

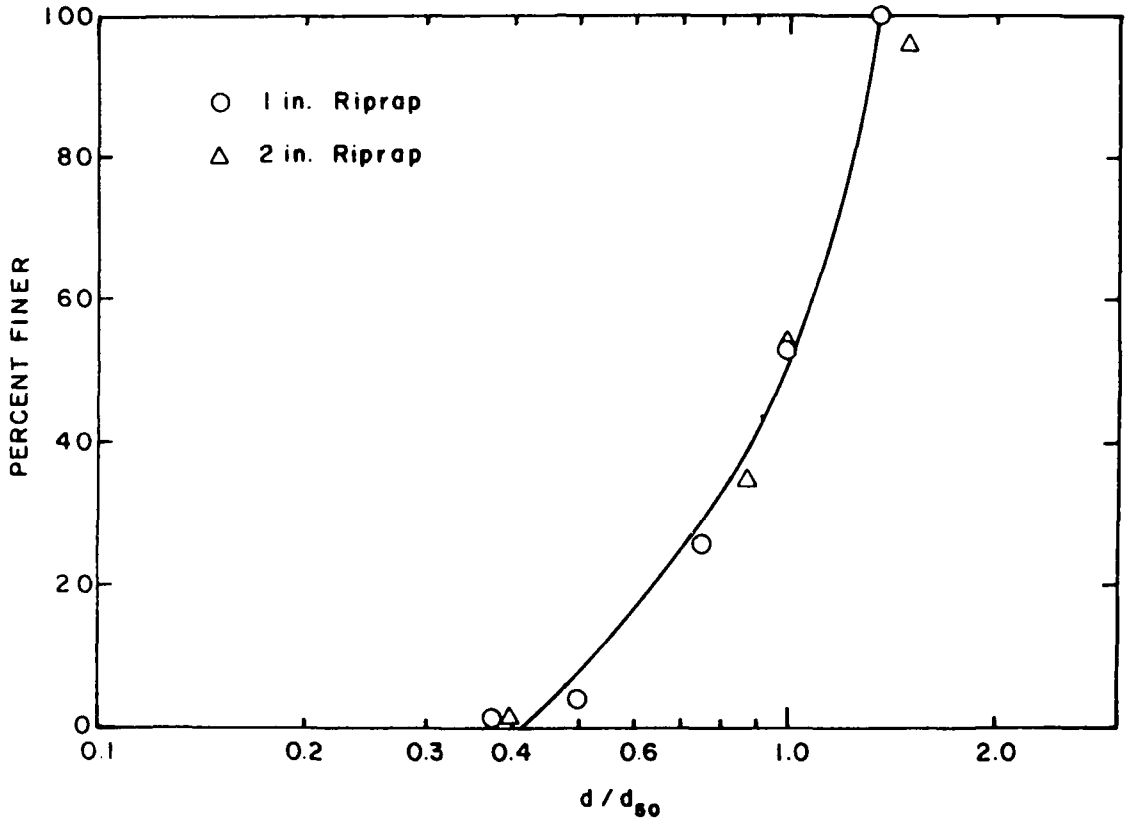

Figure 3.6. Size distribution for CSU Phase III

termed "incipient motion." Applying this technique to different riprap blanket thicknesses would probably yield little variation with thickness. Applying this technique to nonuniform ripraps would give biased results because some of the finer material in nonuniform ripraps will be moved without ultimate failure of the riprap revetment.

Another existing failure criterion is the technique used by Neill (1967), which was a visual observation of first movement. This technique would be successful for uniform materials but unsuccessful for nonuniform (graded) ripraps of varying thickness. The idea of painting rocks in the test section was rejected because it would yield no information about the effects of thickness for nonuniform ripraps.

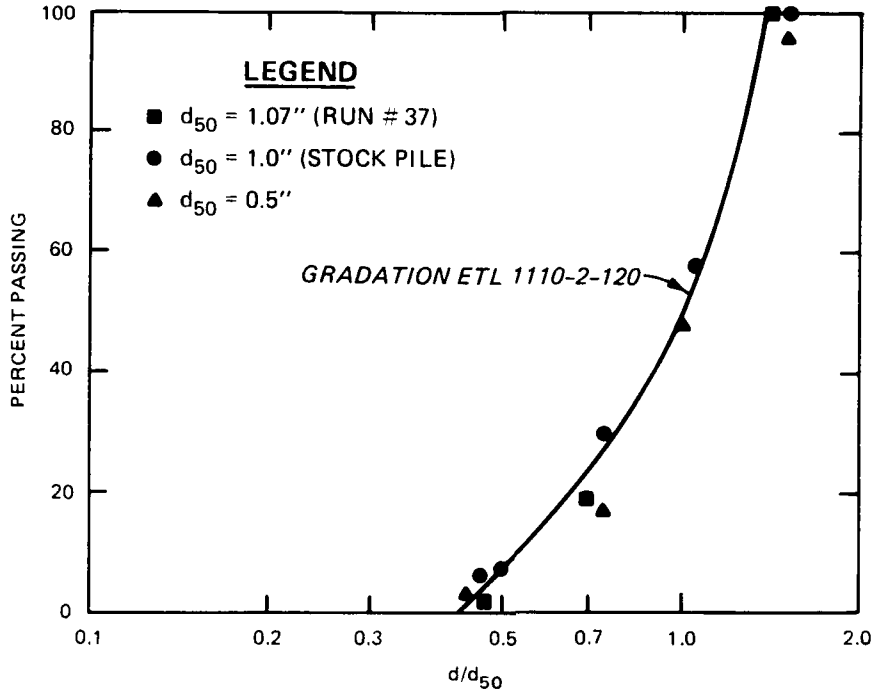

Figure 3.7. Size distribution for CSU Phase IV

An important consideration in riprap stability is that the underlying material should not be exposed to the forces of the flowing water. It is not important if some of the finer material resting on the surface of a nonuniform riprap is washed away. Another factor which must be considered with riprap stability is size segregation during placement. The selected failure criterion must be able to address the effects of size segregation when using nonuniform materials.

To meet these requirements, the concept of incipient failure is used in this investigation to define the flow conditions at which any portion of the underlying material has been exposed. Use of this failure criterion allows determination of the stability of various

gradations and thicknesses. It is the only failure criterion which was considered to address the effects of size segregation. The incipient failure criterion is not the same as the incipient motion criterion used in sediment transport studies. Incipient failure defined the flow conditions which lead to failure of the riprap blanket. Incipient motion defines the flow conditions at which the rate of particle movement approaches zero. Incipient motion could not be used in this study because it would not allow determination of the effects of riprap gradation or thickness.

3.4 TEST PROCEDURE AND DATA COLLECTION

In the CSU and WES trapezoidal channel tests, a fabric was used to separate the riprap from the bed of underlying sand. In the WES tilting flume tests, the fabric was placed directly on the flume floor. While the riprap was being placed, the riprap surface was not tamped or packed to best simulate prototype placement. The flow conditions at which the rock would fail were estimated using existing riprap sizing techniques. The initial test began with low flow rates and slopes well below the estimated failure condition. The riprap was tested for 2 hours, after which the test section was examined for any exposed areas of the underlying fabric. If no exposure of the fabric occurred, the flow rates or slope was increased and the 2-hour test repeated. This process was repeated until the fabric was exposed. After the test section was repaired, the previous stable slope was run for 4-8 hours to ensure stability of the riprap. In case of failure, the slope and/or discharge was further reduced and another 4- to 8-hour run was conducted until stable conditions were found. The WES tilting flume tests differed in

that near the point of failure, all runs used in the analysis were 4- to 8-hour runs.

In the CSU and WES tilting flume studies, uniform flow was maintained by adjusting the tailgate at the downstream end of the flume for subcritical flows. The WES trapezoidal channel tests had a mild, gradually varied flow regime because of the lack of slope variability. Flow uniformity in the WES curved channel model was maintained by keeping the same depth at the upstream and downstream ends of the model.

During the tests at both CSU and WES, discharges were measured by calibrated venturi and orifice meters, velocity was determined with pitot tubes and propeller meters, and depths were measured with point gages.

In the CSU tests, a "general datum" for each rock thickness was established by the following procedures:

1. The flume was set to the horizontal position.
2. Water was added to the flume until about 90 percent of the rocks were covered with water.
3. The elevation of the water surface was measured at the locations where flow depths were measured.
4. These elevations were considered as the elevations of the bottom of channel (general datum) in measuring the flow depth.

In the WES tests, the datum was set by placing a flat plate of known thickness on top of the riprap surface to establish the datum.

3.5 DATA RESTRICTIONS

Two areas of concern generally surface in the course of any flume investigation. First, flow conditions must be turbulent to ensure that viscous forces are insignificant in the flume just as they are in the

prototype. To ensure rough turbulent flow, the following restrictions were placed on the data to be used in the analysis:

1. $\frac{U_* d_{50}}{\nu} > 400$ (Graf 1971)

2. $\frac{V d_{50}}{\nu} > 2.5(10)^3$ (O'Loughlin et al. 1970)

The second area of concern in flume studies is how to handle the effects of the sidewalls. Previous sediment transport studies have frequently used the sidewall correction procedure given in Vanoni (1977). This sidewall correction procedure results in the average bed shear stress. This method takes the central region of the flume (where the flow is essentially two-dimensional) and the two side regions (where the shear stress and velocities are reduced) and determines a weighted average. In this type of study, the riprap generally fails and velocities are measured in the central region of the flume. What is needed is not the weighted average but the values of shear stress and velocity in the central portion of the flume. The velocities pose no difficulty because they are measured in the central portion of the flume, but shear stress needs to be calculated. If the central portion of the flume is sufficiently wide, then the shear stress is best approximated by $\gamma_w DS$. To ensure that the central region is wide enough, Neill (1967) and van Rijn (1982) required that the ratio of flume bottom width B to depth (aspect ratio) be equal to or greater than 5. As part of this study, the limiting aspect ratio was evaluated with velocity measurements taken in a straight, riprapped bottom, smooth sidewall flume. Detailed velocity measurements were taken at aspect ratios of 4.0, 4.9, and 7.3 (Figure 3.8). The tests with aspect ratios of 4.9 and 7.3 show a

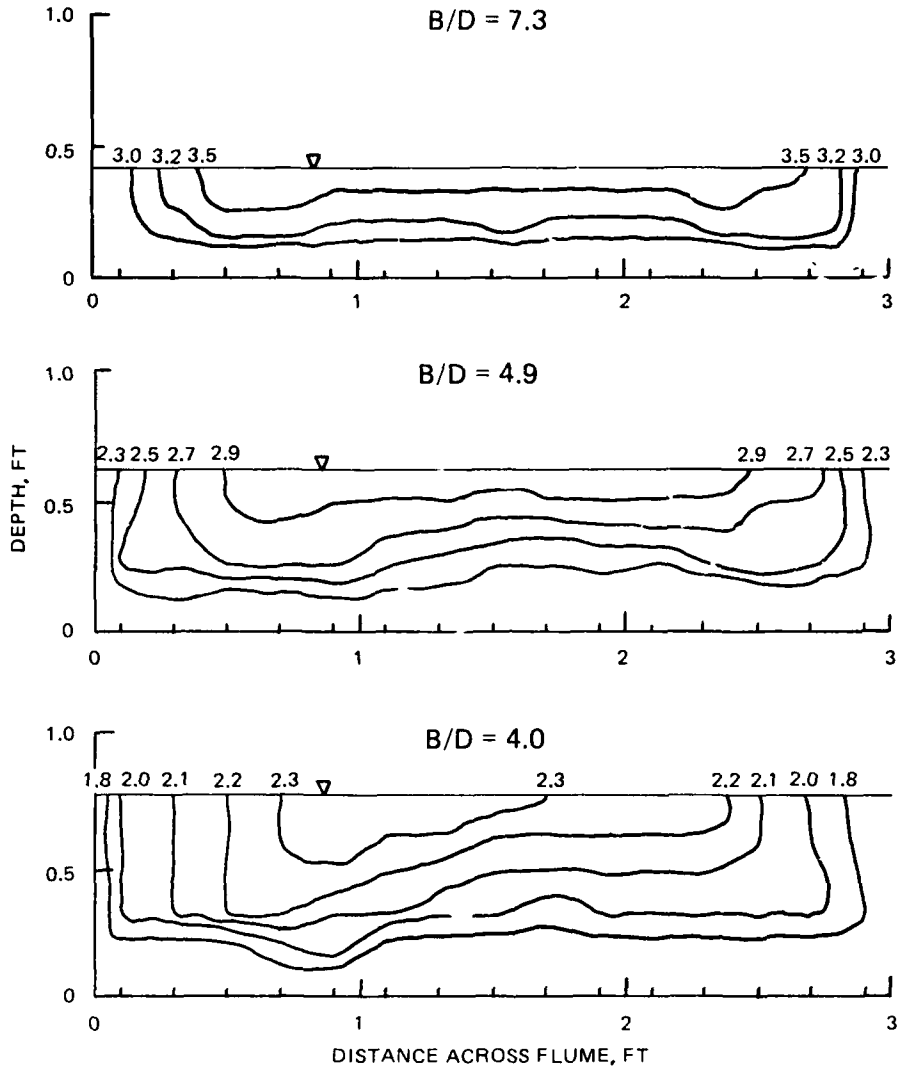

Figure 3.8. Velocity measurements used to evaluate sidewall effects relatively wide center section of essentially two-dimensional flow. The test at an aspect ratio of 4.0 not only shows significant sidewall effects extending out into the flume, but an imbalance of flow across the cross section. All data used in this investigation will have an aspect ratio ≥ 5. This restriction on aspect ratio addresses two other concerns relative to the CSU tests:

1. The CSU tests were generally conducted with sequential discharges of 25, 50, 75, and 100 cfs. By the time the 75- and 100-cfs tests were conducted, the riprap in the flume was "well-seasoned." Any weak spots had already failed and had been repaired. The tests conducted at these higher discharges generally did not meet the width/depth ≥ 5 restriction.
2. At the deeper depths, slopes were mild at the point of failure of the riprap. Only three depths were measured along the test section for each test, which made it difficult either to assume that the bottom slope equaled the energy slope or to compute the energy slope. At mild slopes, errors in determining energy slope can be large. At steeper slopes, the bottom slope dominates the energy slope and errors due to a limited number of depth measurements are small. This factor was probably significant only for the smaller ripraps.

Fortunately, data meeting the width/depth ≥ 5 requirement are sufficient to define riprap stability for the majority of problems.

CHAPTER 4

ANALYSIS AND RESULTS

4.1 APPLICABILITY OF EXISTING SIZING RELATIONS USING A CONSTANT SHIELDS COEFFICIENT OR LOGARITHMIC VELOCITY LAWS

The review of previous work presented in Chapter 2 indicates that numerous investigations have proposed that Shields coefficient should vary with relative roughness. Experimental results from the WES and CSU tilting flumes were used to evaluate Shields coefficient as a function of relative roughness. Results from the WES trapezoidal channel were not used because the test section was not long enough to accurately measure the water-surface slope so that shear stress could be computed. Only those data sets covering a large range of D/d and having the same thickness, gradation, and shape were used in this analysis. Shields coefficients computed for the four data sets meeting these requirements are shown in Figures 4.1-4.4. The data used in Figures 4.1-4.4 are listed in Tables 4.1-4.7. Shields coefficient is computed using a combination of Equations 2.1 and 2.4 or

$$C_c = \frac{\gamma_w DS}{(\gamma_s - \gamma_w) d_{50}} \qquad 4.1$$

and only data meeting the limitations in Chapter 3 are used in the analysis. In a comparison of these results to the Shields (1936) work, the difference in stability criteria must be considered. The Shields (1936) investigation measured low rates of transport and extrapolated these values to a zero rate of transport to obtain incipient conditions.

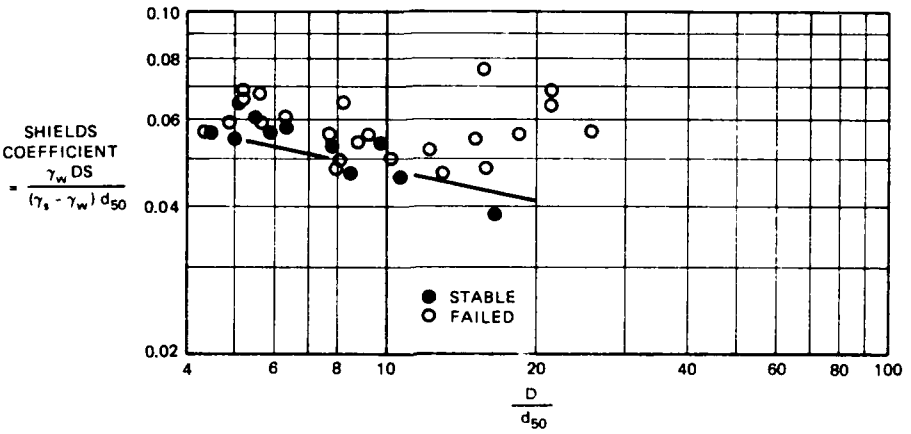

Figure 4.1. Shields' coefficient versus D/d_{50} , thickness = $1d_{100}$, $d_{85}/d_{15} = 1.35$ (data from Table 4.1)

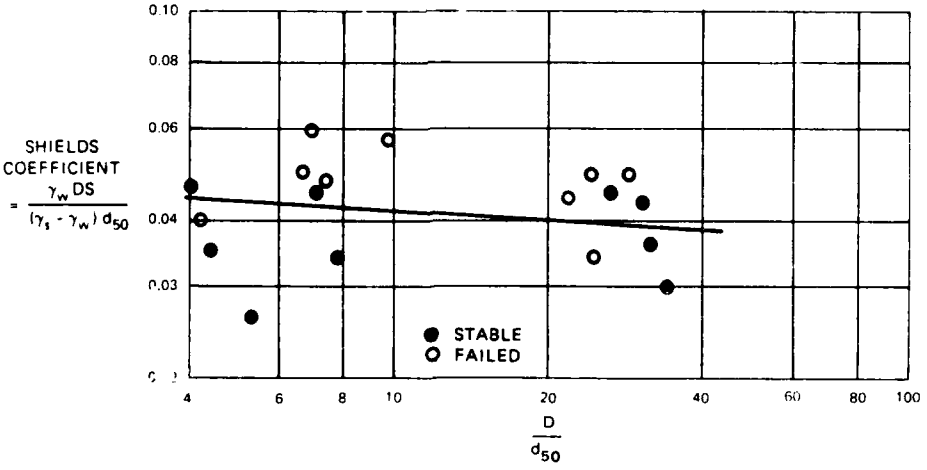

Figure 4.2. Shields' coefficient versus D/d_{50} , thickness = $1d_{100}$, $d_{85}/d_{15} = 2.8$ and 2.5 (data from Tables 4.2 and 4.3)

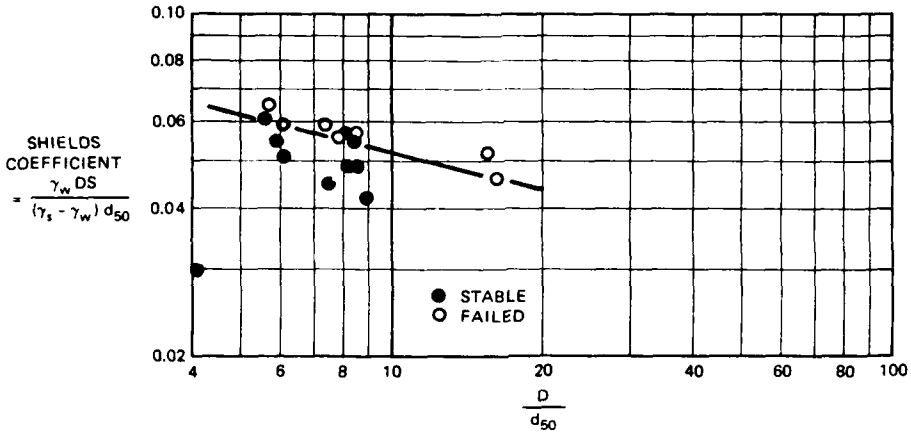

Figure 4.3. Shields' coefficient versus D/d_{50}, thickness = $1.4d_{100}$, d_{85}/d_{15} = 2.1 and 2.3 (data from Tables 4.4 and 4.5)

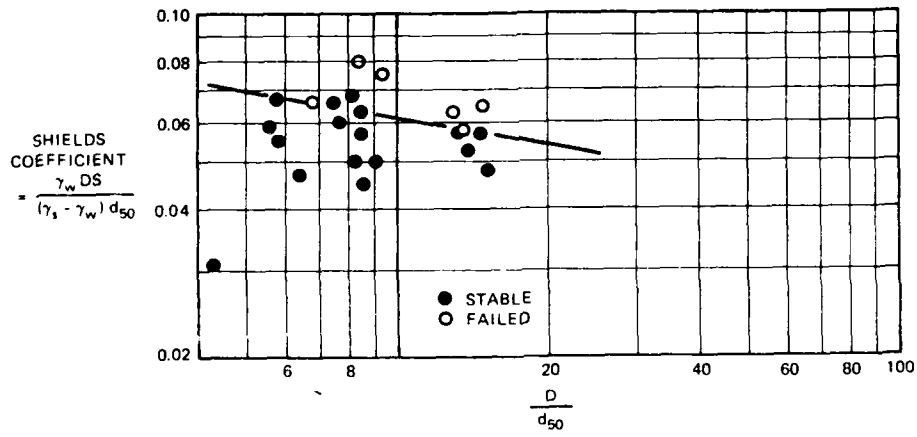

Figure 4.4. Shields' coefficient versus D/d_{50}, thickness = $2.1d_{100}$, d_{85}/d_{15} = 2.1 and 2.3 (data from Tables 4.6 and 4.7)

This investigation used the incipient failure stability criterion given in paragraph 3.3. The best-fit lines on Figures 4.1-4.4 are drawn to separate failure runs from stable runs and are not the result of regression techniques. Three of the four data sets (Figures 4.1, 4.3, and 4.4) show a significant increase in Shields coefficient with a decrease in D/d_{50}. This is the same variation proposed by several investigators cited in Chapter 2. Over the range of D/d_{50} tested, there was no indication that Shields coefficient approached a constant value as proposed by Bathurst, Graf, and Cao (1982) and Bettess (1984). The average of the best-fit lines shown in Figures 4.1, 4.3, and 4.4 show that Shields coefficient should vary according to

$$C_c = C_5 \left(\frac{d_{50}}{D} \right)^{1/5} \qquad 4.2$$

which can be compared to Meyer-Peter and Muller (1948) results given in Equation 2.5.

Logarithmic velocity relations are used in riprap design to relate velocity to shear stress. Several references cited in Chapter 2 show that the logarithmic velocity relations are not applicable to high relative roughness and should be limited to small-scale roughness. The mean velocity logarithmic Equation 2.7 is the equation most frequently used in riprap design problems and will be evaluated in this analysis. The mean velocity relation results from integration of the point velocity relation over the entire depth of flow. This is one problem with the mean velocity equations, if Coleman (1981) is correct in saying that the point velocity logarithmic equation is applicable in only the lower 15 percent of the depth. Another problem is that the origin for the velocity profile is assumed equal to the tops of the roughness elements

in the integration. This assumption is satisfactory for low relative roughness but not for high relative roughness. The effects of both of these assumptions are lumped into the determination of K_s. The experimental data collected in the WES and CSU flumes were used to define the applicability of the logarithmic velocity relations. Analysis of Equation 2.7 was similar to Yalin (1977) in which K_s/d_{90} is determined as a function of relative roughness. Results are presented in Figure 4.5 for tests with no movement and meeting the data requirements given in Chapter 3. Data used in Figure 4.5 are given in Tables 4.2-4.12. Results show that K_s/d_{90} is not constant over the range of data used in this investigation. This result is consistent with Yalin's results showing the point velocity logarithmic relation (Equation 2.6) inapplicable for $D/d_{90} < 10$.

4.2 DEVELOPMENT OF CRITICAL VELOCITY RELATION

One of the objectives of this study is to develop a riprap sizing method based on velocity. Dimensional analysis is used to define the dimensionless variables based on the selection of all relevant parameters. The dimensional analysis is similar to that proposed by Neill (1967) in which mean velocity is used instead of the critical tractive force approach used by many investigators. The relevant parameters governing the stability of riprap in open channels are as follows:

d = characteristic particle size, L

D = flow depth, L

ρ = fluid density, M/L^3

ρ_s = stone density, M/L^3

V = mean velocity, L/T

μ = absolute viscosity, M/LT

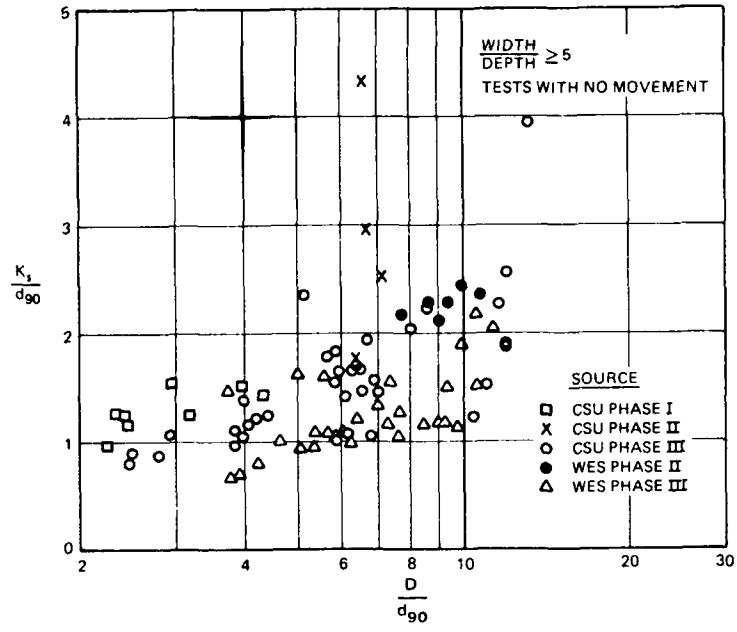

Figure 4.5. Variation of K_s/d_{90} with relative depth (data from Tables 4.2-4.12)

g = gravitational acceleration, L/T^2

F_{SIDE} = side slope factor

S = channel slope

d_{85}/d_{15} = gradation uniformity

N = blanket thickness/d_{100}

F_{SHAPE} = shape factor and surface texture

M,L,T = fundamental dimensions of mass, length, and time, respectively

The mean velocity in this investigation is the average velocity in the vertical at the point of interest. With this concept, the effects of channel alignment or curvature can be incorporated into the design procedure. The designer must determine the velocity at the point of interest, not average cross-section values, in order to determine rock size. Methods to determine this average velocity at the point of interest are

presented in Chapter 5. Neither g nor ρ_s can be independent parameters; they must occur in the combination $g(\rho_s - \rho)$ which is the submerged specific weight of the riprap γ_s'. Replacing μ with $\nu = \mu/\rho$, the relevant parameters can be written

$$f(d, D, \rho, V, \gamma_s', \nu, F_{SIDE}, S, d_{85}/d_{15}, N, F_{SHAPE}) = 0 \qquad 4.3$$

Out of these eleven variables there are six dimensional variables (d, D, ρ, V, γ_s', ν) and five dimensionless quantities (F_{SIDE}, S, d_{85}/d_{15}, N, F_{SHAPE}). Since there are three fundamental dimensions (M, L, and T), there are three nondimensional groups. The statement can be rewritten

$$f(\pi_1, \pi_2, \pi_3, F_{SIDE}, S, d_{85}/d_{15}, N, F_{SHAPE}) = 0 \qquad 4.4$$

Using repeating variables V, D, and γ_s', the π terms are

$$\pi_1 = V^{a_1} D^{b_1} \gamma_s'^{c_1} \rho^{d_1} \qquad 4.5$$

$$\pi_2 = V^{a_2} D^{b_2} \gamma_s'^{c_2} d^{d_2} \qquad 4.6$$

$$\pi_3 = V^{a_3} D^{b_3} \gamma_s'^{c_3} \nu^{d_3} \qquad 4.7$$

Set each of π's equal to $M^oL^oT^o$ and solve simultaneously for a, b, c, and d. This results in

$$\pi_1 = \frac{\rho V^2}{\gamma_s' D} = \left(\frac{\gamma_w}{\gamma_s - \gamma_w}\right)\frac{V}{gD}^2 = \text{Froude Number modified by relative rock weight} \qquad 4.8$$

$$\pi_2 = \frac{d}{D} = \text{relative roughness} \qquad 4.9$$

$$\pi_3 = \frac{VD}{\nu} = \text{Reynolds' number} \qquad 4.10$$

The statement can then be rewritten

$$f\left[\left(\frac{\gamma_w}{\gamma_s - \gamma_w}\right)\frac{V^2}{gD}\ ,\ \frac{d}{D}\ ,\ \frac{VD}{\nu}\ ,\ F_{SIDE},\ S,\ d_{85}/d_{15}\ ,\ N\ ,\ F_{SHAPE}\right] = 0 \qquad 4.11$$

The Reynold's number term $VD/_{\nu}$ is indicative of viscous effects which are not important in prototypes and in the model sizes used in this investigation. The influence of slope is important for steep flows, and Bathurst, Graf, and Cao (1982) found slopes greater than 2 percent to have significant effects on incipient conditions of bed movement. At the condition of incipient failure of riprap, slope and particle size/depth ratio d/D are dependent. A steep slope implies large d/D at incipient conditions. Since this investigation is limited to slopes equal to or less than 2 percent and since d/D is retained in the analysis, slope is omitted. The majority of open channel riprap problems have slopes well below 2 percent. The statement of relevant dimensionless parameters becomes

$$f\left[\left(\frac{\gamma_w}{\gamma_s - \gamma_w}\right)\frac{V^2}{gD}\ ,\ \frac{d}{D}\ ,\ F_{SIDE}\ ,\ d_{85}/d_{15}\ ,\ N\ ,\ F_{SHAPE}\right] = 0 \qquad 4.12$$

Riprap stability data will be used to evaluate the importance of each of these parameters. Channel bottom test series having a relatively large range of d/D and having the same gradation uniformity d_{85}/d_{15}, thickness N, and shape F_{SHAPE} were used to evaluate

$$\frac{d}{D} = \text{function of}\left[\left(\frac{\gamma_w}{\gamma_s - \gamma_w}\right)\frac{V^2}{gD}\right] \qquad 4.13$$

Results in Figures 4.6-4.9 show that the basic equation for threshold of incipient failure of bottom riprap in straight channels has the form

$$\frac{d_{50}}{D} = C_6 \left[\left(\frac{\gamma_w}{\gamma_s - \gamma_w} \right)^{1/2} \frac{V}{\sqrt{gD}} \right]^{2.5} \qquad 4.14$$

These best-fit lines were drawn to separate stable runs from failure runs and were not the result of regression techniques. Equation 4.14 is the same form found by Neill (1967) and Bogardi (1968) and will be used in the evaluation of the effects of gradation, thickness, and shape. Particle size d_{50} was used in this analysis until additional analysis can define a characteristic size.

An equation similar to Equation 4.14 can be derived by combining the following shear or tractive force relations:

$$T = \gamma_w DS \qquad (2.1 \text{ bis})$$

$$T_c = C_c(\gamma_s - \gamma_w)d_{50} \qquad (2.4 \text{ bis})$$

$$T = T_c \text{ (at incipient failure)} \qquad 4.15$$

$$C_c = C_5 \left(\frac{d_{50}}{D} \right)^{1/5} \qquad 4.2 \text{ bis}$$

Manning's equation

$$V = \frac{1.49}{n} D^{2/3} S^{1/2} \qquad 4.16$$

where n = Manning's resistance coefficient and Strictler's equation is

$$n = C_7 d_{50}^{1/6} \qquad 4.17$$

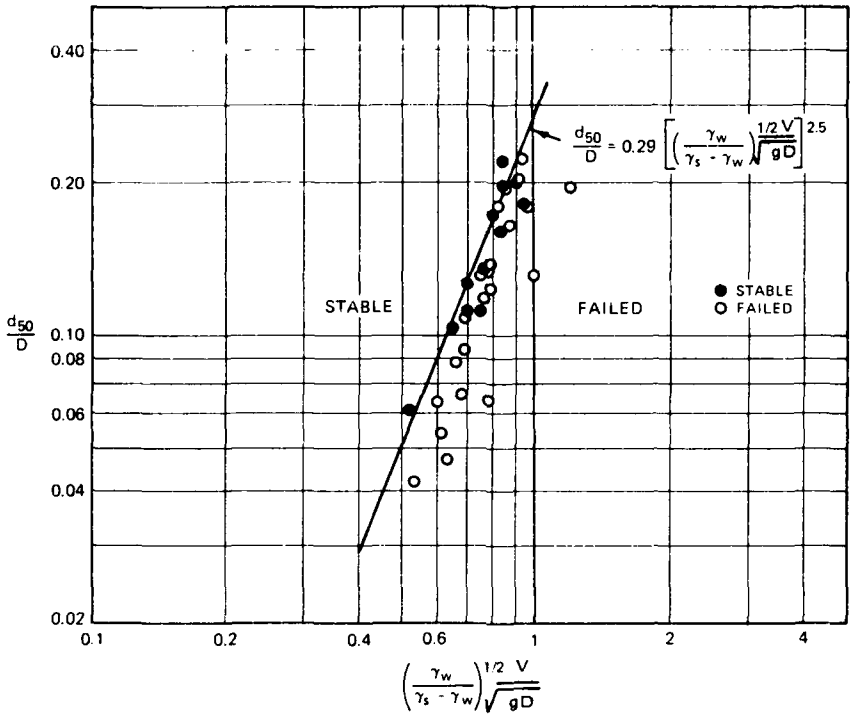

Figure 4.6. d_{50}/D versus modified Froude number, thickness = $1d_{100}$, d_{85}/d_{15} = 1.35, WES Phase I (Data from Table 4.1)

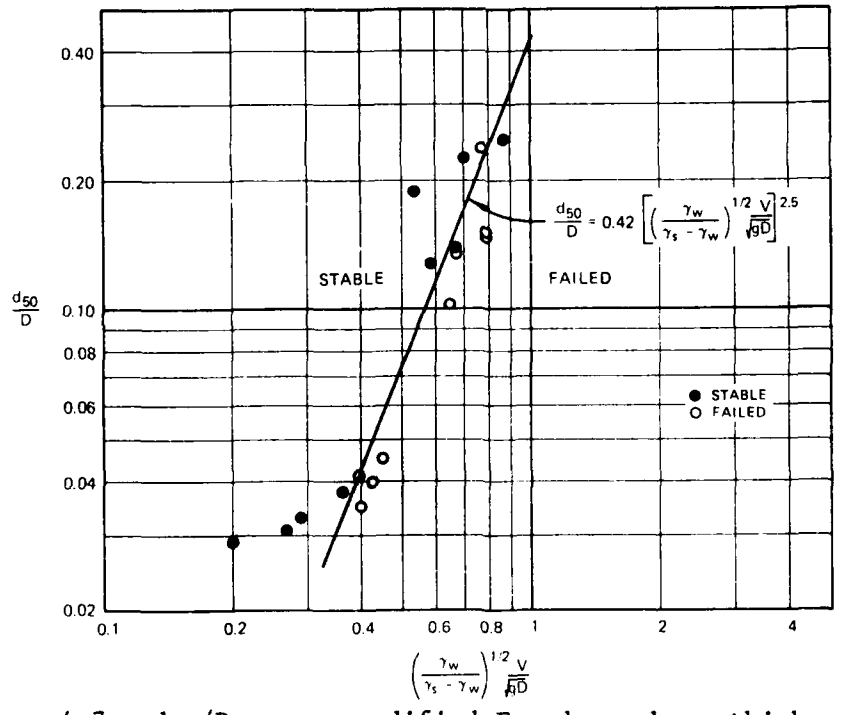

Figure 4.7. d_{50}/D versus modified Froude number, thickness = $1d_{100}$, d_{85}/d_{15} = 2.8 and 2.5, CSU Phases I and II (Data from Tables 4.2 and 4.3)

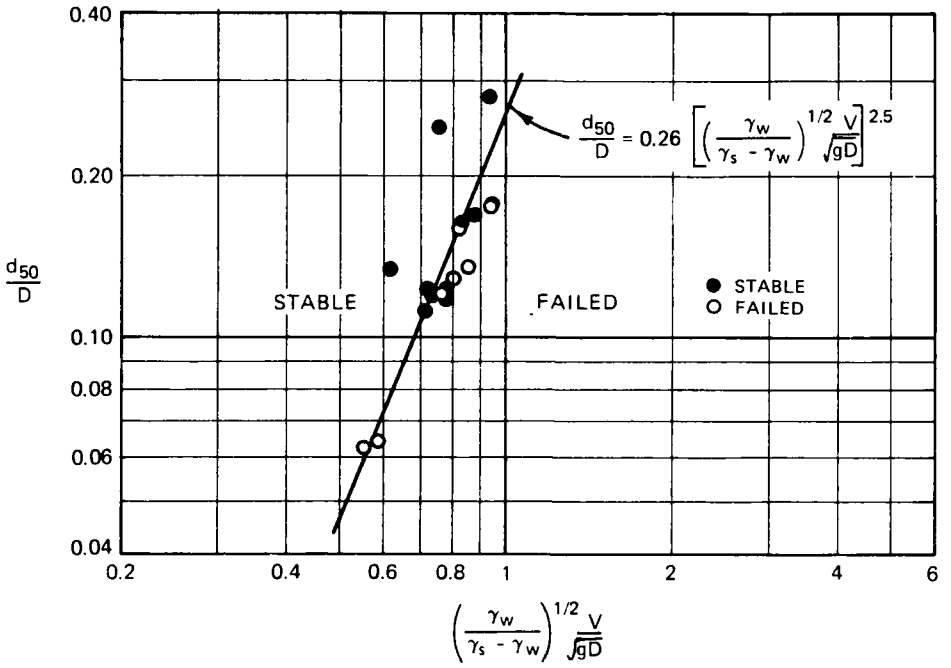

Figure 4.8. d_{50}/D versus modified Froude number, thickness = $1.4d_{100}$, d_{85}/d_{15} = 2.1 and 2.3, CSU Phase III (Data from Tables 4.4 and 4.5)

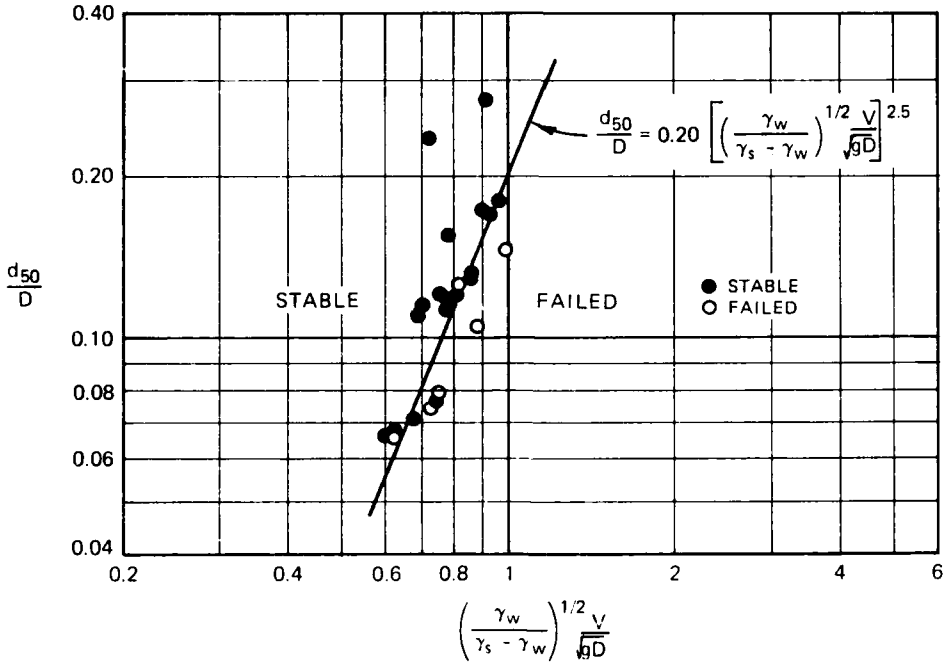

Figure 4.9. d_{50}/D versus modified Froude number, thickness = $2.1d_{100}$, d_{85}/d_{15} = 2.1 and 2.3, CSU Phase III (Data from Table 4.6 and 4.7)

When combined, these equations yield

$$\frac{d_{50}}{D} = C_8 \left[\left(\frac{\gamma_w}{\gamma_s - \gamma_w} \right)^{1/2} \frac{V}{\sqrt{gD}} \right]^{2.31} \qquad 4.18$$

which is similar to Equation 4.14.

Most existing riprap design procedures fall into two categories:

1. Constant Shields coefficient. Equation 2.14 is an average velocity relation which can be derived using a constant Shields coefficient and combining equations 2.1, 2.4, 4.15, 4.16, and 4.17.

$$\frac{d_{50}}{D} = C_4 \left[\left(\frac{\gamma_w}{\gamma_s - \gamma_w} \right)^{1/2} \frac{V}{\sqrt{gD}} \right]^{3} \qquad (2.14 \text{ bis})$$

2. Isbash type relations. These can be expressed as

$$d_{50} = C_9 V^2 \qquad 4.19$$

Many US Army Corps of Engineers (CE) offices have charts relating riprap size to velocity which use this relation. This relation can be rewritten in the form

$$\frac{d_{50}}{D} = C_{10} \left[\left(\frac{\gamma_w}{\gamma_s - \gamma_w} \right)^{1/2} \frac{V}{\sqrt{gD}} \right]^{2} \qquad 4.20$$

using the full form of the Isbash equation and dividing both sides by depth.

Comparing Equations 2.14 and 4.20 to the equation proposed in this investigation (previously proposed by Neill (1967) and Bogardi (1968))

$$\frac{d_{50}}{D} = C_6 \left[\left(\frac{\gamma_w}{\gamma_s - \gamma_w} \right)^{1/2} \frac{V}{\sqrt{gD}} \right]^{2.5} \qquad (4.14 \text{ bis})$$

shows that riprap stability is best described by a relationship with an exponent that falls halfway between the two most commonly used methods of design.

4.3 EFFECTS OF GRADATION, THICKNESS, AND SHAPE ON RIPRAP STABILITY

4.3.1 Gradation. Variation of gradation uniformity was accounted for by using a characteristic size less than the average size given in several references cited in the literature review. Size segregation can be a significant factor when using highly nonuniform materials and is probably one reason the characteristic size was found to be less than the average size. The ratio d_{85}/d_{15} is used to describe the uniformity of riprap gradations. Standard CE gradations given in OCE (1971) have $d_{85}/d_{15} = 1.8\text{-}2.1$. In addition to the results presented in Figures 4.6-4.9, data from the following test series were evaluated using Equation 4.14 (these data sets were not used in the development of Equation 4.14 because they do not cover a wide enough range of d/D) .

Source	d_{85}/d_{15}	Thickness	Table	Figure
CSU Phase I	3.9	$1d_{100}$	4.8	4.10
CSU Phase II	4.6	$1d_{100}$	4.9	4.11

To evaluate the effects of gradation for riprap placed to a thickness of $1d_{100}$, the coefficients from the equations shown in Figures 4.6, 4.7, 4.10, and 4.11 are plotted against d_{85}/d_{15} in Figure 4.12. Results show that the coefficient varies with d_{85}/d_{15} , which means that d_{50} is not the characteristic size for the range of gradations tested. Equation 4.14 was evaluated using different characteristic sizes, and only d_{30} (Figure 4.12) was shown to give a

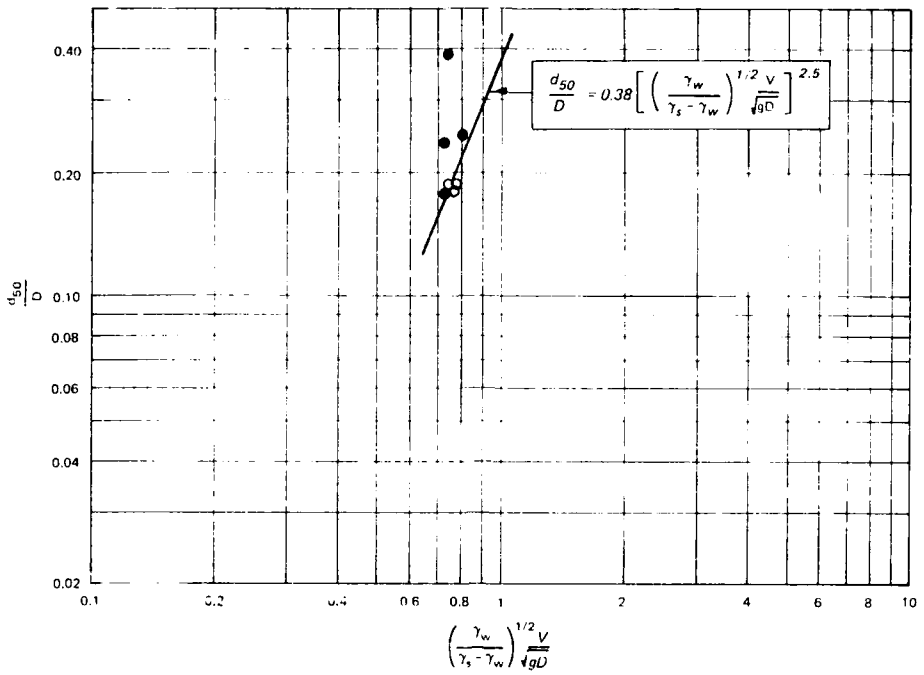

Figure 4.10. d_{50}/D versus modified Froude number, thickness = $1.0d_{100}$, d_{85}/d_{15} = 3.9 , CSU Phase I
(Data from Table 4.8)

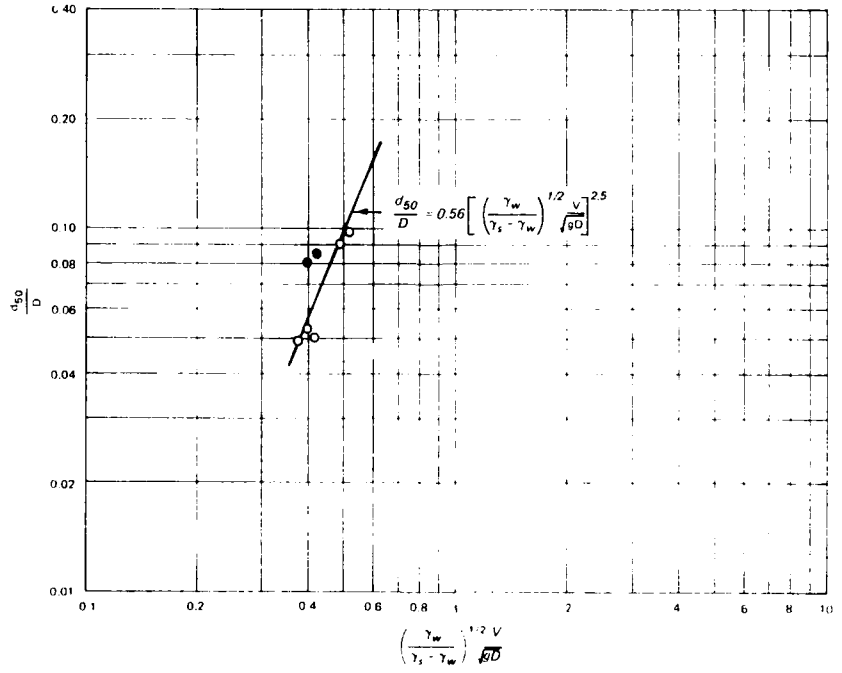

Figure 4.11. d_{50}/D versus modified Froude number, thickness = $1.0d_{100}$, d_{85}/d_{15} = 4.6 , CSU Phase II
(Data from Table 4.9)

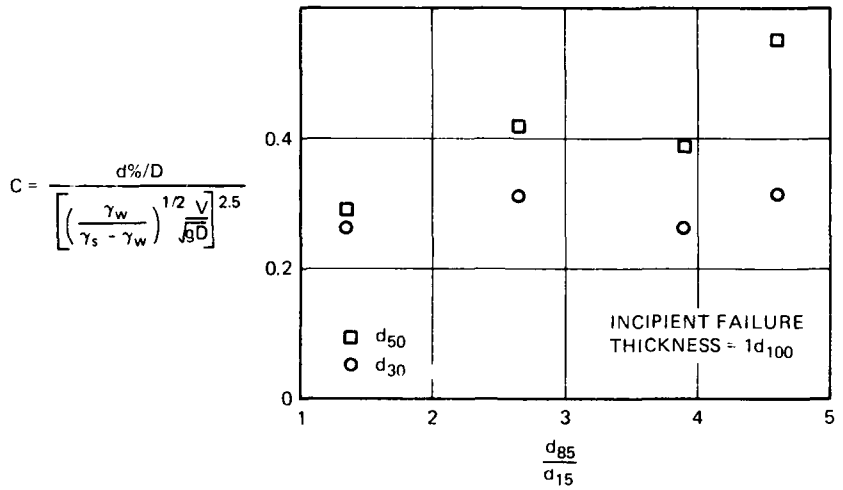

Figure 4.12. Coefficient in Equation 4.14 versus d_{85}/d_{15} , thickness = $1d_{100}$, bottom riprap

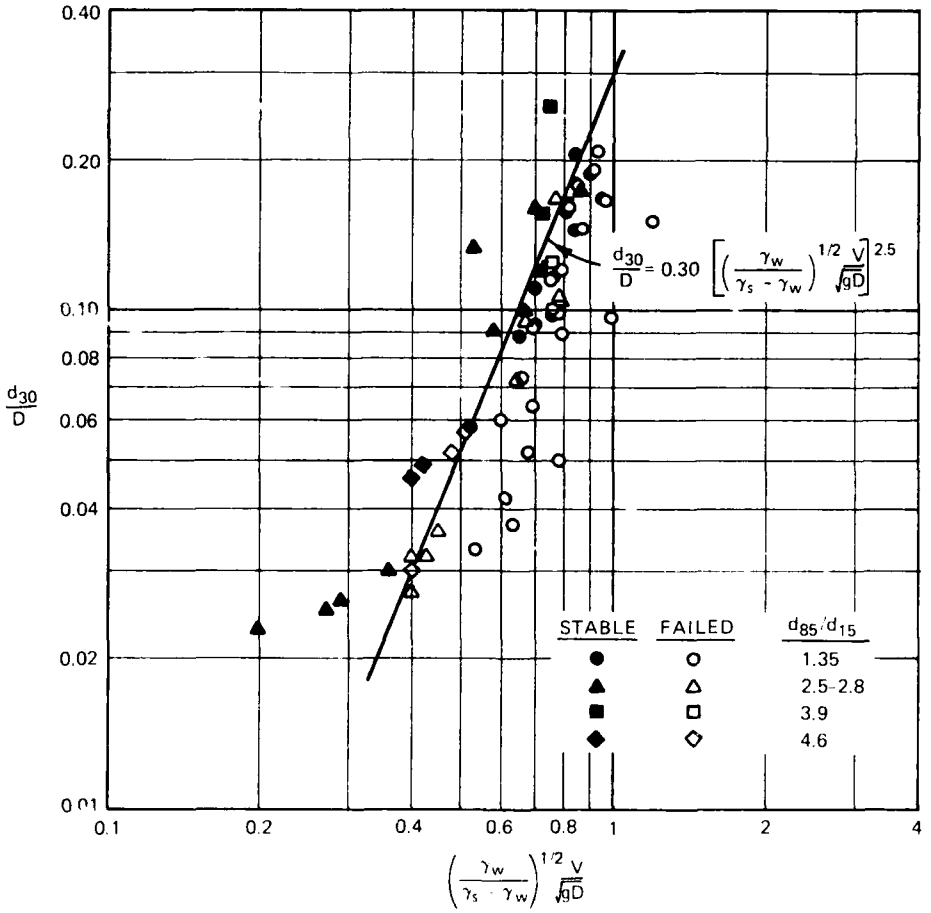

Figure 4.13. d_{30}/D versus modified Froude number, thickness = $1d_{100}$, d_{85}/d_{15} = 1.35-4.6 , bottom riprap

relatively constant C in Equation 4.14. All data are plotted in Figure 4.13. The equation

$$\frac{d_{30}}{D} = 0.30 \left[\left(\frac{\gamma_w}{\gamma_s - \gamma_w} \right)^{1/2} \frac{V}{\sqrt{gD}} \right]^{2.5} \qquad 4.21$$

is applicable to threshold of incipient failure of riprap placed to a thickness of $1d_{100}$, $d_{85}/d_{15} \leq 4.6$, $d_{30}/D = 0.020\text{-}0.25$, $F < 1.2$, on the bottom of straight channels. This analysis shows that either d_{50} can be used in Equation 4.14 with a coefficient which varies with gradation or d_{30} can be used in Equation 4.21.

4.3.2 Thickness. Several of the test series were used to determine the effects of blanket thickness on riprap stability. Any comparison of different thicknesses of riprap must be conducted with the same gradation. Data from Maynord (1978) are shown in Figure 4.14 for a thickness of $1.5d_{100}$. The following tabulation summarizes the test series used in the analysis of thickness effects:

Source	d_{85}/d_{15}	Thickness	d_{30}/d_{50}	Table	Figure
WES trapezoidal channel	2.0	$1.5d_{100}$	0.83	See Maynord (1978)	4.14
CSU Phase III	2.1-2.3	$1.4d_{100}$	0.80	4.4, 4.5	4.8
CSU Phase III	2.1-2.3	$2.1d_{100}$	0.80	4.6, 4.7	4.9

The coefficients from these equations are determined for a characteristic size d_{30} and plotted against thickness in Figure 4.15. For thickness of $1.0d_{100}$, the coefficient from Equation 4.21 is used. Results show that increased thickness decreases the size required to remain stable up to a thickness of $2.0\text{-}2.5d_{100}$. Additional tests are needed to evaluate the effects of thickness for other gradations. Note that d_{30} was shown to be the characteristic size for a thickness of $1.0d_{100}$ only. As riprap thickness increases, the likelihood of areas having

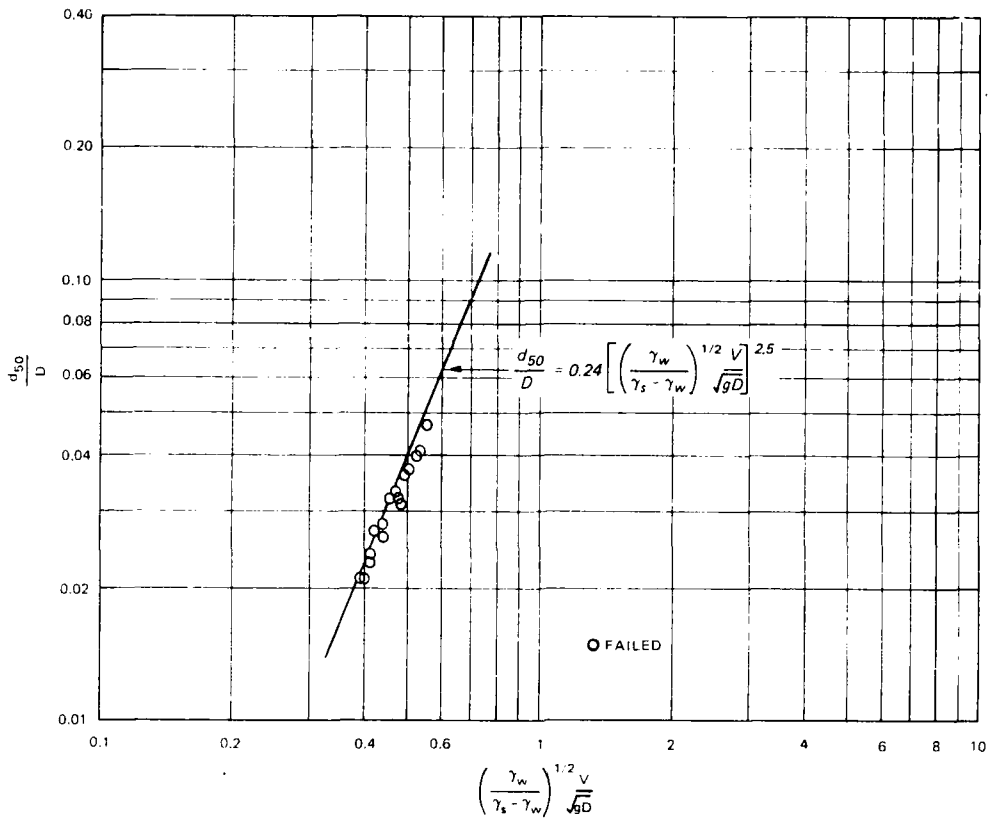

Figure 4.14. d_{50}/D versus modified Froude number, thickness = $1.5d_{100}$, d_{85}/d_{15} = 2.0 , WES trapezoidal

$$C = \frac{d_{30}/D}{\left[\left(\frac{\gamma_w}{\gamma_s - \gamma_w}\right)^{1/2}\frac{V}{\sqrt{gD}}\right]^{2.5}}$$

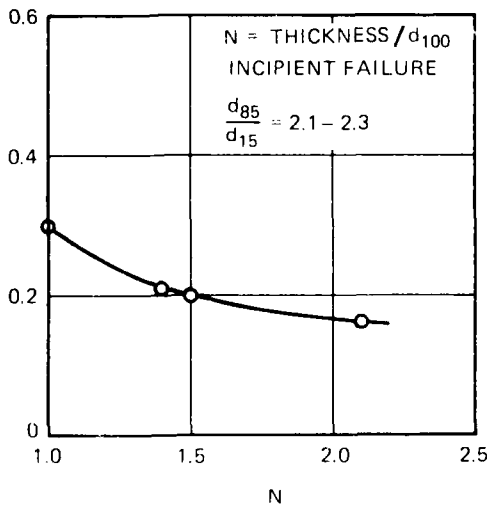

Figure 4.15. Coefficient in Equation 4.21 (using d_{30}) versus blanket thickness, d_{85}/d_{15} = 2.1-2.3 , bottom riprap

only small particles (due to size segregation) decreases. Another mechanism, armoring, may also exert a significant influence on riprap stability. These may be the reasons that thickness is seen to be so significant in Figure 4.15.

4.3.3 Shape. Two of the test series conducted during the CSU Phase III tests allow a comparison of the effects of riprap shape. OCE (1970) shape guidance requires the following:

1. Stone predominantly angular
2. No more than 25 percent of stones having $\ell/b > 2.5$
3. No stone having $\ell/b > 3.0$

Riprap meeting this guidance was tested and compared with riprap having the following characteristics:

1. All stone angular
2. Thirty percent of stone had $\ell/b > 2.5$
3. Eighteen percent of stone had $\ell/b > 3.0$

Results of these two test series are plotted in Figure 4.16. Data used in Figure 4.16 are from Tables 4.4 and 4.10. Results show that shape effects are insignificant within the range tested in this investigation. Neill (1967) also found shape effects to be small. The stability of rounded rock such as cobbles was not addressed in this investigation.

4.4 EFFECTS OF SIDE SLOPE ON RIPRAP STABILITY

Three areas must be addressed in defining the effects of channel side slopes on riprap stability. First, the effects of the gravity component acting downslope and the influence of angle of repose must be evaluated. Second, the effects of the side slope on the velocity profile and distribution must be incorporated into the average velocity relations for sizing riprap. Third, side slope stability tests must be

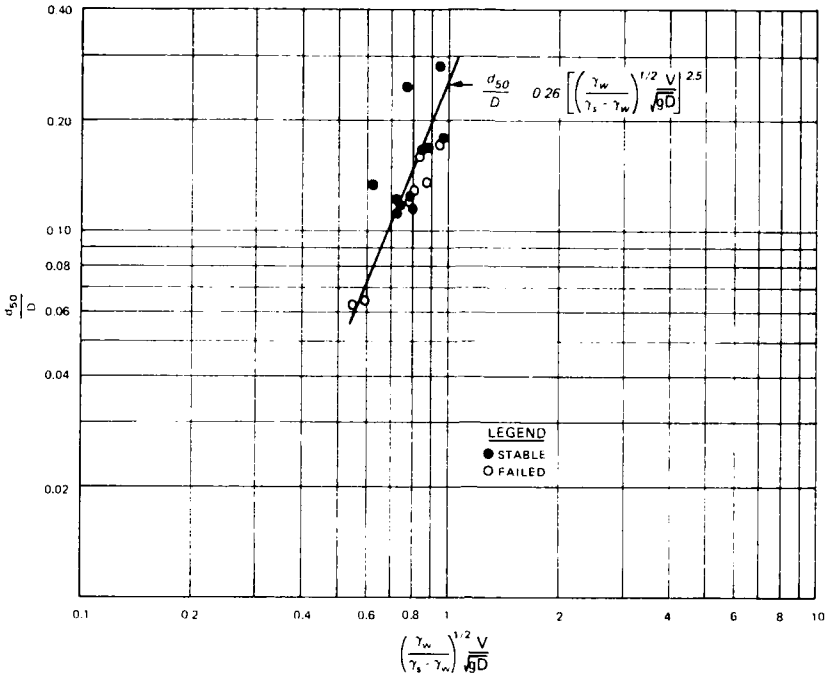

a. Meets Corps shape criteria (Data from Table 4.4)

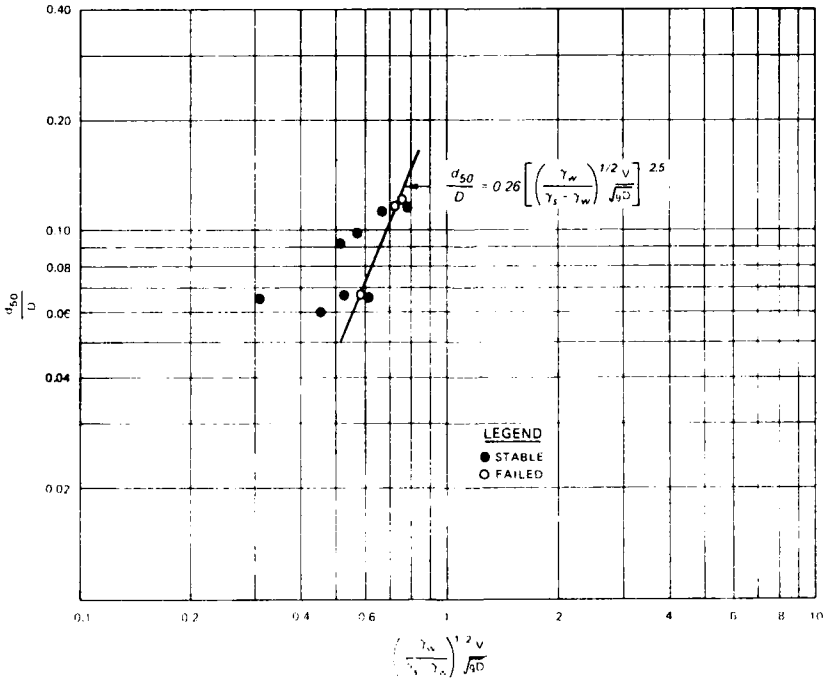

b. Does not meet Corps shape criteria because of excess elongated particles (Data from Table 4.10)

Figure 4.16. Shape effects comparison, d_{85}/d_{15} = 2.1-2.3, thickness = $1.4d_{100}$, CSU Phase III

conducted to determine the combined effect of the gravity component and the velocity profile.

4.4.1. Effect of Gravity Component Acting Downslope. As indicated in the literature review, several different methods including equilibrium of moments and equilibrium of forces have been used to define the stability of a particle resting on a channel side slope. As part of this investigation, tests were conducted in the WES tilting flume (Phase IV) to compare the stability of riprap resting on various side slopes. A schematic of the test facility is shown in Figure 4.17. The side slope was hinged at the bottom of the slope to facilitate changing the side slope. The riprap surrounding the test section was the same size as used in the test section and was glued to the side slope to ensure that the velocity profile and turbulence characteristics of the approach flow did not vary from test to test. Results for six different side slopes using uniform riprap with a thickness of $1d_{100}$ are shown in Table 4.13. Bottom velocity was used to define the imposed velocity and was measured $2.9d_{50}$ above the side slope as shown in Figure 4.18. Results show decreasing bottom velocity for increasing side slope.

The tractive force ratio as used by Carter, Carlson, and Lane (1953) is

$$K = \frac{T_s}{T_c} = \cos\,\Theta \sqrt{1 - \frac{\tan^2\Theta}{\tan^2\Phi}} = \sqrt{1 - \frac{\sin^2\Theta}{\sin^2\Phi}} \qquad \text{(2.17 bis)}$$

Given the same fluid, particle characteristics, and depth, shear stress is proportional to the second power of the velocity

$$T = C_{11}V^2 \qquad 4.22$$

The WES tilting flume side slope tests were conducted with the same fluid, particle characteristics, and depth. The only factor that varied

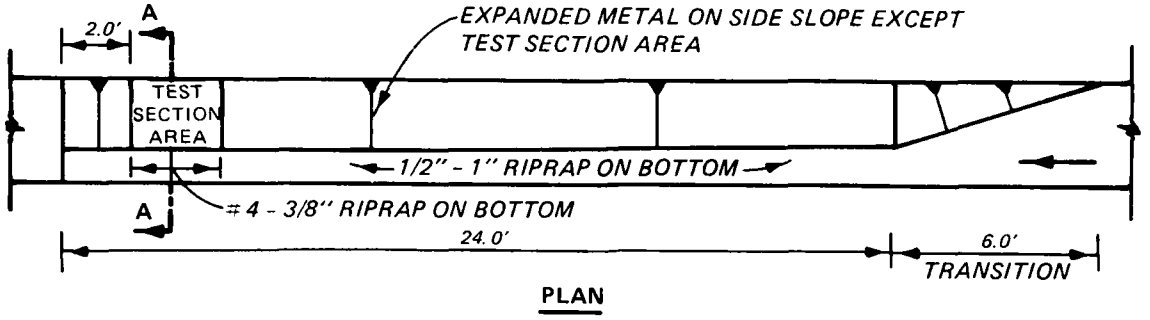

PLAN

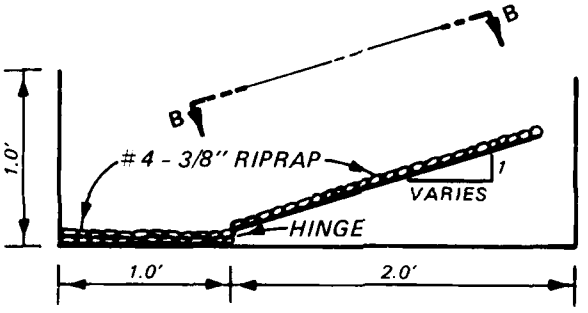

SECTION A-A

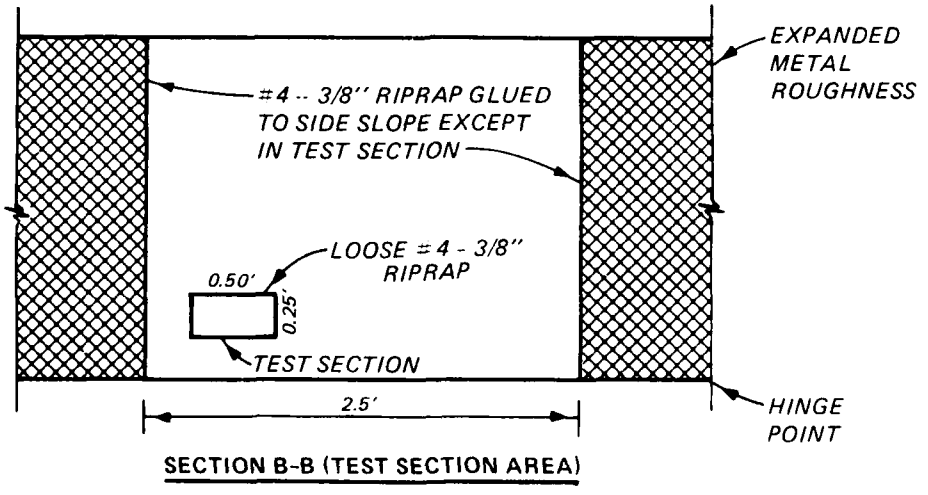

SECTION B-B (TEST SECTION AREA)

Figure 4.17. WES side slope test flume

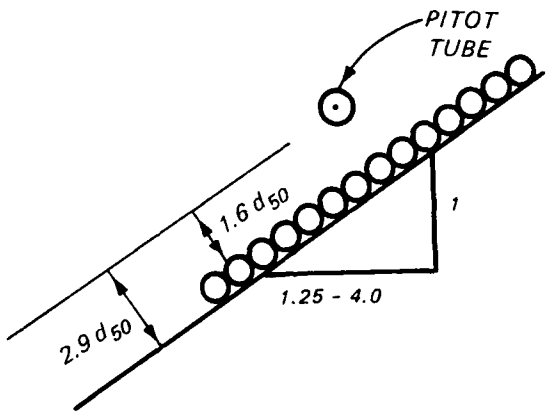

Figure 4.18. Location of bottom velocity measurements in WES tilting flume side slope tests

was the side slope angle. Having established these conditions Equation 4.22 can be substituted into 2.17 to obtain

$$K = \frac{T_s}{T_c} = \frac{V_s^2}{V_c^2} \qquad 4.23$$

where

V_s = critical velocity for particle on side slopes

V_c = critical velocity for particle on horizontal bed

The flattest side slope, 1V:4H, and the horizontal test yield essentially the same critical velocity and will be used for V_c in this analysis. The tractive force ratio K from Equation 4.23 is plotted against the side slope angle θ in Figure 4.19. Also shown in this figure is the analysis of Carter, Carlson, and Lane (1953) using an angle of repose of 40 deg (OCE 1970). The Carter, Carlson, and Lane method shows a greater decrease in stability than the experimental data. The experimental results are consistent with the findings of Hughes, Urbonas, and Stevens (1983) stating that "rock size does not need to be

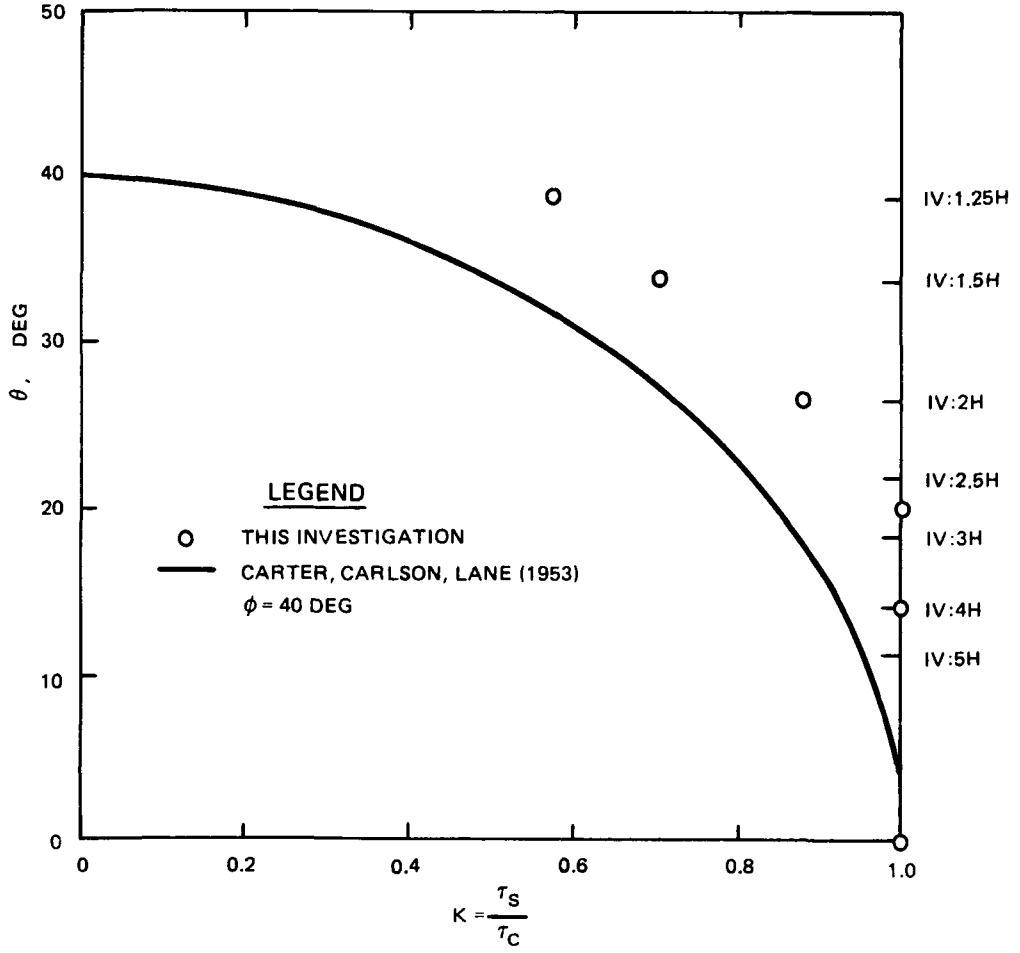

Figure 4.19. Tractive force ratio K versus side slope angle θ (Data from Table 4.13)

increased for steeper channel side slopes, provided the side slopes are no steeper than 2H:1V."

Tests were conducted to see if the assumed angle of repose of 40 deg was correct for the revetment used in these stability tests. The question arises, "Is the angle of repose of a revetment of varying height and thickness the same as the bulk angle of repose obtained from a pile of material?" The same revetment configuration used in the stability tests was placed on the hinged sloping side. The side slope angle was gradually increased until the revetment failed by sliding down

the slope. The average value of repose angle obtained for this revetment configuration under dry conditions was 52 deg (see Table 4.14). These tests were repeated with the test section submerged, and the average repose angle was 53 deg. A third series of tests was conducted using pressure fluctuations to simulate the turbulent fluctuations that occur when water flows over the riprap. A pressure transducer was installed flush with the sloping side on which the riprap was placed. Measurements of pressure were taken for flow conditions close to the conditions that resulted in failure of the riprap. With the test section submerged but without flow, a variable speed vibrator was attached to the flume sidewall. The speed of the vibrator was varied until the amplitude of the measured fluctuation was approximately equal to the maximum amplitude measured under flowing water conditions. This vibrator speed was used in all subsequent angle of repose tests. The third series with pressure fluctuations resulted in an average repose angle of 53 deg. The vibrator resulted in higher frequency fluctuations than did the flowing water condition but the amplitudes were similar.

The predictive technique of Carter, Carlson, and Lane (1953) was again tested against the experimental data using the measured angle of repose of 53 deg. Results given in Figure 4.20 show a much better comparison between predicted and observed values when the repose angle of 53 deg is used in the Carter, Carlson, and Lane equation, Equation 2.16.

Additional tests were conducted to determine why the measured repose angle was significantly higher than that predicted by existing techniques (Anderson, Paintal, and Davenport 1970). These tests were conducted to determine the effects of revetment height, bank smoothness, and revetment thickness. Results shown in Table 4.14 were plotted in

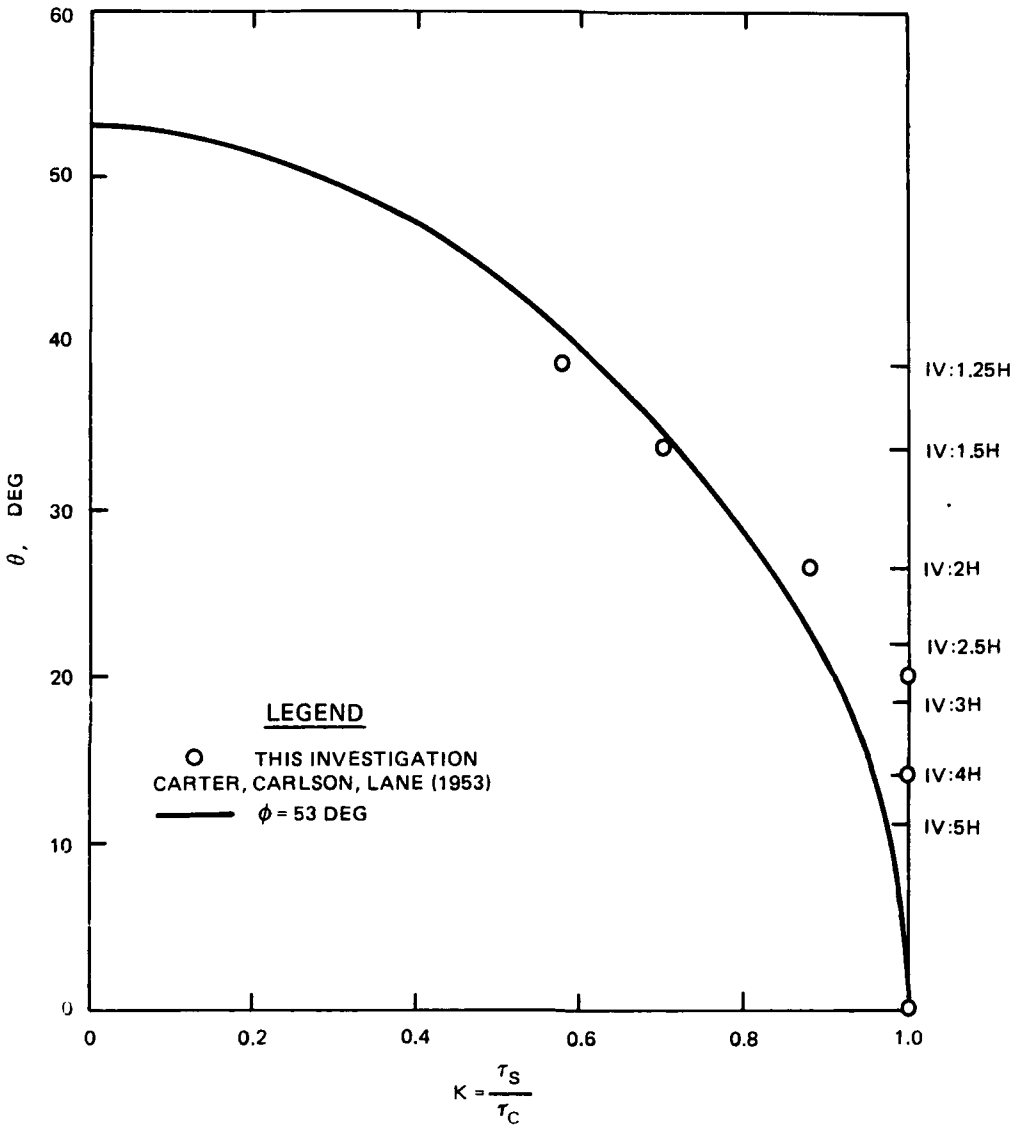

Figure 4.20. Tractive force ratio K versus θ (Data from Table 4.13)

Figure 4.21. The relative height of the revetment is defined as the length along the slope L_s divided by the average riprap size d_{50}. Revetment height L_s was included to determine if a 50-ft-high channel bank is less stable or has a different angle of repose than a 10-ft-high channel bank. Also shown on Figure 4.21a is the repose angle for crushed rock from Anderson, Paintal, and Davenport (1970). These results show that revetment height and thickness have a significant effect on

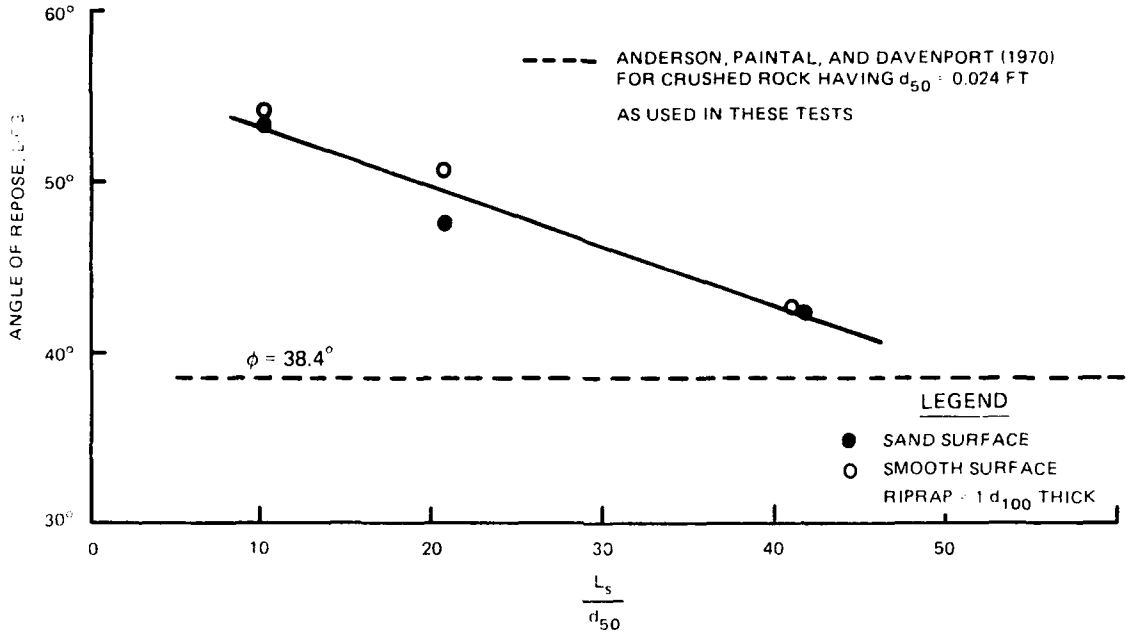

a. Angle of repose versus revetment height

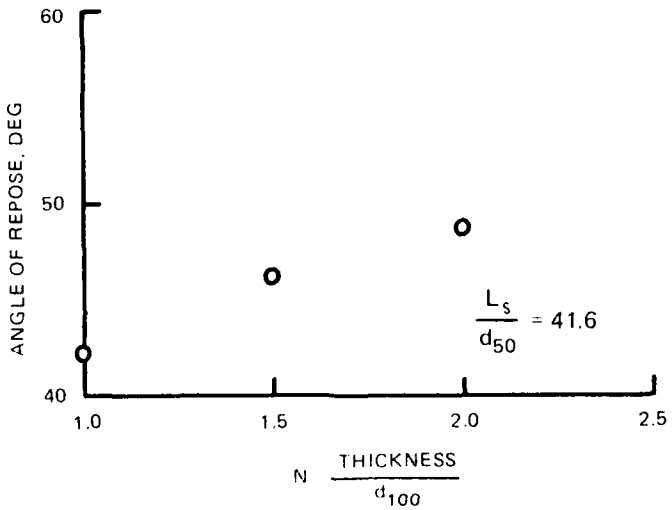

b. Angle of repose versus riprap thickness

Figure 4.21. Angle of repose of a revetment

the angle of repose. Surface smoothness was tested by comparing the repose angle for a smooth piece of marine plywood to that of a surface having sand glued to the marine plywood. The smooth surface yields a slightly higher value than the sand surface. The difference is small and surface roughness is not considered to be a big factor in angle of repose for the two surfaces used in these tests.

The California Division of Highways (1970) uses a repose angle of 70 deg in the predictive equations. Blodgett and McConaughy (1986) report that this was based on tests in which

> They constructed a model streambank on which small stones were arranged as riprap, and underlying stones were cemented in a plaster of paris base. The side slope was increased until the first outer stone was displaced. It was determined that 65° to 70° was the maximum angle attained before a stone fell out.

Miller and Byrne (1965) found the angle of repose of a single sand grain on a fixed rough bed to be as high as 70 deg when the fixed rough bed particles were equal in size to the single sand grain. Both the California study and Miller and Byrne show that surface roughness becomes important when the underlying material size becomes large relative to the size of the riprap. Hudson (1958) did not include the coefficient of friction (angle of repose) in the development of his widely used equations for the design of quarrystone cover layers subjected to wave attack. He cited several factors that presented difficulty in using angle of repose. Method of placement was one of the factors that caused variation in the repose angle.

The following results summarize angle of repose:

1. The angle of repose of a revetment is not always equal to the bulk angle of repose reported in the literature.

2. The angle of repose of a revetment is affected by revetment height, thickness, method of placement, and possibly other factors that were not investigated.

Similar to Hudson (1958), this investigation will omit repose angle from the analysis of side slope stability and incorporate repose angle effects into the empirically derived coefficients.

4.4.2 Velocity Profiles Over Channel Side Slopes. As part of the CSU Phase IV riprap stability tests, velocities were measured over the 1V:2H side slope in a straight flume. Results from tests having similar depth were averaged. Velocities were made dimensionless by dividing observed point velocity by the average velocity of a single vertical traverse over the toe of the slope, and depths were expressed in percentage of the total depth. Results shown in Figure 4.22 indicate reduced velocities over the slope and that the influence of the slope extends out from the toe of the slope approximately 0.5 times the depth of flow. The measured depth at the toe of the slope was generally 95 percent of the depth in the horizontal portion of the channel. This is shown in Figure 4.22 where the cross section is rounded at the toe of the slope. These profiles are for straight channels without the effects of upstream channel curvature. An analysis of the shear distribution of the profiles was conducted using the approach given in Section 4.4.1. The shear stress was evaluated relative to the shear stress in the horizontal portion of the cross section at $X/D = -1.0$. The velocity along the channel bottom was determined at a distance of $0.1D$ above the bed,

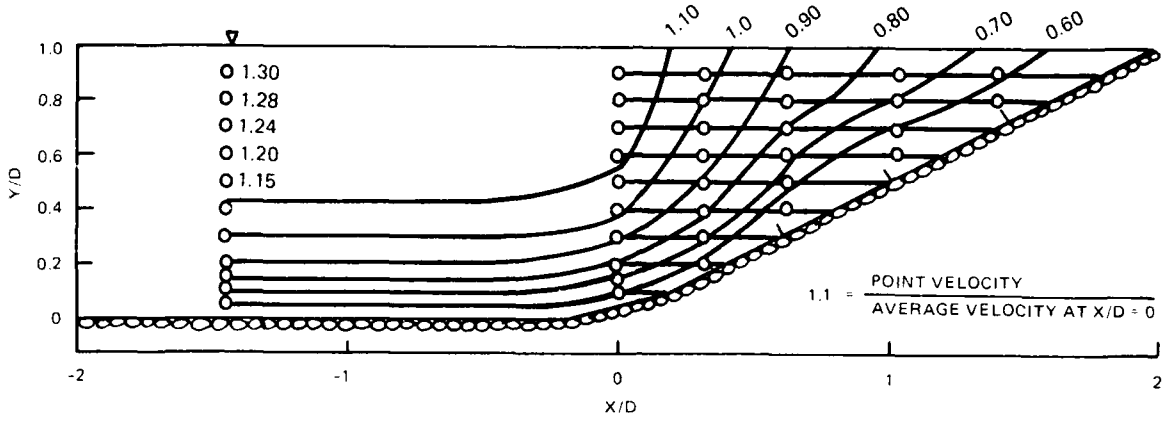

Tests 21, 22, and 23, d_{50} = 1 in. , thickness = 2 in.

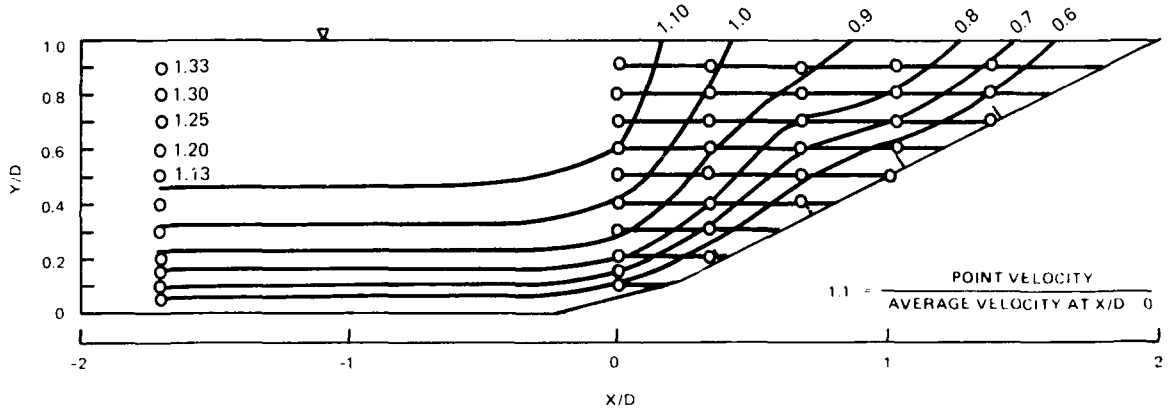

Tests 16 and 18, d_{50} = 1 in. , thickness = 2 in.

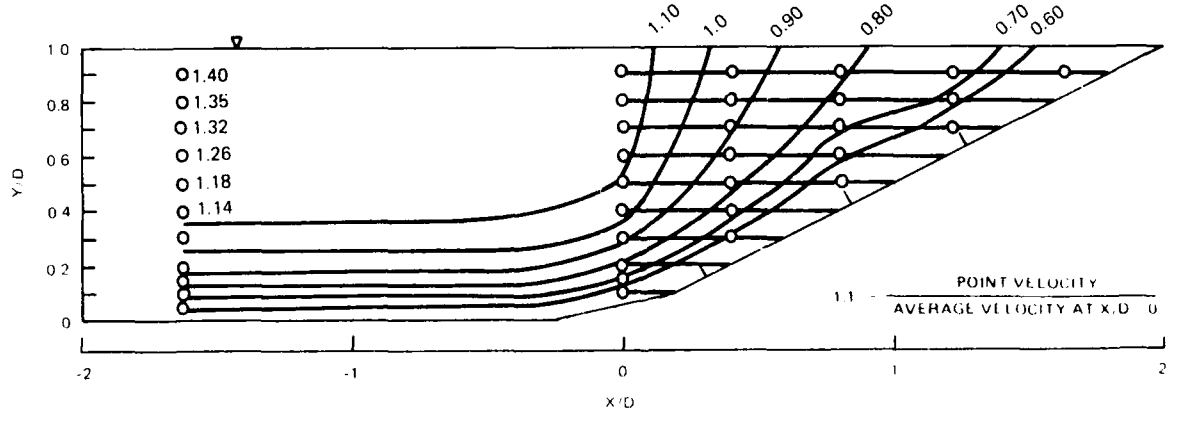

Tests 42, 43, 44 d_{50} = 1 in. , thickness = 1.5 in.

Figure 4.22. Velocity profiles, CSU Phase IV side slope tests

where D is the depth at $X/D = -1.0$. The relative shear is determined from

$$\frac{T}{T \text{ at } \frac{X}{D} = -1.0} = \frac{V^2}{V^2 \text{ at } \frac{X}{D} = -1.0} \qquad 4.24$$

Results from the three profiles, plotted in Figure 4.23, show that the shear stress is less on the channel side slope than on the channel bottom.

Another series of velocity measurements was conducted in a curved channel at WES to determine velocity profiles over side slopes that have strong upstream curvature effects. Profiles were measured at stations 11.6, 16.6, 21.6, 65.0, 70.0, and 75.0, shown in Figure 4.24. These stations correspond to the regions of maximum velocity over the toe of the slope. Nondimensional profiles were determined (Figures 4.25 and 4.26) and are significantly different from the profiles having a straight upstream alignment. These curved channel profiles show a velocity maximum over the toe of the slope, with the maximum located below the water surface.

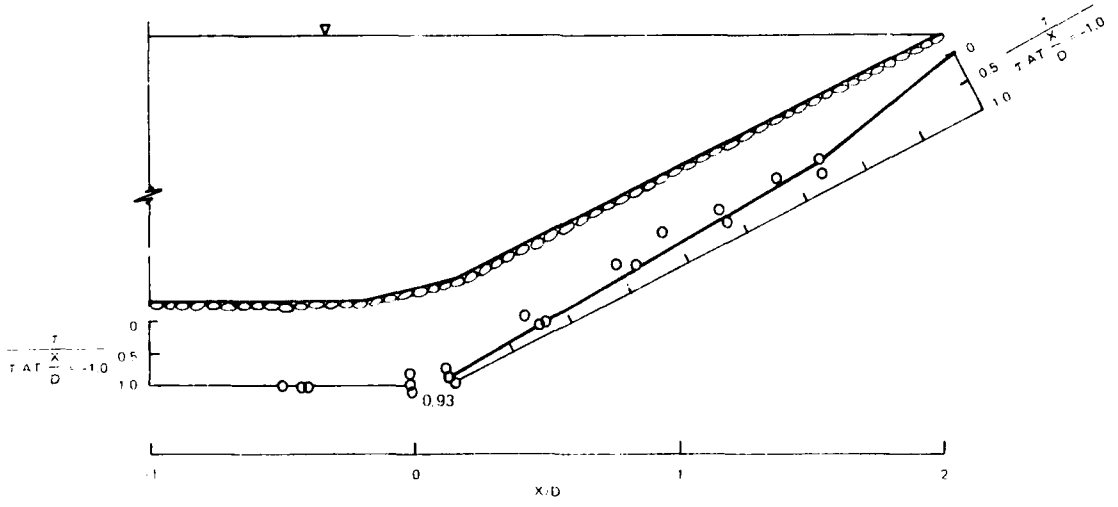

Figure 4.23. Shear stress distribution, 1V:2H side slope, straight channel

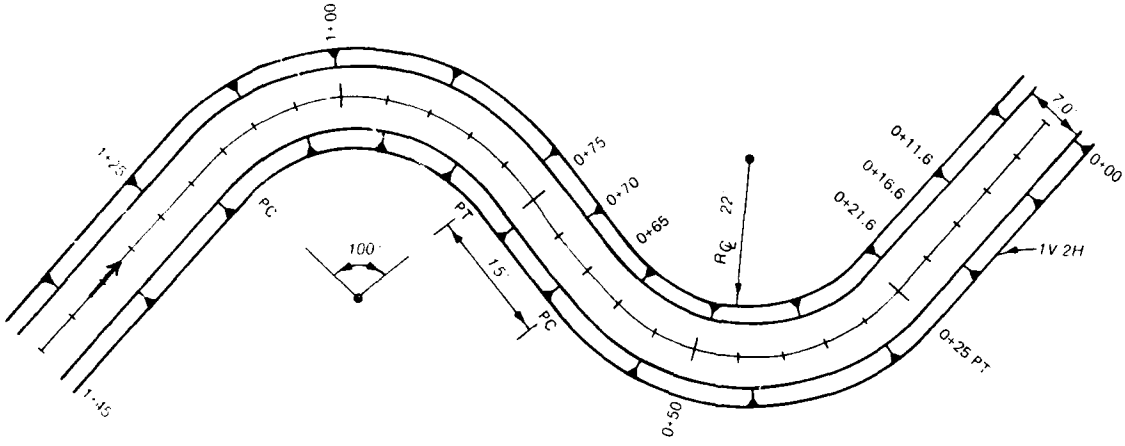

Figure 4.24. WES curved channel model, plan view

An analysis of the shear in the straight versus curved section was conducted using the same analysis used in Equation 4.24. For equal average velocity over the toe of the slope, the maximum stress on the curved channel side slope (located at $X/D = 0.5$) is equal to approximately 1.5 times the shear stress at $X/D = 0.5$ in the straight channel side slope.

4.4.3 Side Slope Stability Tests. Before side slope stability tests are analyzed, a characteristic velocity and depth must be selected. This velocity and depth must be representative of the conditions on the side slope and must also be values which a designer has some hope of determining or estimating. Average channel velocity is the easiest to determine but not very representative of conditions on the side slope. Depth and average velocity over the toe of the slope will be used in this investigation for the side slope stability analysis. These values were selected based on the two requirements stated previously and the results from the WES curved channel, which showed that

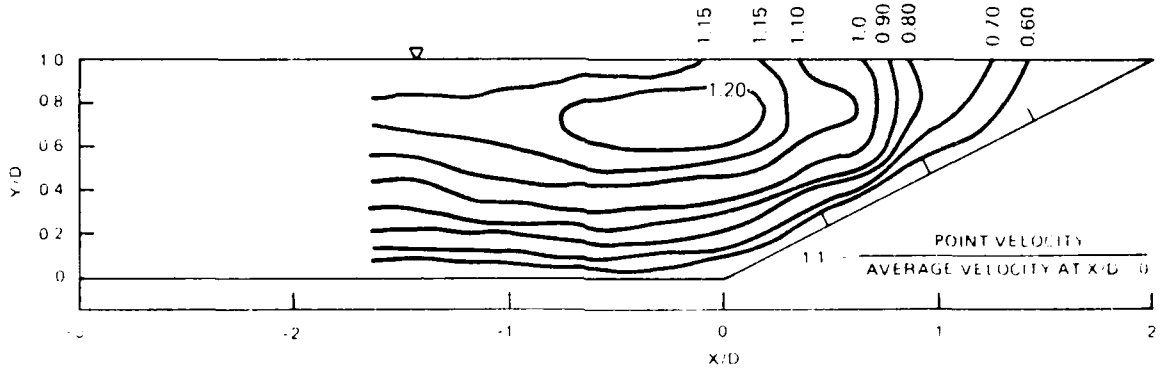

a. Station 11.6

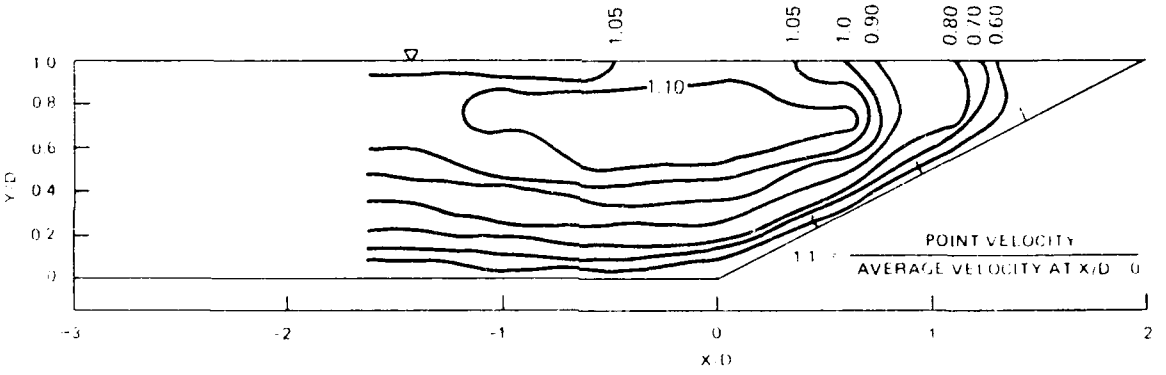

b. Station 16.6

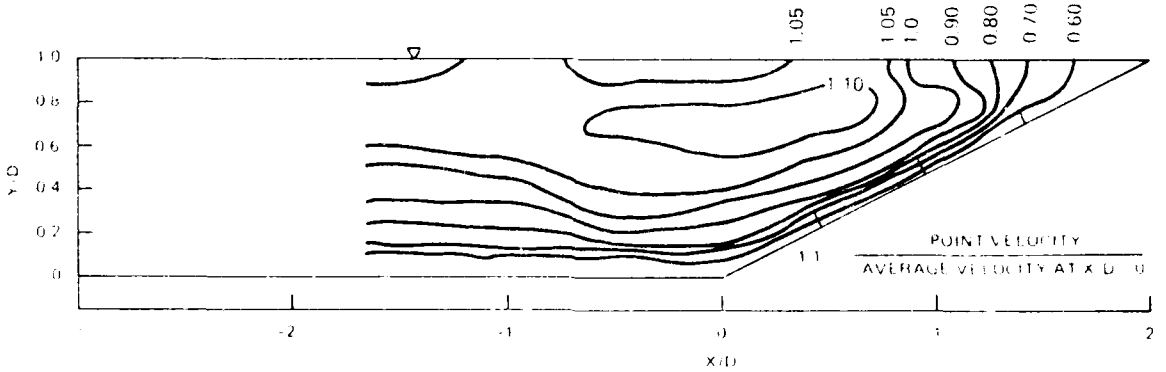

c. Station 21.6

Figure 4.25. Velocity profiles, WES curved channel facility, stations 11.6, 16.6, and 21.6

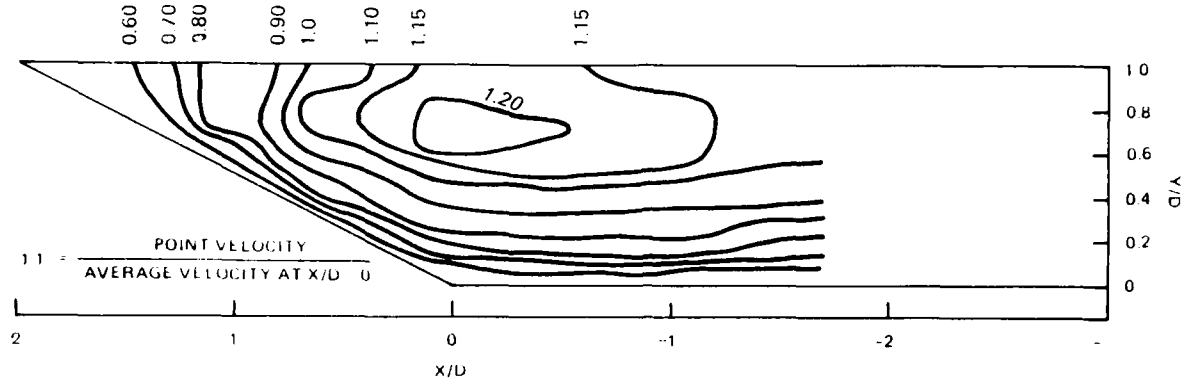

a. Station 65

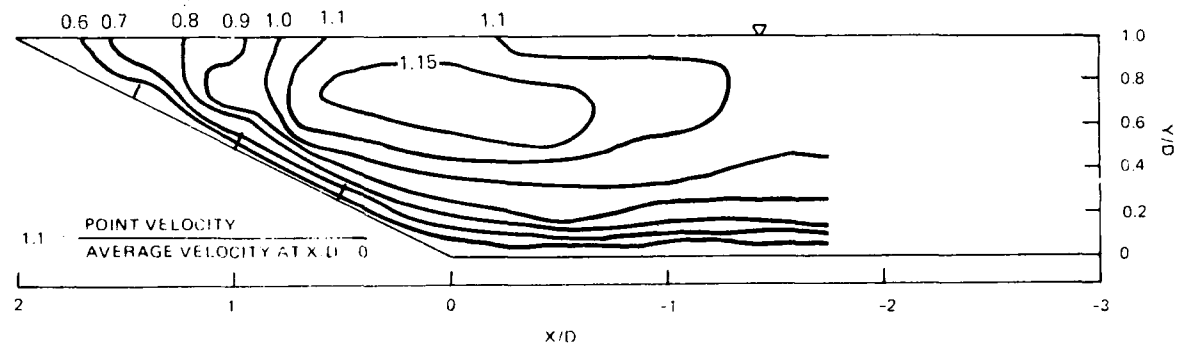

b. Station 70

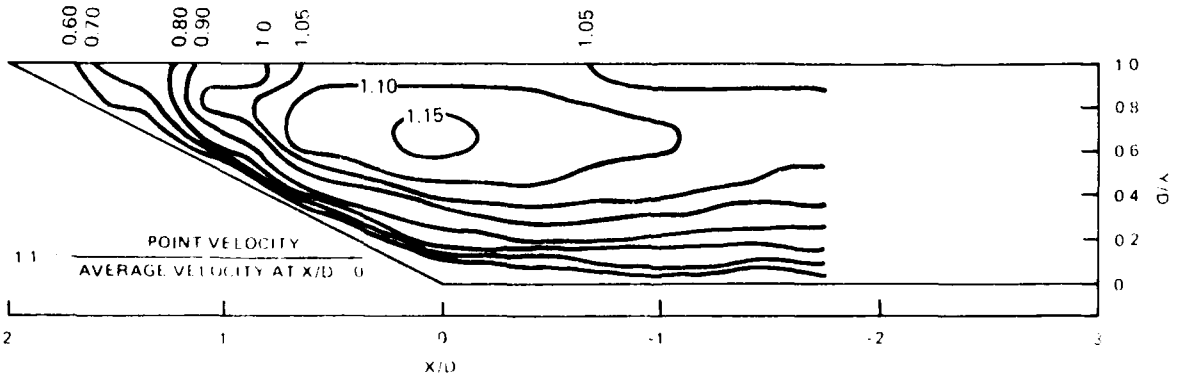

c. Station 75

Figure 4.26. Velocity profiles, WES curved channel facility, stations 65, 70, and 75

the maximum velocity in the cross section occurred over the toe of the side slope.

Prior to the CSU Phase IV side slope stability tests, an analysis was conducted of the Dorena Dam prototype tests reported by the US Army Engineer District, Portland (1952). These tests were conducted downstream of Dorena Dam in a channel having a grouted riprap bottom and 1V:2H side slopes with riprap placed to a thickness of $1d_{100}$. Results are shown in Table 4.15 and Figure 4.27. The curve for threshold of incipient failure, thickness of $1d_{100}$, 1V:2H side slope, and straight channel is

$$\frac{d_{30}}{D} = 0.23 \left[\left(\frac{\gamma_w}{\gamma_s - \gamma_w} \right)^{1/2} \frac{V}{\sqrt{gD}} \right]^{2.5} \qquad 4.25$$

based on the Dorena Dam prototype tests. The depth and velocity over the toe of the slope were used in the analysis. The velocities were measured for several tests, and these were used to estimate the velocity in the remaining tests.

In the CSU Phase IV tests, stability was determined for the following:

d_{50} in.	Thickness / d_{100}	Table
1.0	1.33	4.16
1.0	1.0	4.17
0.5	1.0	4.18

Like the Dorena Dam tests, these tests were conducted in a straight channel without upstream curvature effects.

The results given in Tables 4.16-4.18 show that the bottom riprap fails more often or with greater severity than the side slope riprap.

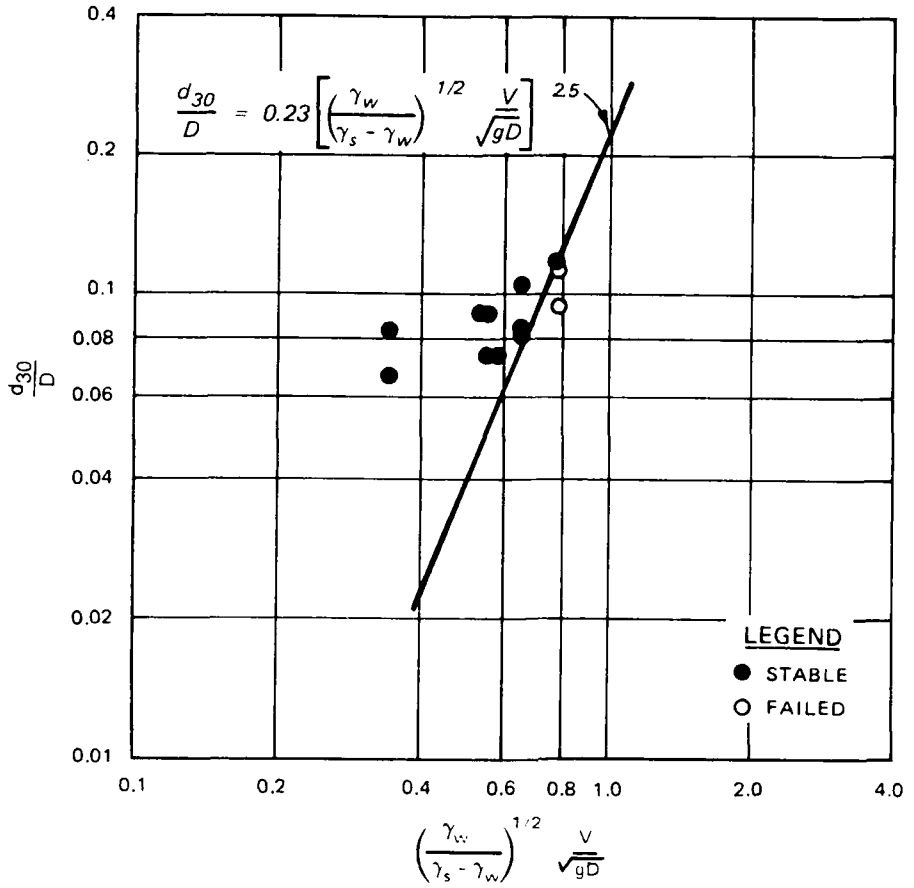

Figure 4.27. d_{30}/D versus modified Froude number, thickness of $1.0d_{100}$, 1V:2H side slope, Dorena Dam prototype tests (Data from Table 4.15)

In tests 29-35 (Table 4.16) with the 1-in. d_{50} riprap placed 2 in. thick, the bed was stabilized with a wire screen to ensure failure on the side slopes. Results from tests with a thickness of $1d_{100}$ are shown in Figure 4.28. A failure point from test 21 is located to the left of the incipient failure line. This test had a total failed area of less than 0.1 sq ft. Due to the small failure area and the position of this point relative to several stable runs, this point was not used in the determination of the best-fit line. The curve for threshold of

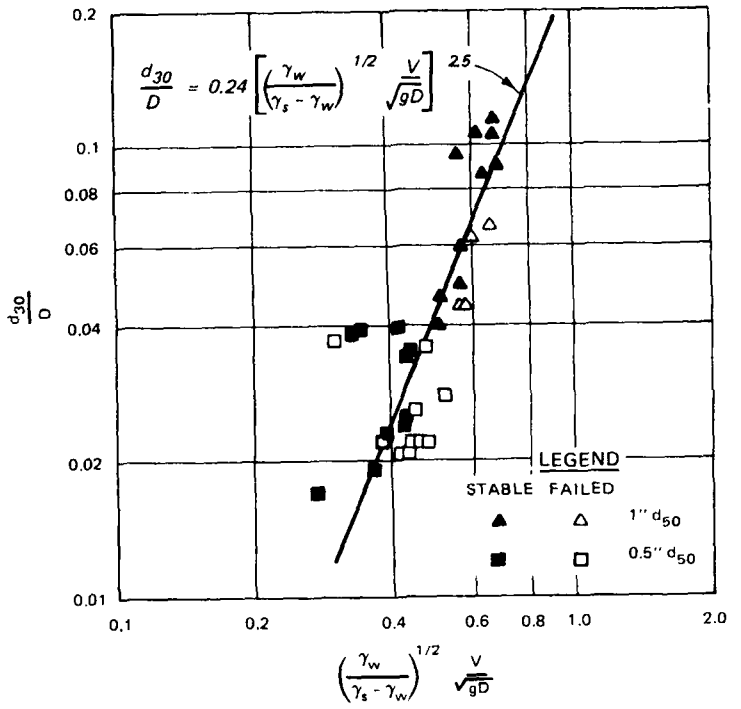

Figure 4.28. d_{30}/D versus modified Froude number, thickness of $1d_{100}$, 1V:2H side slope, CSU Phase IV (Data from Tables 4.17 and 4.18)

incipient failure, a thickness of $1d_{100}$, 1V:2H side slope, and straight channel is

$$\frac{d_{30}}{D} = 0.24\left[\left(\frac{\gamma_w}{\gamma_s - \gamma_w}\right)^{1/2} \frac{V}{\sqrt{gD}}\right]^{2.5} \qquad 4.26$$

based on the CSU Phase IV tests. This relation is in close agreement with the Dorena Dam prototype test results.

Results from the CSU tests with a thickness of $1.33d_{100}$ are shown in Figure 4.29. The effects of thickness for side slope riprap are

$$\frac{C_{12}(N = 1.33)}{C_{13}(N = 1.00)} = \frac{0.19}{0.24} = 0.79$$

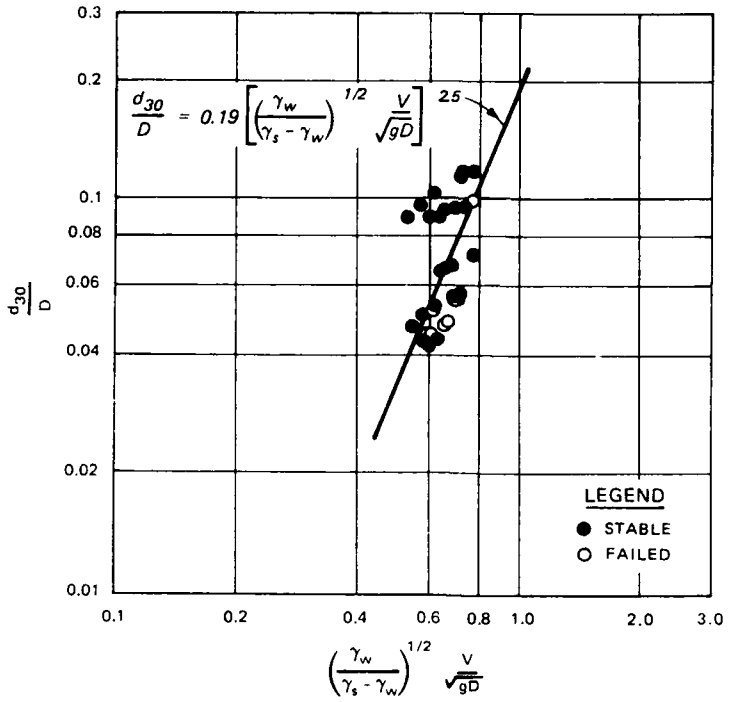

Figure 4.29. d_{30}/D versus modified Froude number, a thickness of $1.33d_{100}$, 1V:2H side slope, CSU Phase IV (Data from Table 4.16)

From Figure 4.15 the effect of thickness for bottom riprap is

$$\frac{C_{14}(N = 1.33)}{C_{15}(N = 1.00)} = \frac{0.225}{0.30} = 0.75$$

which is essentially the same thickness effect as the side slope riprap. Note that these thickness results apply only to gradations having a d_{85}/d_{15} ratio of 2-2.3.

A limited series of stability tests was conducted in the WES curved channel facility shown in Figure 4.24. These tests were limited in the sense that only a narrow range of rock size could be failed while maintaining a high enough Reynolds number based on the limitations given in section 3.5. Results are shown in Table 4.19 and Figure 4.30. With so few data points, the basic relation given by Equation 4.21 is used to define the slope of the power function. The relation describing the

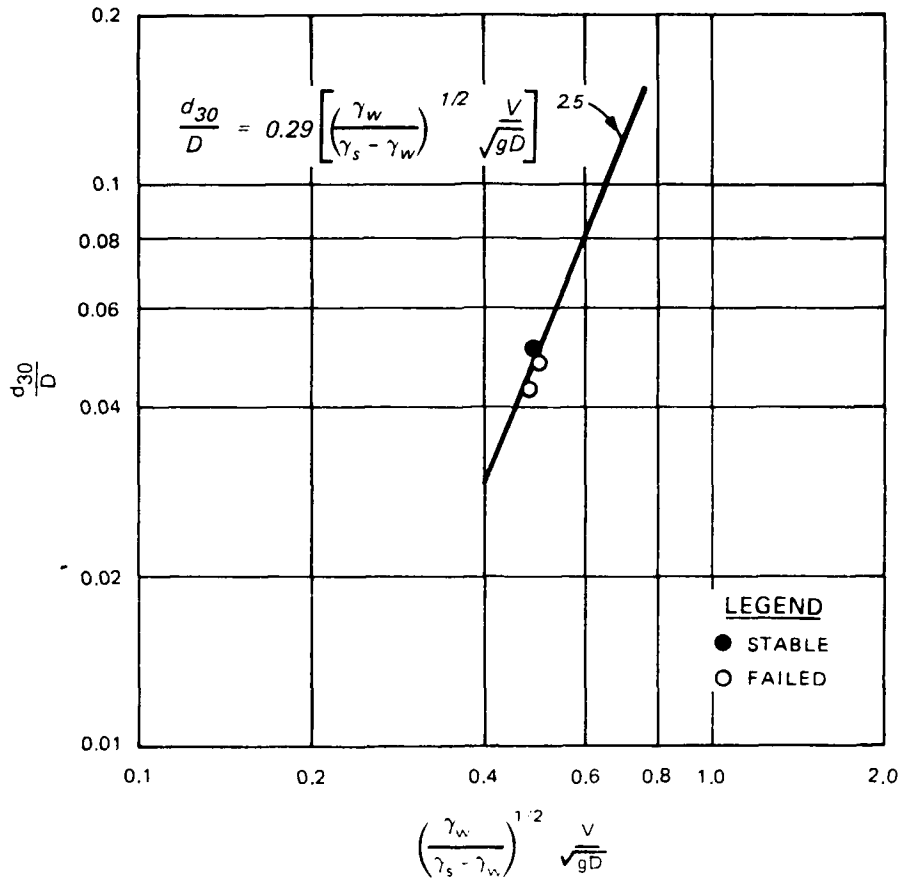

Figure 4.30. d_{30}/D versus modified Froude number, thickness of $1d_{100}$, 1V:2H side slope, WES curved channel (Data from Table 4.19)

threshold incipient failure for a thickness of $1d_{100}$, 1V:2H side slope, and curved channel is

$$\frac{d_{30}}{D} = 0.29\left[\left(\frac{\gamma_w}{\gamma_s - \gamma_w}\right)^{1/2} \frac{V}{\sqrt{gD}}\right]^{2.5} \qquad 4.27$$

based on the WES curved channel model using depth and average velocity over the toe of the side slope.

This model derived relationship can be compared to the prototype data of Blodgett and McConaughy (1986). These data were taken mainly from curved channels. Since side slope angle is generally considered to

be significant, only sites with the cotangent of the side slope angle between 1.8 and 2.2 were used in this analysis. To best estimate the average velocity and depth over the toe of the slope, the maximum depth and maximum velocity were used in the analysis. In cases where the maximum velocity was not measured, the relation

$$V_{max} = 1.53V_{avg} \qquad 4.28$$

was derived from the Blodgett and McConaughy data and used to estimate maximum velocity. A similar approach was used to estimate d_{30} for measurements where sufficient data were not given. The values used in the analysis are shown in Table 4.20 and Figure 4.31. Only sites with particle erosion or no damage were considered in the analysis. Blanket thicknesses are not given, and these results are considered applicable to a thickness of $1d_{100}$ since most prototype sites are constructed to this thickness. The incipient failure curve shown in Figure 4.31 is drawn to the right of two failure points (measurements 6 and 7). The site of these measurements was a channel curved only 18 deg. The failure for measurement 6 was on the upper 6 ft of the channel side slope, which is unusual. Blodgett and McConaughy state that the velocity for measurement 6 "may have been greater than estimated." The data for measurement 7 show a relatively low velocity but an extremely high shear stress. The high-water profile shows some unusual conditions such as an adverse water-surface slope over the point of failure. Considering these problems and the proximity of points 6 and 7 to other stable points, these failure points were not considered in the analysis. The resulting threshold of incipient failure curve for 1V:2H side slope, a thickness of $1d_{100}$, and curved channels is the same as that proposed for bottom riprap or

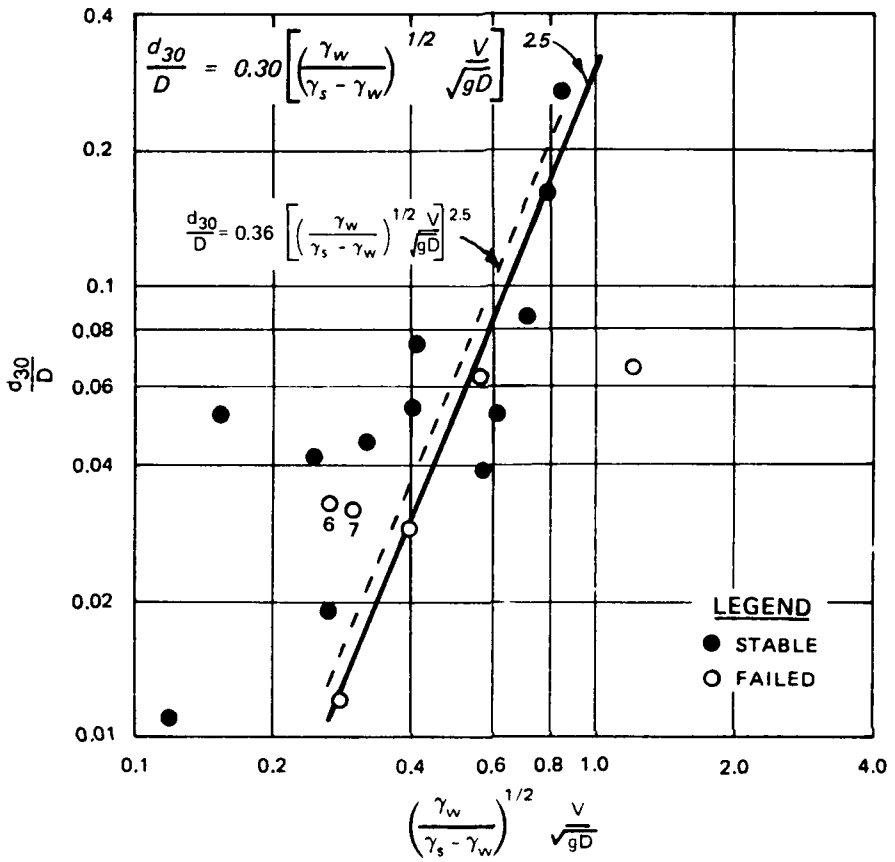

Figure 4.31. d_{30}/D versus modified Froude number, thickness of $1d_{100}$, 1V:1.8H to 1V:2.2H side slope, Blodgett and McConaughy (1986) prototype data (Data from Table 4.20)

$$\frac{d_{30}}{D} = 0.30\left[\left(\frac{\gamma_w}{\gamma_s - \gamma_w}\right)^{1/2} \frac{V}{\sqrt{gD}}\right]^{2.5} \qquad (4.21 \text{ bis})$$

which is in close agreement with the model relation determined in the WES curved channel model. This relation uses the depth and average velocity over the toe of the side slope.

CHAPTER 5

SAFETY FACTORS, SIZING NOMOGRAPH, AND DESIGN APPLICATION

5.1 SAFETY FACTORS

The threshold of incipient failure for bottom riprap and 1V:2H side slope riprap in curved channels was shown to be described by

$$\frac{d_{30}}{D} = 0.30 \left[\left(\frac{\gamma_w}{\gamma_s - \gamma_w} \right)^{1/2} \frac{V}{\sqrt{gD}} \right]^{2.5} \qquad \text{(4.21 bis)}$$

Until additional tests can be conducted to define the relationship for other side slopes, Equation 4.21 should be used for all slopes equal to or flatter than 1V:2H. This relation is applicable to a thickness of $1d_{100}$, which is the most common thickness used in open channel riprap. Since this relation describes incipient failure, a safety factor must be used in design. A common problem that should be avoided in design of riprap is the addition of safety factors at all steps in the design procedure. The use of available gradations often adds a safety factor to the design because the computed riprap size falls between two available gradations and the designer must choose the larger gradation. A safety factor of 1.2 times the d_{30} riprap size given by Equation 4.21 provides stability above the failure points used the analysis of the Blodgett and McConaughy prototype data. Using this safety factor yields

$$\frac{d_{30}}{D} = 0.36 \left[\left(\frac{\gamma_w}{\gamma_s - \gamma_w} \right)^{1/2} \frac{V}{\sqrt{gD}} \right]^{2.5} \qquad 5.1$$

This equation is shown by the dashed line in Figure 4.31.

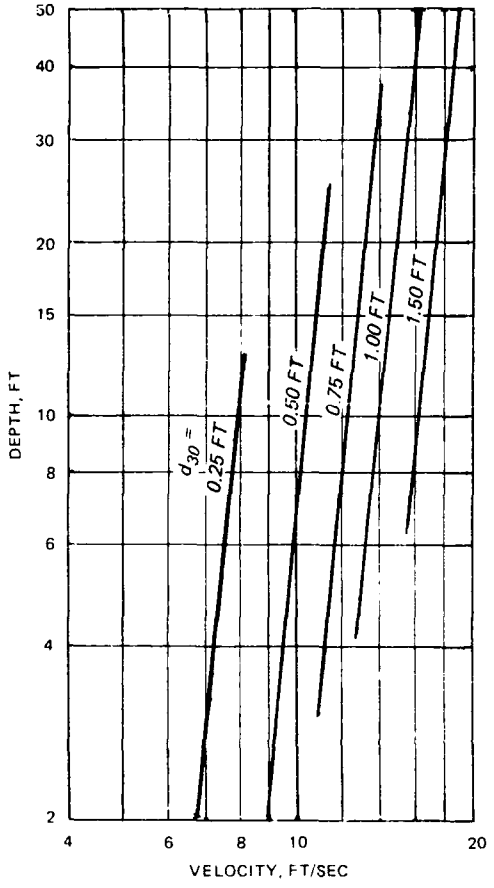

a. Velocity versus depth versus d_{30} for unit stone weight = 165 pcf, thickness = $1d_{100}$

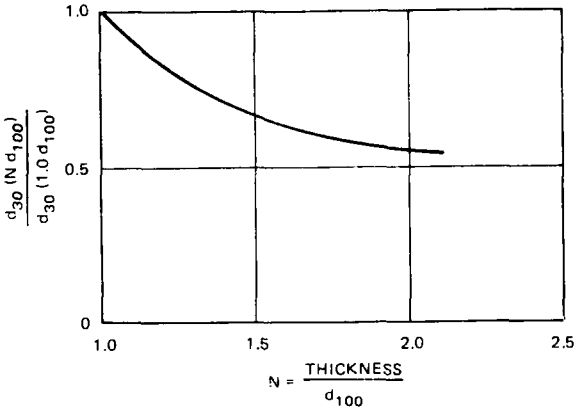

b. Thickness adjustment for d_{85}/d_{15} = 2.0-2.3

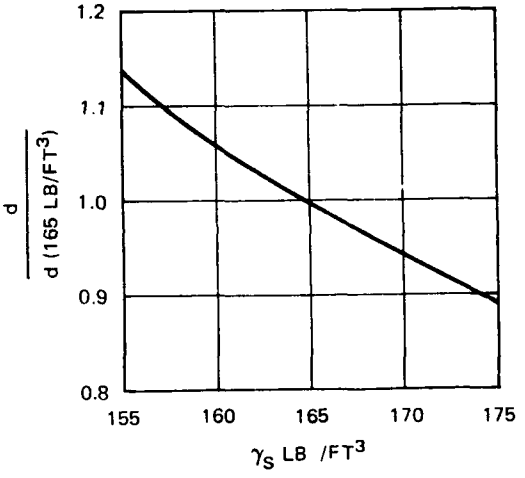

c. Correction for unit stone weight

Figure 5.1. Sizing nomograph for riprap

5.2 SIZING NOMOGRAPH

A sizing nomograph of Equation 5.1 is shown in Figure 5.1. In Figure 5.1a, the relationship of average velocity in the vertical, depth, and d_{30} are given for a specific weight of 165 pcf and a blanket thickness of $1d_{100}$. In Figure 5.1b, the adjustment for thickness is given for gradations having d_{85}/d_{15} = 2.0-2.3, which is similar to the gradations given in OCE (1971). In Figure 5.1c, the correction for unit weight of rock is given.

5.3 DESIGN APPLICATION

This design procedure is based on the premise that a variety of tools are available for estimating the average velocity in the vertical for use in this design procedure. The average velocity in the vertical at the point of interest is used, not average cross-section values. The available tools for determining velocities include the following:

1. Numerical Models: one-dimensional water-surface profile programs and multidimensional models
2. Physical models
3. Prototype measurements
4. Analytical techniques such as the California Division of Highways (1970) equation

$$V_{max} = 4/3(\text{Average Channel Velocity}) \qquad 5.2$$

which should be limited to prismatic channels, and the analysis of the data by Blodgett and McConaughy (1986) which gave the relation

$$V_{max} = 1.53(\text{Average Channel Velocity}) \qquad (4.28 \text{ bis})$$

which would be applicable to natural channels.

Analytical techniques that need to be developed include

V_{max} = f(average channel velocity, bend radius/ water-surface width, channel shape (natural or prismatic), side slope angle, aspect ratio, bend angle, different bed and bank roughness)

5.4 EXAMPLE DESIGN

Determine size of side slope riprap for the design problem at Pinole Creek given in Blodgett and McConaughy (1986) having the following conditions:

Average channel velocity = 7.7 ft/sec

Average depth = 4.8 ft

Maximum depth = 7.7 ft

γ_s = 175 pcf

Curved channel (radius/width = 2.5)

Water-surface width = 61 ft

Thickness = $1d_{100}$

Cotangent of side slope angle = 2

As in most riprap design problems, only the average channel velocity is known. The maximum average velocity in the vertical over the toe of the outer bank can be estimated by

$$V_{max} = 1.53V_{avg} = 11.78 \text{ ft/sec} \qquad (4.28 \text{ bis})$$

This velocity and the maximum depth are used in equation 5.1. The size required for stability is d_{30} = 0.64 ft . At Pinole Creek prototype, riprap having a d_{30} of 0.45 ft and a unit stone weight of 178 pcf failed under the given hydraulic conditions.

Using OCE (1971) gradations given in Table 4.21, a blanket thickness of 18 in. provides a d_{30} (minimum) of 0.73 ft for a unit stone weight of 175 pcf. A blanket thickness of 15 in. cannot be used because the d_{30} (minimum) of 0.61 ft is less than 0.64 ft.

For comparison, OCE (1970 and 1971) riprap sizing guidance using a constant Shields coefficient and the logarithmic velocity relations results in a d_{50} of 1.17 ft. The 24-in. blanket thickness given in Table 4.21 for a unit stone weight of 175 pcf provides a d_{50} (minimum) of 1.17 ft.

5.5 SUMMARY OF LIMITATIONS

This design procedure is limited to the following conditions:

1. Straight and curved open channels that are not immediately downstream of a structure that creates a hydraulic jump.
2. Channel bottoms and channel side slopes less than or equal to 1V:2H.
3. Slopes less than 2 percent, no overtopping embankment flows.
4. Froude number less than 1.2.
5. Ratio of flow depth to d_{30} riprap size from 4 to 50.
6. For thickness equal $1d_{100}$, d_{85}/d_{15}, less than or equal to 4.6. For thickness greater than $1d_{100}$, d_{85}/d_{15} from 2.0-2.3.
7. Angular rock.

CHAPTER VI

CONCLUSIONS AND RECOMMENDATIONS

This investigation has shown that a constant Shields coefficient and the logarithmic velocity laws are not applicable to such high relative roughness problems as riprap design.

The critical velocity relation developed in this study for the threshold of incipient failure of riprap is

$$\frac{d_{30}}{D} = C_{16} \left[\left(\frac{\gamma_w}{\gamma_s - \gamma_w} \right)^{1/2} \frac{V}{\sqrt{gD}} \right]^{2.5}$$

This relation was developed for straight channel bottoms, straight channel side slopes of 1V:2H, and curved channel side slopes of 1V:2H. Average velocity in the vertical at the point of interest is used, not average cross-sectional values. A relation of this form was first proposed by Neill (1967) and Bogardi (1968).

This critical velocity relation was compared to the two most common riprap sizing methods: (1) critical shear stress using a constant Shields coefficient and (2) Isbash type relations ($d_{50} = C_9 V^2$). This critical velocity relation has an exponent that falls halfway between these two methods.

Riprap gradation uniformity was shown to affect riprap stability if d_{50} is used in the analysis. Use of particle size d_{30} in the stability relations eliminates the effects of gradation uniformity for riprap thickness of $1d_{100}$ and is used as the characteristic size in this investigation.

Riprap thickness was shown to have a significant affect on riprap stability for riprap gradation having d_{85}/d_{15} of 2.1-2.3.

Within the range tested, riprap shape did not have a significant effect on riprap stability. Gradations having 18 percent elongated particles ($\ell/b > 3$) exhibited the same stability as gradations not having elongated particles.

Existing side slope relations used in the critical shear stress equation overestimate the decrease in stability that occurs when a particle is placed on a sloping bank. This was demonstrated in two ways:

1. Comparison with the Hudson (1958) wave equation that showed the effects of side slope angle are more significant in channel flow than in wave attack.
2. Stability tests on sloping sides conducted in this investigation. The existing side slope stability relations matched the observed data when a repose angle of 53 deg was used in the analysis instead of the commonly used 40 deg. This led to a series of repose angle tests which suggested that repose angle varies with revetment height, riprap thickness, surface texture, and placement method. Revetment height is important because the higher the bank, the greater the amount of material being supported by the rock at the toe of the slope. Because of these difficulties, repose angle was not used in the critical velocity relation and was included in the empirical coefficients just as Hudson did in his wave equation.

Comparison of velocity profiles over channel side slopes in straight and curved reaches shows that for the same average velocity

over the toe of the side slope, the velocity and shear stress on the side slope are significantly higher on the outer bank of the curved channel. Side slope stability tests in straight channels cannot be used in channel bends. The representative velocity used herein for side slope riprap stability is the average velocity in the vertical over the toe of the side slope. Maximum velocities in the curved channel tests occurred over the toe of the side slope.

Using depth and velocity over the toe of the side slope, the threshold of incipient failure of 1V:2H side slope riprap in straight channels is described by

$$\frac{d_{30}}{D} = 0.24 \left[\left(\frac{\gamma_w}{\gamma_s - \gamma_w} \right)^{1/2} \frac{V}{\sqrt{gD}} \right]^{2.5}$$

based on model and prototype data for thickness = $1d_{100}$.

For 1V:2H side slope riprap in curved channels

$$\frac{d_{30}}{D} = 0.30 \left[\left(\frac{\gamma_w}{\gamma_s - \gamma_w} \right)^{1/2} \frac{V}{\sqrt{gD}} \right]^{2.5}$$

based on model and prototype data for thickness of $1d_{100}$. This relation was also found applicable to bottom riprap in straight channels.

Since these relations define the threshold of incipient failure, safety factors must be determined before they can be used. A common problem in the design of riprap is the addition of safety factors at each step in the design procedure. A safety factor of 1.2 times the d_{30} riprap size given by the threshold of incipient failure curve is used in the sizing nomograph (Figure 5.1) developed in this investigation. The designer can easily use other safety factors and apply them to the incipient failure relations.

During this study, the following areas were identified as needing additional study relative to open channel riprap design:

1. Effects of blanket thickness for gradations other than those studied in this investigation.
2. Effects of riprap shape outside the range covered in this study, including the effects of surface texture such as stability of cobble particles.
3. Side slope stability tests of 1V:1.5H and 1V:3H.
4. Determining repose angle of riprap revetment so that it can be included in the design procedure.
5. Effect of revetment side slope height on stability. Side slope riprap in shallow channels may be much more stable than in deep channels due to the amount of material being supported by the toe of the slope.
6. Analytical methods for determining velocity in straight and curved channels for use in riprap sizing.
7. Using the experience of others involved in riprap design to better define appropriate safety factors.

REFERENCES

Anderson, A. G., Paintal, A. S., and Davenport, J. T. (1968). "Tentative design procedure for riprap lined channels." Project Report No. 96, St. Anthony Falls Hydraulic Laboratory, University of Minnesota, Minneapolis, Minn.

Anderson, A. G., Paintal, A. S., and Davenport, J. T. (1970). "Tentative design procedure for riprap-lined channels." National Cooperative Highway Research Program Report 108, University of Minnesota, Minneapolis, Minn.

Ashida, K., and Bayazit, M. (1973). "Initiation of motion and roughness of flows in steep channels." Proceedings, 15th Congress of the International Association on Hydraulic Research, 1, 475-484.

Barr, D. I., and Herbertson, J. G. (1966). Discussion of "Sediment transportation mechanics: initiation of motion," by Task Committee on Preparation of Sedimentation Manual, Journal of the Hydraulics Division, American Society of Civil Engineers, 92(HY6), 248-251.

Bathurst, J. C., Graf, W. H., and Cao, H. H. (1982). "Initiation of sediment transport in steep channels with coarse bed material." Proceedings of Euromech 156: Colloquium on Mechanics of Sediment Transport, Istanbul, 207-213.

Bayazit, M. (1976). "Free Surface Flow in a Channel of Large Relative Roughness." Journal of Hydraulic Research, International Association on Hydraulic Research, 14(2), 115-126.

Bayazit, M. (1982). "Flow structure and sediment transport mechanics in steep channels." Proceedings of Euromech 156: Colloquium on Mechanics of Sediment Transport, Istanbul, 197-206.

Bettess, R. (1984). "Initiation of sediment transport in gravel streams." Proceedings of the Institution of Civil Engineers, Technical Note 407, Part 2, 77.

Blench, T. (1966). Discussion of "Sediment transportation mechanics: initiation of motion," by Task Committee on Preparation of Sedimentation Manual, Journal of the Hydraulics Division, American Society of Civil Engineers, 92(HY5), 287-288.

Blodgett, J. C., and McConaughy, C. E. (1986). "Rock riprap design for protection of stream channels near highway structures; Vol 2, Evaluation of riprap design procedures." Water-Resources Investigations Report 86-4128, US Geological Survey, Sacramento, Calif.

Bogardi, J. L. (1968). "Incipient sediment motion in terms of critical mean velocity." Acta Technica Academiae Scientarium Hungaricae, Budapest, 62 (1-2), 1-24.

Bogardi, J. L. (1978). Sediment transport in alluvial streams. Akademiai Kiado, Budapest.

California Division of Highways. (1970). "Bank and shore protection in California highway practice." State of California, Department of Public Works, Sacramento, Calif.

Carter, A. C., Carlson, E. J., and Lane, E. W. (1953). "Critical tractive forces on channel side slopes in coarse, non-cohesive material." Hydraulic Laboratory Report No. HYD-366, US Bureau of Reclamation, Denver, Colo.

Chen, C. K., and Roberson, J. A. (1974). "Turbulence in wakes of roughness elements." Journal of the Hydraulics Division, American Society of Civil Engineers, 100(HY1), 53-67.

Christensen, B. A. (1972). "Incipient motion on cohesionless channel banks." Sedimentation, H. W. Shen, ed., 4-1--4-22, Fort Collins, Colo.

Coleman, H. W., Hodge, B. K., and Taylor, R. P. (1984). "A re-evaluation of Schlichting's surface roughness experiment." Journal of Fluids Engineering, American Society of Mechanical Engineers, 106, 60-65.

Coleman, N. L. (1981). "Velocity profiles with suspended sediment." Journal of Hydraulic Research, 19(3), 211-229.

Cooper, R. H. (1970). "A study of bed-material transport based on the analysis of flume experiments," thesis presented to the University of Alberta, Edmonton, Alberta, Canada, in partial fulfillment of the requirements for the degree of Doctor of Philosophy.

Daido, A. (1983). "Incipient motion and bed load of sediment in steep channel." International Association for Hydraulic Research, 20th Congress, Moscow, Seminar 2, 3, 293-296.

Dubuat, P. 1786. Principes d'Hydraulique. 2nd Edition, Paris.

Einstein, H. A. (1942). "Formulas for the transportation of bed load," Transactions, American Society of Civil Engineers, 107, 561-597.

Einstein, H. A., and El-Samni, E. A. 1949. "Hydrodynamic forces on a rough wall." Reviews of Modern Physics, 21(3), 520-524.

Escoffier, F. F. (1968). "Third summary of progress, riprap study." US Army Engineer Waterways Experiment Station, Vicksburg, Miss.

Fiuzat, A. A., Chen, Y. H., and Simons, D. B. (1982). "Stability tests of riprap in flood control channels." Prepared under Contract No. CER81-82AAF-YHC-DB556 by Colorado State University, Fort Collins, Colo., for the US Army Engineer Waterways Experiment Station, Vicksburg, Miss.

Fiuzat, A. A., and Richardson, E. V. (1983). "Supplemental stability tests of riprap in flood control channels." Prepared under Contract No. CER83-84AAF-EVR18 by Colorado State University, Fort Collins, Colo., for the US Army Engineer Waterways Experiment Station, Vicksburg, Miss.

Forchheimer, P. (1914). Hydraulik. Teubner, Leipzig/Berlin.

Gessler, J. (1971). "Beginning and ceasing of sediment motion," River Mechanics, Fort Collins, Colo., H. W. Shen, ed., 1, 7-1--7-22.

Grace, J. L., Jr., Calhoun, C. C., Jr., and Brown, D. N. (1973). "Drainage and erosion control facilities, field performance investigation," Miscellaneous Paper No. H-73-6, US Army Engineer Waterways Experiment Station, Vicksburg, Miss.

Graf, W. H. (1971). Hydraulics of Sediment Transport. McGraw-Hill, New York.

Hey, R. D. (1979). "Flow resistance in gravel-bed rivers," Journal of the Hydraulics Division, American Society of Civil Engineers, 105(HY9), 365-379.

Hudson, R. Y. (1958). "Design of quarry-stone cover layers for rubble-mound breakwaters." Research Report 2-2, US Army Engineer Waterways Experiment Station, Vicksburg, Miss.

Hughes, W. C., Urbonas, B., and Stevens, M. A. (1983). "Guidelines for the design of riprap channel linings." D. B. Simons Symposium on Erosion and Sedimentation, R. M. Li and P. S. Lagasse, Fort Collins, Colo., 4.106-4.127.

Isbash, S. V. (1935). "Construction of dams by dumping stones in flowing water." Translated by A. Dorijikov, US Army Engineer District, Eastport, Me.

Kamphius, J. W. (1974). "Determination of sand roughness for fixed beds." Journal of Hydraulic Research, International Association on Hydraulic Research, 12(2), 193-203.

Keulegan, G. H. (1938). "Laws of turbulent flow in open channels." Journal of Research of the National Bureau of Standards, Research Paper RP115, 21, 707-741.

Knight, D. W., and McDonald, J. A. (1979). "Hydraulic resistance of artificial strip roughness." Journal of the Hydraulics Division, American Society of Civil Engineers, 105(HY6), 675-690.

Lane, E. W. (1953). "Progress report on results of studies on the design of stable channels." Hydraulic Laboratory Report No. HYD-352, US Bureau of Reclamation, Denver, Colo.

Li, R. M., Simons, D. B., Blinco, P. H., and Samad, M. A. (1976). "Probabilistic approach to design of riprap for river bank protection." Symposium on Inland Waterways for Navigation, Flood Control, and Water Diversions, Colorado State University, Fort Collins, Colo., II, 1572-1591.

Maynord, S. T. (1978). "Practical riprap design." Miscellaneous Paper H-78-7, US Army Engineer Waterways Experiment Station, Vicksburg, Miss.

_____. "Open channel riprap design: incipient failure and friction coefficients for channel bottom riprap" (in preparation). US Army Engineer Waterways Experiment Station, Vicksburg, Miss.

Meyer-Peter, E., and Muller, R. (1948). "Formulas for bed-load transport." International Association for Hydraulic Structures Research, Second Meeting, Stockholm, Appendix 2, 39-64.

Miller, R. L., and Byrne, R. J. (1965). "The angle of repose of a single grain on a fixed rough bed." Prepared under Contract Nonr -2121(26) by the University of Chicago, Chicago, Ill., for Office of Naval Research.

National Crushed Stone Association. (1978). "Quarried stone for erosion and sediment control." Washington, D. C.

Neill, C. R. (1967). "Mean-velocity criterion for scour of coarse uniform bed-material." International Association on Hydraulic Research, 12th Congress, Paper C6, 3, C6.1-C6.9.

Neill, C. R. (1968). "Note on initial movement of coarse uniform bed-material." Journal of Hydraulic Research, International Association on Hydraulic Research, 6(2), 173-176.

Neill, C. R., and Hey, R. D. (1982). "Gravel-bed rivers: engineering problems." Gravel-Bed Rivers, R. D. Hey, J. C. Bathurst, and C. R. Thorne, ed., Wiley and Sons, Chichester, N. Y.

Neill, C. R., and Van Der Giessen. (1966). Discussion of "Sediment transportation mechanics: initiation of motion," by Task Committee on Preparation of Sedimentation Manual, Journal of the Hydraulics Division, American Society of Civil Engineers, 92(HY5), 280-287.

Office, Chief of Engineers, US Army. (1970). "Hydraulic design of flood control channels." EM 1110-2-1601, US Government Printing Office, Washington, D. C.

Office, Chief of Engineers, US Army. (1971). "Additional guidance for riprap channel protection." ETL 1110-2-120, US Government Printing Office, Washington, D. C.

Olivier, H. (1967). "Through and overflow rockfill dams - new design techniques." Proceedings of the Institution of Civil Engineers, 36 (7012), 433-471.

O'Loughlin, E. M., and McDonald, E. G. (1964). "Some roughness-concentration effects on boundary resistance." La Houille Blanche, 7, 773-782.

O'Loughlin, E. M., Mehrotra, S. C., Chang, Y. C., and Kennedy, J. F. (1970). "Scale effects in hydraulic model tests of rock protected structures." IIHR Report No. 124, Iowa Institute of Hydraulic Research, Iowa City, Ia.

Peterka, A. J. (1958). "Hydraulic design of stilling basins and energy dissipators." Engineering Monograph No. 25, US Bureau of Reclamation, Denver, Colo.

Reese, A. (1984). "Riprap sizing - four methods." Proceedings of the American Society of Civil Engineers Hydraulics Specialty Conference, Coeur d'Alene, Ida., 397-401.

Ruff, J. F., Shaikh, A., Abt, S. R., and Richardson, E. V. (1985). "Riprap tests in flood control channels." Prepared under Contract No. CER85-86-JFR-AS-SRA-EVR-17 by Colorado State University, Fort Collins, Colo., for the US Army Engineer Waterways Experiment Station, Vicksburg, Miss.

Ruff, J. F., Shaikh, A., Abt, S. R., and Richardson, E. V. (1987). "Riprap stability in side sloped channels." Prepared under Contract No. DACW39-83-C-0045, by Colorado State University, Fort Collins, Colo., for the US Army Engineer Waterways Experiment Station, Vicksburg, Miss.

Schoklitsch, A. (1914). Uber Schleppkraft und Geschiebebewegung. Engelmann, Leipzig.

_____. 1962. Handbuch des Wasserbaues. Springer-Verlag, Vienna.

Shen, H. W., and Lu, J. (1983). "Development and prediction of bed armoring." Journal of Hydraulic Engineering, American Society of Civil Engineers, 109(4), 611-629.

Shields, A. (1936). Application of Similarity Principles and Turbulence Research to Bed-load Movement. English translation by W. P. Ott and J. C. van Uchelon, California Institute of Technology, publication 167.

Simons, D. B., and Senturk, F. (1977). Sediment Transport Technology. Water Resources Publications, Fort Collins, Colo.

Stevens, M. A., and Simons, D. B. (1971). "Stability analysis for coarse granular material on slopes." River Mechanics, H. W. Shen, ed., Fort Collins, Colo., 1, 17-1--17-27.

Straub, L. G. (1953). "Dredge fill closure of Missouri River at Fort Randall." Proceedings of Minnesota International Hydraulics Convention, Minneapolis, Minn., 61-75.

Uram, E. M. (1981). "Analysis of the roughness function and wall law slope for rough surface turbulent boundary layers." Bioengineering, Fluids Engineering and Applied Mechanics Conference, American Society of Mechanical Engineers/American Society of Civil Engineers, Boulder, Colo., 81-FE-36, 1-9.

US Army Corps of Engineers. "Hydraulic design criteria." Prepared for Office, Chief of Engineers, by US Army Engineer Waterways Experiment Station, Vicksburg, Miss., issued serially since 1952.

US Army Engineer District, Portland. (1952). "High velocity revetment tests." Civil Works Investigation-485, Portland, Ore.

US Army Engineer Division, Lower Mississippi Valley. (1982). "Report on standardization of riprap gradations" (Revised). Vicksburg, Miss.

US Department of Transportation. (1975). "Design of stable channels with flexible linings." Hydraulic Engineering Circular No. 15, Federal Highway Administration, Washington, D. C.

Vanoni, V. A. (1977). "Sedimentation engineering." American Society of Civil Engineers Manuals and Reports on Engineering Practice No. 54, New York.

van Rijn, L. C. (1982). "Equivalent roughness of alluvial bed." Journal of the Hydraulics Division, American Society of Civil Engineers, Technical Note, 108(HY10), 1215-1218.

Yalin, M. S. (1965). "Similarity in sediment transport by currents." Hydraulics Research Paper No. 6, HM Stationery Office, London.

Yalin, M. S. (1977). Mechanics of sediment transport. Pergamon Press, Elmsford, N. Y.

Table 3.1

Model Riprap

Flume	Test Phase	d_{50} in.	Thickness	$\frac{d_{85}}{d_{15}}$	Gradation, in.	γ_s pcf
CSU	I	1.87	$1.0d_{100}$	2.8	Figure 3.4[a]	170
CSU	I	3.0	$1.0d_{100}$	3.9	Figure 3.4[a]	170
CSU	II	0.5	$1.0d_{100}$	4.6	Figure 3.5[b]	166
CSU	II	1.0	$1.0d_{100}$	4.6	Figure 3.5[b]	166
CSU	III	1.0	$1.4d_{100}$ & $2.1d_{100}$	2.1	Figure 3.6[c]	167
CSU	III	2.0	$1.4d_{100}$ & $2.1d_{100}$	2.3	Figure 3.6[c]	165
CSU	IV	0.5	$1.0d_{100}$	2.0	Figure 3.7[d]	167
CSU	IV	1.0	$1.0d_{100}$ & $1.3d_{100}$	2.3	Figure 3.7[d]	167
WES Trapezoidal	I	0.31	$1.5d_{100}$	2.0	OCE (1971)[e]	167
WES Trapezoidal	I	0.38	$1.5d_{100}$	2.0	OCE (1971)[e]	167
WES Trapezoidal	I	0.44	$1.5d_{100}$	2.0	OCE (1971)[e]	167
WES Tilting	I	0.86	$1.0d_{100}$	1.23	3/4-1	167
WES Tilting	I	0.61	$1.0d_{100}$	1.33	1/2-3/4	167
WES Tilting	I	0.43	$1.0d_{100}$	1.24	3/8-1/2	167

(Continued)

[a] See Figure 3.4 for gradation.
[b] See Figure 3.5 for gradation.
[c] See Figure 3.6 for gradation.
[d] See Figure 3.7 for gradation.
[e] See OCE (1971) for gradation.

Table 3.1 (Concluded)

Flume	Test Phase	d_{50} in.	Thickness	$\frac{d_{85}}{d_{15}}$	Gradation, in.	γ_s pcf
WES Tilting	I	0.30	$1.0d_{100}$	1.56	#4 - 3/8	167
WES Tilting	II	0.43	$1.0d_{100}$	2.5	33% 1/2-3/4 33% 3/8-1/2	167
WES Tilting	III	0.43	$1.0d_{100}$	2.5	33% #4 - 3/8	167
WES Tilting	III	0.61	$1.0d_{100}$	2.1	33% 3/4-1 33% 1/2-3/4 33% 3/8-1/2	167
WES Tilting	IV	0.30	Varied	1.56	#4 - 3/8	167
WES Curved	I	0.38	$1.0d_{100}$	2.0	50% #4 - 3/8 50% 3/8-1/2	167

Table 3.2

Shape Characteristics of Model Riprap

Test Rock	Rock Size, in.	Percent Greater than $\ell/b = 2.5$	Percent Greater than $\ell/b = 3$
WES	#4 - 1	29	17
CSU (1st test series)	2 - 6	16	7
CSU (2nd test series)	3/8 - 1-1/2	37	25
CSU (3rd test series)	#4 - 1-1/2	30	18
CSU (4th test series)	#4 - 1-1/2	30	18

Table 4.1

WES Tilting Flume, Phase I Test Results for d_{85}/d_{15} = 1.35, Thickness = $1.18d_{50} = 1d_{100}$ γ_s = 167 psf, Shape Characteristics Not Meeting Corps Guidance

Energy Slope ft/ft	Average Velocity ft/sec[a]	Average Depth ft	d_{30}/ft	d_{50}/ft	d_{90}/ft	Sieve Size, in.	Stable or Failed or Unknown[b]
0.01800	4.34	0.400	0.068	0.072	0.081	3/4-1	S
0.02000	4.45	0.405	0.068	0.072	0.081	3/4-1	F
0.01600	3.20	0.301	0.047	0.051	0.060	1/2-3/4	S
0.01700	3.23	0.290	0.047	0.051	0.060	1/2-3/4	F
0.02100	3.23	0.227	0.047	0.051	0.060	1/2-3/4	F
0.02100	2.90	0.228	0.047	0.051	0.060	1/2-3/4	S
0.00900	3.60	0.501	0.047	0.051	0.060	1/2-3/4	S
0.01000	3.80	0.470	0.047	0.051	0.060	1/2-3/4	F
0.01100	3.49	0.402	0.047	0.051	0.060	1/2-3/4	S
0.01200	3.58	0.391	0.047	0.051	0.060	1/2-3/4	F
0.01500	3.47	0.327	0.047	0.051	0.060	1/2-3/4	S
0.01600	3.56	0.319	0.047	0.051	0.060	1/2-3/4	F
0.02100	3.11	0.258	0.047	0.051	0.060	1/2-3/4	S
0.02100	3.17	0.263	0.047	0.051	0.060	1/2-3/4	F
0.00500	3.34	0.530	0.019	0.025	0.029	3/8-#4	F
0.00530	3.37	0.534	0.019	0.025	0.029	3/8-#4	F
0.00680	3.38	0.400	0.019	0.025	0.029	3/8-#4	?[c]
0.00800	3.52	0.389	0.019	0.025	0.029	3/8-#4	F
0.02100	3.06	0.131	0.019	0.025	0.029	3/8-#4	?
0.02200	3.11	0.129	0.019	0.025	0.029	3/8-#4	F
0.00900	2.44	0.205	0.019	0.025	0.029	3/8-#4	?
0.01000	2.53	0.198	0.019	0.025	0.029	3/8-#4	F
0.01200	3.17	0.210	0.019	0.025	0.029	3/8-#4	?
0.01300	3.26	0.204	0.019	0.025	0.029	3/8-#4	F
0.00570	2.59	0.325	0.019	0.025	0.029	3/8-#4	?
0.00700	2.75	0.303	0.019	0.025	0.029	3/8-#4	F
0.00940	3.75	0.310	0.019	0.025	0.029	3/8-#4	?
0.01000	2.71	0.220	0.019	0.025	0.029	3/8-#4	F
0.00500	2.82	0.402	0.019	0.025	0.029	3/8-#4	?
0.00600	3.03	0.377	0.019	0.025	0.029	3/8-#4	F
0.00400	2.88	0.487	0.019	0.025	0.029	3/8-#4	?
0.00500	3.00	0.461	0.019	0.025	0.029	3/8-#4	F

(Continued)

[a] Velocity based on discharge/area.
[b] S = stable; F = failed; ? = unknown.
[c] Stable but tested for a short duration compared to the other tests.
[d] Width/depth < 5.

Table 4.1 (Concluded)

Energy Slope ft/ft	Average Velocity ft/sec[a]	Average Depth ft	d_{30}/ft	d_{50}/ft	d_{90}/ft	Sieve Size, in.	Stable or Failed or Unknown[b]
0.00300	2.73	0.633[d]	0.019	0.025	0.029	3/8-#4	?
0.00400	2.95	0.589	0.019	0.025	0.029	3/8-#4	F
0.00500	3.28	0.564	0.034	0.036	0.041	1/2-3/8	F
0.00390	2.93	0.591	0.034	0.036	0.041	1/2-3/8	S
0.00800	3.06	0.368	0.034	0.036	0.041	1/2-3/8	F
0.00900	3.23	0.353	0.034	0.036	0.041	1/2-3/8	S
0.00700	2.93	0.386	0.034	0.036	0.041	1/2-3/8	S
0.01810	2.77	0.181	0.034	0.036	0.041	1/2-3/8	S
0.01950	2.82	0.178	0.034	0.036	0.041	1/2-3/8	F
0.00930	2.91	0.297	0.034	0.036	0.041	1/2-3/8	?
0.01000	2.95	0.293	0.034	0.036	0.041	1/2-3/8	F
0.00900	2.82	0.306	0.034	0.036	0.041	1/2-3/8	S
0.00520	3.03	0.494	0.034	0.036	0.041	1/2-3/8	?
0.00600	3.28	0.463	0.034	0.036	0.041	1/2-3/8	F

[a] Velocity based on discharge/area.
[b] S = stable; F = failed; ? = unknown.

Table 4.2

CSU Phase I,

Test Results for d_{85}/d_{15} = 2.8, Thickness = $2d_{50}$ = $1d_{100}$,

d_{50} = 1.87 in., γ_s = 170 pcf, Angular Particles, Does Not

Meet Corps Shape Guidance

Run No.	Orifice Discharge cfs	Flume Slope	Average Velocity fps	Average Depth ft	Stable (S) or Failed (F)
1	25	0.00852	3.62	0.825	S
2		0.01378	4.34	0.687	S
3		0.01667	4.62	0.653	F
4		0.01973	5.11	0.629	S
5	50	0.00761	4.78	1.218	S
6		0.01089	5.24	1.110	S
7		0.01451	5.92	1.032	F
8		0.01266	6.01	1.051	F
9		0.01089	5.35	1.151	F
10	75	0.00537	5.39	1.868[a]	S
11		0.00769	5.38	1.716[a]	S
12		0.01025	5.92	1.509	F
13		0.00894	5.64	1.604[a]	F
14		0.00769	5.39	1.700[a]	S
15	100	0.00420	5.39	2.325[a]	S
16		0.00601	5.32	2.111[a]	S
17		0.00801	6.03	2.010[a]	F
18		0.00699	5.86	2.012[a]	F
19		0.00601	5.68	2.062[a]	S

[a] Width/depth < 5 .

Table 4.3

CSU Phase II,

Test Results for d_{85}/d_{15} = 2.5, Thickness = $2d_{50}$ = $1d_{100}$,

d_{50} = 0.5 in., γ_s = 166 pcf

Run No.	Nominal Discharge cfs	Flume Slope	Average Velocity fps	Average Depth ft	Stable (S) or Failed (F)
1	25	0.00143	1.763	1.434	S
2	25	0.00185	2.269	1.335	S
3	25	0.00231	2.391	1.277	S
4	25	0.00280	2.779	1.106	S
5	25	0.00331	2.940	1.021	F
6	25	0.00331	3.147	0.922	F
7	25	0.00280	3.212	1.201	F
8	25	0.00231	3.155	1.030	F
9	50	0.00102	3.022	1.961[a]	F
10	50	0.00128	3.135	1.894[a]	F
12	50	0.00102	3.085	2.047[a]	F
13	75	0.00072	3.410	2.958[a]	F
14	75	0.00090	3.610	2.724[a]	F
15	75	0.00072	3.372	2.855[a]	F
16	75	0.00056	3.154	3.026[a]	S
17	100	0.00056	3.469	3.550[a]	S

[a] Width/depth < 5 .

Table 4.4

CSU Phase III,

Test Results for d_{85}/d_{15} = 2.1, Thickness = $2d_{50}$ = $1.4d_{100}$,

d_{50} = 1 in., γ_s = 167 pcf, Shape Characteristics

Meeting Corps Guidance

Run No.	Nominal Discharge cfs	Flume Slope	Average Velocity fps	Average Depth ft	Stable (S) or Failed (F)
33	25	0.00998	4.40	0.684	S
34	25	0.01088	4.51	0.703	S
35	25	0.01186	4.72	0.672	S
36	25	0.01337	4.95	0.618	F
37	25	0.01204	4.77	0.651	F
32	50	0.00558	4.90	1.300	F
41	50	0.00475	4.71	1.353	F
38	75	0.00402	5.02	1.832[a]	F
39	75	0.00377	5.00	1.842[a]	F
40	75	0.00345	4.84	1.918[a]	S
42	100	0.00314	4.97	2.371[a]	S
43	100	0.00403	4.90	2.415[a]	S
44	100	0.00436	5.20	2.210[a]	F
45	100	0.00354	5.09	2.332[a]	F

[a] Width/depth < 5 .

Table 4.5

CSU Phase III,

Test Results for d_{85}/d_{15} = 2.3, Thickness = $2d_{50}$ = $1.4d_{100}$,

d_{50} = 2 in., γ_s = 165 pcf, Shape Characteristics

Meeting Corps Guidance

Run No.	Nominal Discharge cfs	Flume Slope	Average Velocity fps	Average Depth ft	Stable (S) or Failed (F)
76	25	0.01193	4.55	0.681	S
77	25	0.01858	5.27	0.598	S
65	50	0.00998	5.03	1.246	S
66	50	0.01378	6.13	1.019	S
67	50	0.01519	6.36	0.987	S
68	50	0.01796	6.71	0.935	S
69	50	0.01888	6.63	0.948	F
78	50	0.01579	6.14	1.022	F
70	75	0.01110	6.65	1.410	F
71	75	0.00781	6.33	1.483	S
72	75	0.00937	6.81	1.423	S
73	100	0.00731	6.43	1.954[a]	S
74	100	0.00840	6.62	1.891[a]	S
75	100	0.01066	7.00	1.804[a]	F

[a] Width/depth < 5 .

Table 4.6

CSU Phase III,

Test Results for d_{85}/d_{15} = 2.1, Thickness = $3d_{50}$ = $2.1d_{100}$,

d_{50} = 1 in., γ_s = 167 pcf, Shape Characteristics

Meeting Corps Guidance

Run No.	Nominal Discharge cfs	Flume Slope	Average Velocity fps	Average Depth ft	Stable (S) or Failed (F)
46	25	0.00880	4.37	0.720	S
47	25	0.01011	4.61	0.688	S
48	25	0.01313	5.02	0.640	S
57	25	0.01475	5.02	0.625	S
58	25	0.01626	5.52	0.568	F
49	50	0.00526	4.94	1.268	S
50	50	0.00636	5.36	1.169	S
52	50	0.00726	5.74	1.096	S
53	50	0.00802	5.66	1.095	F
54	50	0.00732	5.64	1.111	F
55	50	0.00732	5.03	1.245	F
56	50	0.00647	5.11	1.231	S
59	75	0.00423	4.90	1.907[a]	S
60	75	0.00517	5.11	1.814[a]	S
61	75	0.00621	5.50	1.714[a]	F
62	100	0.00406	4.63	2.513[a]	S
63	100	0.00457	5.25	2.210[a]	F
64	100	0.00409	5.10	2.298[a]	S

[a] Width/depth < 5 .

Table 4.7

CSU Phase III,

Test Results for d_{85}/d_{15} = 2.3, Thickness = $3d_{50}$ = $2.1d_{100}$,

d_{50} = 2 in., γ_s = 165 pcf, Shape Characteristics

Meeting Corps Guidance

Run No.	Nominal Discharge cfs	Flume Slope	Average Velocity fps	Average Depth ft	Stable (S) or Failed (F)
79	25	0.01180	4.42	0.710	S
80	25	0.01870	5.17	0.607	S
81	50	0.01205	5.90	1.068	S
82	50	0.01544	6.47	0.966	S
83	50	0.01724	6.76	0.928	S
84	50	0.01879	6.61	0.970	S
85	75	0.00898	6.19	1.519	S
86	75	0.01095	6.58	1.414	S
87	75	0.01206	6.63	1.423	S
88	75	0.01359	6.88	1.372	S
89	75	0.01565	6.84	1.399	F
90	100	0.00866	6.97	1.808[a]	S
91	100	0.00938	6.96	1.796[a]	S
92	100	0.01084	7.39	1.711[a]	S
93	100	0.01189	7.44	1.698[a]	S
94	100	0.01300	8.02	1.572	F

[a] Width/depth < 5 .

Table 4.8

CSU Phase I,

Test Results for d_{85}/d_{15} = 3.9, Thickness = $2d_{50}$ = $1d_{100}$,

d_{50} = 3 in., γ_s = 170 pcf, Angular Particles, Does Not

Meet Corps Shape Guidance

Run No.	Orifice Discharge cfs	Flume Slope	Average Velocity fps	Average Depth ft	Stable (S) or Failed (F)
1	25	0.02000	4.51	0.655	S
2	50	0.01544	5.55	1.064	S
3		0.02000	6.09	1.026	S
4	75	0.01500	6.60	1.348	F
5		0.01719	6.55	1.363	F
6		0.01500	6.72	1.387	F
7		0.01291	6.41	1.401	S
8	100	0.01009	6.14	1.831[a]	S
9		0.01343	6.54	1.703[a]	F
10		0.01172	6.37	1.825[a]	F

[a] Width/depth < 5 .

Table 4.9

CSU Phase II,

Test Results for d_{85}/d_{15} = 4.6, Thickness = $2d_{50}$ = $1d_{100}$,

d_{50} = 1 in., γ_s = 166 pcf

Run No.	Nominal Discharge cfs	Flume Slope	Average Velocity fps	Average Depth ft	Stable (S) or Failed (F)
1	25	0.00348	2.952	1.047	S
3	25	0.00451	3.027	0.978	S
4	25	0.00562	3.427	0.848	F
5	25	0.00451	3.373	0.926	F
6	50	0.00249	3.568	1.689[a]	F
7	50	0.00310	3.653	1.581	F
8	50	0.00249	3.880	1.660[a]	F
10	75	0.00176	3.922	2.561[a]	F
11	75	0.00219	4.119	2.416[a]	F
12	75	0.00265	4.360	2.284[a]	F
13	75	0.00219	4.056	2.478[a]	F
14	75	0.00176	3.796	2.442[a]	S
15	100	0.00106	3.710	3.310[a]	F

[a] Width/depth < 5 .

Table 4.10

CSU Phase II,

Test Results for $d_{85}/d_{15} = 2.1$, Thickness = $2d_{50} = 1.4d_{100}$,

d_{50} = 1 in., γ_s = 167 pcf, Shape Characteristics

Not Meeting Corps Guidance

Run No.	Nominal Discharge cfs	Flume Slope	Average Velocity fps	Average Depth ft	Stable (S) or Failed (F)
1	25	0.00367	2.57	1.273	S
2	25	0.00490	3.55	0.906	S
3	25	0.00617	3.87	0.846	S
4	25	0.00749	4.22	0.745	S
5	25	0.00872	4.45	0.714	F
6	25	0.01012	4.59	0.689	F
7	25	0.00869	4.77	0.714	S
28	50	0.00409	3.85	1.386	S
29	50	0.00490	4.30	1.262	S
30	50	0.00561	4.76	1.252	F
31	50	0.00561	5.06	1.262	S
20	75	0.00284	5.03	2.018[a]	S
21	75	0.00333	5.14	1.886[a]	S
22	75	0.00407	4.64	1.802[a]	F
23	75	0.00343	5.02	1.885[a]	S
24	100	0.00225	4.86	2.479[a]	S
25	100	0.00266	4.62	2.397[a]	S
26	100	0.00308	5.15	2.286[a]	F
27	100	0.00318	5.06	2.337[a]	F

[a] Width/depth < 5 .

Table 4.11

WES Tilting Flume, Phase II

Bottom Slope ft/ft	Average Velocity ft/sec	Average Depth, ft	d_{50}/ft	d_{90}/ft
0.00100	1.62	0.707[a]	0.036	0.055
0.00200	1.90	0.647[a]	0.036	0.055
0.00300	2.34	0.592	0.036	0.055
0.00400	2.52	0.547	0.036	0.055
0.00500	2.75	0.517	0.036	0.055
0.00600	2.98	0.497	0.036	0.055
0.00700	3.06	0.477	0.036	0.055
0.00900	3.23	0.427	0.036	0.055

NOTE: These resistance tests were conducted using riprap with one-third (by weight) 3/4-1/2 in., one-third 1/2-3/8 in., and one-third 3/8 in.-#4. The stone had thickness of $1d_{100}$. Velocity was based on the average of two vertical profiles taken at the flume center line. Stability was not studied in these tests.

[a] Width/depth < 5 .

Table 4.12

WES Tilting Flume, Phase III

Bottom Slope ft/ft	Average Velocity, ft/sec	Average Depth, ft	d_{50}/ft[a]	d_{90}/ft
0.00300	1.94	0.346	0.036	0.055
0.00400	2.09	0.320	0.036	0.055
0.00500	2.26	0.296	0.036	0.055
0.00600	2.38	0.279	0.036	0.055
0.00700	2.99	0.407	0.036	0.055
0.01600	2.72	0.207	0.036	0.055
0.00200	2.10	0.582	0.036	0.055
0.00250	2.37	0.538	0.036	0.055
0.00300	2.48	0.511	0.036	0.055
0.00350	2.60	0.490	0.036	0.055
0.00400	2.69	0.466	0.036	0.055
0.00200	1.73	0.423	0.036	0.055
0.00300	1.96	0.369	0.036	0.055
0.00400	2.16	0.338	0.036	0.055
0.00500	2.28	0.314	0.036	0.055
0.00600	2.40	0.298	0.036	0.055
0.00200	2.06	0.624[b]	0.036	0.055
0.00250	2.16	0.585	0.036	0.055
0.00300	2.33	0.548	0.036	0.055
0.00350	2.54	0.513	0.036	0.055
0.00300	1.81	0.353	0.051	0.076
0.00400	2.07	0.323	0.051	0.076
0.00500	2.26	0.298	0.051	0.076
0.00600	2.42	0.287	0.051	0.076
0.00200	2.12	0.580	0.051	0.076
0.00300	2.30	0.531	0.051	0.076
0.00400	2.55	0.488	0.051	0.076
0.00500	2.76	0.446	0.051	0.076
0.01300	3.50	0.379	0.051	0.076
0.01200	3.70	0.425	0.051	0.076

NOTE: These resistance tests were conducted with stone having a thickness equal to $1d_{100}$. Velocity was based on the average of four vertical velocity profiles. Stability was not studied in these tests.

[a] Gradation used for d_{50} = 0.036 ft was same as WES Phase II tests. Gradation used for d_{50} = 0.051 ft was one-third 3/4-1 in., one-third 1/2-3/4 in., and one-third 3/8-1/2 in.

[b] Width/depth < 5 .

Table 4.13

Side Slope Versus Critical Bottom Velocity

Slope	Critical Bottom Velocity, ft/sec
Horizontal	2.64
	2.58
	2.53
1V:4H	2.63
	2.58
	2.63
1V:2.75H	2.51
	2.58
	2.61
	2.61
1V:2H	2.41
	2.44
	2.41
	2.46
1V:1.5H	2.15
	2.20
1V:1.25H	2.06
	2.06
	1.87
	1.94
	1.91
	2.00

Table 4.14

Angle of Repose

Pressure Fluctuations	Submerged	Revetment Thickness $\frac{d}{d_{100}}$	Revetment Height $\frac{L_s}{d_{50}}$	Surface	No. of Tests	Average Angle of Repose deg
No	No	1.0	10.4	Sand	14	52.3
No	Yes	1.0	10.4	Sand	14	52.8
Yes	Yes	1.0	10.4	Sand	21	53.5
Yes	Yes	1.0	10.4	Smooth	10	54.3
Yes	Yes	1.0	20.8	Sand	9	47.5
Yes	Yes	1.0	20.8	Smooth	9	50.5
Yes	Yes	1.0	41.7	Sand	8	42.3
Yes	Yes	1.0	41.7	Smooth	9	42.5
Yes	Yes	1.5	41.7	Smooth	12	46.3
Yes	Yes	2.0	41.7	Smooth	7	48.8

Table 4.15

Analysis of Dorena Dam Prototype Data

1V:2H Side Slope, Straight Channel

Test	Station	Right or Left Bank	Gradation[a]	Estimated V Over Toe	Depth Over Toe	$\left(\frac{\gamma_w}{\gamma_s-\gamma_w}\right)^{1/2}\frac{V}{\sqrt{gD}}$	$\frac{d_{30}}{D}$	Failed or Stable
3	2+80	L	A	7.1	7.3	0.34	0.067	S
3	2+80	R	B	7.1	7.3	0.34	0.084	S
3	3+46	L	A	11.5	6.6	0.58	0.074	S
3	3+46	R	B	10.5	6.6	0.53	0.092	S
3	3+90	L	C	14.5	6.0	0.77	0.095	F
3	3+90	R	D	14.5	6.0	0.77	0.120	S
3	4+12	L	C	13.0	6.7	0.65	0.085	S
3	4+12	R	D	13.0	6.7	0.65	0.107	S
3	4+75	L&R	D	15.0	6.3	0.77	0.114	F
4	3+46	L	A	10.9	6.6	0.55	0.074	S
4	3+46	R	B	10.9	6.6	0.55	0.092	S
4	4+12	L	C	13.0	6.7	0.65	0.085	S
4	4+12	R	D	13.0	6.7	0.65	0.107	S

[a] Rock Characteristics:

Gradation	d_{30} ft	d_{100} ft	Thickness / d_{100}
A	0.49	1.08	1.08
B	0.61	1.28	1.02
C	0.57	?	?
D	0.72	1.79	1.12

Table 4.16

CSU Phase IV

Test Results for d_{85}/d_{15} = 2.3, Thickness = $1.3d_{100}$, d_{50} = 1 in., γ_s = 167 pcf, Shape Characteristics Not Meeting Corps Criteria

Run No.[a]	Discharge, cfs	Water-Surface Slope, ft/ft	Average Velocity Over Toe of Slope ft/sec	Average Depth, Over Toe, ft	Stable (S) or Failed (F)	
					Bottom	Side Slope
1	15	0.00768	3.44	0.81	S	S
3	15	0.00929	3.59	0.76	S	S
4	15	0.01127	3.73	0.70	F	S
5	15	0.01077	4.15	0.64	F	S
6	15	0.00907	4.18	0.64	F	S
7	15	0.00957	4.40	0.62	S	S
12	20	0.00491	3.91	0.81	S	S
13	20	0.00804	4.19	0.78	S	S
14	20	0.00945	4.41	0.77	S	S
15	20	0.01074	4.61	0.77	F	S
16	30	0.00685	4.86	1.11	S	S
17	30	0.00723	4.97	1.09	S	S
18	30	0.00677	5.13	1.07	S	S
19	30	0.00796	5.55	1.00	F	S
20	40	0.00515	4.87	1.51	S	S
21	40	0.00595	4.98	1.42	S	S
22	40	0.00536	5.25	1.36	S	S
23	40	0.00669	5.61	1.28	S	F
25	40	0.00729	5.76	1.26	F	F
8	50	0.00547	5.47	1.57	S	F
9	50	0.00498	5.46	1.58	S	F
10	50	0.00526	5.45	1.60	F	S
11	50	0.00292	5.56	1.64	S	S

(Continued)

[a] Test numbers omitted did not have velocities measured over toe.

Table 4.16 (Concluded)

Run No.[a]	Discharge, cfs	Water-Surface Slope, ft/ft	Average Velocity Over Toe of Slope ft/sec	Average Depth, Over Toe, ft	Stable (S) or Failed (F)	
					Bottom	Side Slope
29	50	0.00451	5.77	1.61	--b	S
30	50	0.00449	5.89	1.50	--b	F
31	40	0.00560	5.71	1.28	--b	F
33	20	0.00921	4.15	0.81	--b	S
34	20	0.01112	4.64	0.76	--b	S
35	20	0.01310	4.77	0.74	--b	F

[a] Test numbers omitted did not have velocities measured over toe.
[b] Bottom fixed with wire mesh to ensure side slope failure.

Table 4.17

CSU Phase IV

Test Results for d_{85}/d_{15} = 2.3, Thickness = $1d_{100}$, d_{50} = 1 in., γ_s = 167 pcf, Shape Characteristics Not Meeting Corps Criteria

Run No.	Discharge, cfs	Water-Surface Slope, ft/ft	Average Velocity Over Toe of Slope ft/sec[a]	Average Depth Over Toe, ft	Stable (S) or Failed (F) Bottom	Side Slope
36	15	--[b]	3.54	0.76	S	S
37	15	0.01002	3.73	0.68	S	S
38	15	0.01165	3.91	0.64	F	S
39	15	0.01090	4.03	0.69	S	S
40	20	0.00900	4.42	0.80	F	S
41	20	0.00832	4.26	0.84	S	S
42	30	0.00711	4.97	1.09	F	F
43	30	0.00482	4.56	1.20	S	S[c]
44	30	0.00649	4.68	1.16	F	F[c]
45	40	0.00464	4.93	1.45	F	S
46	40	0.00408	4.62	1.54	S	S
47	50	0.00287	4.93	1.77	S	S[c]
48	50	0.00434	5.27	1.63	F	F[c]
49	50	--[b]	5.36	1.63	S	F
50	50	--[b]	5.46	1.61	F	F

[a] Estimated from results given in Table 4.16.
[b] Not determined.
[c] Failed area less than 0.1 ft^2.

Table 4.18

CSU Phase IV

Test Results for d_{85}/d_{15} = 2.0, Thickness = $1d_{100}$, d_{50} = 0.5 in., γ_s = 167 pcf, Shape Characteristics Not Meeting Corps Criteria

Run No	Discharge, cfs	Water-Surface Slope, ft/ft	Average Velocity Over Toe of Slope ft/sec	Average Depth Over Toe, ft	Stable (S) or Failed (F)	
					Bottom	Side Slope
1	15	0.00203	2.15	1.02	S	S
2	15	0.00269	2.31	0.93	S	S
3	15	0.00207	2.39	0.91	F	S
5	15	0.00197	2.87	0.91	S	S
21	15	0.00375	2.50	0.97	S	F[a]
15	20	0.00295	3.24	1.07	S	S
16	20	0.00400	3.46	1.00	F	F
17	20	0.00347	3.25	1.03	S	S
10	30	0.00242	3.51	1.54	S	S
11	30	0.00234	3.75	1.48	S	S
12	30	0.00221	3.55	1.57	S	F
13	30	0.00206	3.73	1.43	S	S
14	30	0.00322	3.83	1.39	F	F
23	30	0.00270	4.27	1.29	F	F
18	35	0.00240	3.88	1.68	S	F
19	35	0.00250	4.08	1.62	S	F
6	40	0.00241	4.38	1.62	F	F
7	40	0.00170	4.28	1.65	F	F
8	40	0.00268	4.10	1.70	F	F
9	40	0.00159	3.63	1.88	S	S
22	40	0.00158	2.93	2.17	S	S

[a] Failed area less than 0.10 ft^2

Table 4.19

Test Results From WES Curved Channel Model

Discharge cfs	Average Velocity Over Toe of Slope ft/sec[a]	Average Depth Over Toe, ft	Stable (S) or Failed (F)	Number of 6-Hour Runs
7.0	2.44	0.47	S	10
8.0	2.57	0.50	F	1
9.0	2.62	0.56	F	3

[a] For stable runs this was the maximum average velocity in the vertical over the toe. For failure, run velocity was measured at the location of the failure. Failure points and maximum velocities were always between stations 70 and 75.

Table 4.20

Prototype Data

(From Blodgett and McConaughy (1986))

Measurement Number	d_{30} ft	$\frac{d_{30}}{D_{max}}$	$\frac{d_{85}}{d_{15}}$	V_{max}, ft/sec	$\left(\frac{\gamma_w}{\gamma_s-\gamma_w}\right)^{1/2} \frac{V_{max}}{\sqrt{gD_{max}}}$	Stable (S) or Failure (F)	cot
2	0.54	0.011	2.0	6.17	0.119	S	1.9
5	0.55	0.045	2.5	8.17	0.320	S	1.8
6	0.55	0.033	2.5	7.97	0.266	F	1.8
7	0.55	0.032	2.5	9.33[a]	0.300	F	1.8
8	0.46	0.063	2.7	11.75[a]	0.564	F	2.0
9	1.75	0.273	--[b]	16.22[a]	0.842	S	2.1
10	0.42	0.075	3.0	7.43	0.412	S	2.1
14	0.52	0.042	--[b]	6.46[a]	0.243	S	2.1
15	0.52	0.054	--[b]	9.46	0.402	S	2.1
22	0.63	0.052	--[b]	15.90[a]	0.611	S	2.0
25	0.63	0.066	--[b]	27.24[a]	1.205	F	1.9
27	1.12	0.052	1.6	5.2	0.153	S	2.0
28	1.12	0.039	1.6	22.34	0.569	S	2.0
33	1.05	0.086	2.8	19.05[a]	0.713	S	2.0
34	1.05	0.162	2.8	15.30[a]	0.784	S	2.0
37	0.38	0.019	2.1	8.54	0.264	S	1.8
38	0.38	0.012	2.1	11.17[a]	0.278	F	1.8
39	0.38	0.029	2.1	10.25[a]	0.397	F	1.8

[a] Estimated using Equation 4.28.
[b] Not given.

Table 4.21

Gradations for Riprap Placement in the Dry, Low-Turbulence Zones

Riprap Thickness, in.	Limits of Stone Weight, lb[a] Percent Lighter by Weight 100 Max	100 Min	50 Max	50 Min	15 Max	15 Min	d_{30}(min) ft
			Specific Weight = 155 pcf				
12	81	32	24	16	12	5	0.48
15	159	63	47	32	23	10	0.61
18	274	110	81	55	41	17	0.73
21	435	174	129	87	64	27	0.85
24	649	260	192	130	96	41	0.97
27	924	370	274	185	137	58	1.10
30	1,268	507	376	254	188	79	1.22
33	1,688	675	500	338	250	105	1.34
36	2,191	877	649	438	325	137	1.46
42	3,480	1,392	1,031	696	516	217	1.70
48	5,194	2,078	1,539	1,039	769	325	1.95
54	7,396	2,958	2,191	1,479	1,096	462	2.19
			Specific Weight = 165 pcf				
12	86	35	26	17	13	5	0.48
15	169	67	50	34	25	11	0.61
18	292	117	86	58	43	18	0.73
21	463	185	137	93	69	29	0.85
24	691	276	205	138	102	43	0.97
27	984	394	292	197	146	62	1.10
30	1,350	540	400	270	200	84	1.22
33	1,797	719	532	359	266	112	1.34
36	2,331	933	691	467	346	146	1.46
42	3,704	1,482	1,098	741	549	232	1.70
48	5,529	2,212	1,638	1,106	819	346	1.95
54	7,873	3,149	2,335	1,575	1,168	492	2.19
			Specific Weight = 175 pcf				
12	92	37	27	18	14	5	0.48
15	179	72	53	36	27	11	0.61
18	309	124	92	62	46	19	0.73
21	491	196	146	98	73	31	0.85
24	733	293	217	147	109	46	0.97

(Continued)

[a] Stone weight limit data from OCE 1971.

Table 4.21 (Concluded)

Riprap Thickness, in.	Limits of Stone Weight, lb[a] Percent Lighter by Weight						d_{30}(min) ft
	100		50		15		
	Max	Min	Max	Min	Max	Min	
	Specific Weight = 175 pcf						
27	1,044	417	309	209	155	65	1.10
30	1,432	573	424	286	212	89	1.22
33	1,906	762	565	381	282	119	1.34
36	2,474	990	733	495	367	155	1.46
42	3,929	1,571	1,164	786	582	246	1.70
48	5,864	2,346	1,738	1,173	869	367	1.95
54	8,350	3,340	2,474	1,670	1,237	522	2.19

[a] Stone weight limit data from OCE 1971.

APPENDIX A

NOTATION

a = effective area of particle

b = stone breadth or thickness

bis = equation is repeated

B = flume bottom width

C_1, C_2, C_3 = generic coefficients

C_c = Shields coefficient

C_d = drag coefficient

C_ℓ = lift coefficient

D = flow depth

d, d_{90}, d_{50}, etc. = particle size of which a certain percent is finer by weight

d_{85}/d_{15} = gradation uniformity

F_L = lift force

F_{SHAPE} = shape factor and surface texture

F_{SIDE} = side slope factor

g = universal gravitational constant

H = wave height

K = tractive force ratio

K_1, K_2, K_3 = generic coefficients

K_D = stability coefficient

K_s = equivalent sand grain roughness

ℓ = stone length

L_s = length along channel side slope

M,L,T = fundamental dimensions of mass, length, and time, respectively

n = Manning's roughness coefficient

N = blanket thickness/d_{100}

R = hydraulic radius

S = energy slope; channel slope

U_* = shear velocity = $\sqrt{gDS}$ = $\sqrt{T/\rho}$

V = average flow velocity

V_a = cross-section average channel velocity

V_b = bottom velocity

V_c = critical velocity for particle on horizontal bed

V_s = critical velocity for particle on side slopes

V_y = local velocity at distance y

W = unsubmerged stone weight

W_s = submerged stone weight

y = distance above origin of logarithmic velocity profile

y_o = distance below top of roughness element to origin of profile

α = bottom angle with horizontal in flow direction

β = angle of inclination of drag force as a result of secondary motion

γ_s = specific weight of stone

γ_w = specific weight of water

θ = angle of side slope with horizontal

κ = von Karman coefficient

μ = absolute viscosity

ν = kinematic viscosity

ρ = fluid density

ρ_s = stone density

T = tractive force imposed by flowing water

T_c = critical tractive force for given particle size on bottom

T_s = critical tractive force for particle on side slope

Φ = angle of repose